

Abstract

STOVER, TRACY EUGENE, JR. Quantification of Back End Fuel Cycle Metrics Uncertainties Due to Cross Sections. (Under the direction of Paul J. Turinsky).

This work examines uncertainties in the back end fuel cycle metrics of isotopic composition, decay heat, radioactivity, and radiotoxicity. Most advanced fuel cycle scenarios, including the ones represented in this work, are limited by one or more of these metrics, so that quantification of them becomes of great importance in order to optimize or select one of these scenarios. Uncertainty quantification, in this work, is performed by propagating cross-section covariance data, and later number density covariance data, through a reactor physics and depletion code sequence. Propagation of uncertainty is performed primarily via the Efficient Subspace Method (ESM). ESM decomposes the covariance data into singular pairs and perturbs input data along independent directions of the uncertainty and only for the most significant values of that uncertainty. Results of these perturbations being collected, ESM directly calculates the covariance of the observed output posteriori. By exploiting the rank deficient nature of the uncertainty data, ESM works more efficiently than traditional stochastic sampling, but is shown to produce equivalent results. ESM is beneficial for very detailed models with large amounts of input data that make stochastic sampling impractical.

In this study various fuel cycle scenarios are examined. Simplified, representative models of pressurized water reactor (PWR) and boiling water reactor (BWR) fuels composed of both uranium oxide and mixed oxides are examined. These simple models are intended to give a representation of the uncertainty that can be associated with open uranium oxide fuel cycles and closed mixed oxide fuel cycles. The simplified models also serve as a

demonstration to show that ESM and stochastic sampling produce equivalent results, because these models require minimum computer resources and have amounts of input data small enough such that either method can be quickly implemented and a numerical experiment performed. The simplified models are followed by more rigorous reactor physics and depletion models showing a PWR uranium oxide fuel and various metal fast reactor fuels composed of transuranics. The more rigorous models include multi-group cross sections, multiple burnup steps, neutron transport calculations to update cross sections, and multi-scale multi-physics code sequences to simulate a complete fuel lifetime. Finally, the fast reactor and PWR fuels are combined in a closed fast reactor recycle fuel cycle, and uncertainties on the resulting equilibrium cycle examined.

Quantification of Back-End Fuel Cycle Metrics Uncertainties Due to Cross Sections

By

Tracy E. Stover, Jr.

A thesis submitted to the Graduate Faculty of
North Carolina State University
in partial fulfillment of the
requirements for the Degree of
Master of Science

Nuclear Engineering

Raleigh, North Carolina

2007

APPROVED BY:

Dr. Hany S. Abdel-Khalik
Co-Chair

Dr. Harvey Charlton

Dr. Paul J. Turinsky
Chair of Advisory Committee

Dedication

*I can do all things through Christ which strengthens me.
(Philippians 4:13, NKJV)*

Biography

Tracy Eugene Stover, Jr. was born in Fairlea, West Virginia on December 1, 1983 to Tracy and Gay Stover of Smoot, West Virginia. He received elementary and secondary education at Smoot Jr. High and Elementary School. He graduated as salutatorian from Greenbrier West High School of Charmco, West Virginia in 2002.

After high school Tracy attended Murray State University of Murray, Kentucky as a major in the area of Engineering Physics. In the summer of 2004 he received the Summer Undergraduate Research Fellowship at the National Institute of Standards and Technology in Gaithersburg, Maryland. Research conducted there in the area of Compton suppression, under the supervision of Dr. George Lamaze, led to his first journal publication in Nuclear Instruments and Methods B in 2004. In his senior year, Tracy assisted Dr. Arthur Pallone of Murray State in restoring the Murray State particle accelerator laboratory to full operation after years out of service. After graduation from Murray State in May of 2005 he enrolled at North Carolina State University for graduate studies in Nuclear Engineering where he is currently pursuing a higher degree under the direction of Dr. Paul J. Turinsky.

Acknowledgements

There are so many people involved in my life that need to be acknowledged here and I'm sure I will miss someone. First I need to recognize and thank my parents, Tracy and Gay Stover, who have supported me through my entire educational career from grade school to graduate school. I would like to next thank my advisor Dr. Paul Turinsky whose enthusiastic guidance and commanding knowledge of the subject have been crucial to both this work and my post-graduate development. Next, I thank Dr. Hany Abdel-Khalik who has been continuously available to assist me in this work and help me through the many difficulties in the subject matter. I would also like to thank Dr. Masood Iqbal for very helpful conversation and instruction in the use of alternative cross-section processors and depletion codes.

I offer sincere gratitude to my professors both at Murray State University and North Carolina State for their academic instruction and encouragement. I would also like to thank all my friends, classmates, and co-workers who've helped me in many ways with my work. In particular I must thank Mr. Matthew Jessee for his vast support in dealing with and understanding the implementation of mathematics involved in this research, and Mr. Ross Hays, Mr. Christopher Briggs, and Mr. Jason Elkins for their thoughtful advice on advanced programming and instruction in the use of various models. To anyone I may have missed please accept my apologies and my thanks.

Finally, and most importantly, I must thank God, my Lord and Savior Jesus Christ. My faith has given me both strength and comfort in even the worst of times so I must thank Him for the spiritual support.

Table of Contents

List of Figures	vii
List of Tables	ix
Nomenclature	xii
1. Introduction.....	1
1.1 Importance to the Nuclear Fuel Cycle	1
1.2 Cross Sections and Uncertainty	2
1.3 Review of Uncertainty Propagation Techniques	3
1.4 Overview of Computational Modeling Software.....	8
1.5 Fuel Types and Scenarios of Interest.....	12
2. Methodology	13
2.1 Use of SCALE Covariance Data.....	13
2.2 Use of REBUS Covariance Data	16
2.3 Verification of Model Linearity.....	17
2.4 Implementation of Stochastic Sampling Method.....	21
2.5 Implementation of the ESM.....	23
2.6 Computational Models Employed for Each Method	26
2.7 TRITON Recycle Methodology	33
2.8 Statistical Analysis Performed on Results	37
3. Numerical Results.....	42
3.1 Simplified ORIGEN Models.....	42
3.1.1 Equivalency of ESM and Stochastic Methods.....	42
3.1.2 PWR Model with UOX Fuel	44
3.1.3 Typical LWR with UOX Fuel.....	49
3.1.4 BWR Models with UOX Fuel.....	50
3.1.5 PWR Models with MOX Fuels.....	53
3.1.6 Comparison of Results, Simplified ORIGEN Models.....	56
3.1.7 A Brief Experiment with Operational Uncertainties	63
3.2 TRITON Models.....	65
3.2.1 PWR Model in TRITON with UOX Fuel.....	65

3.2.2	Fast Reactor Models with Transuranic Fuels.....	76
3.2.3	Fast Reactor Model with Transuranic Fuel and Recycling.....	80
3.2.4	Comparison of Results, TRITON Models	84
3.3	REBUS Fast Reactor Equilibrium Model.....	90
4.	Discussion and Conclusions	94
4.1	Discussion of the Use of ESM in this Study.....	94
4.2	Discussion Concerning the Results of the Models	94
4.3	Recommendations and Future Work	98
	References.....	100
	Appendices.....	102
	Appendix A: Fuel Models.....	103
I.	The Typical LWR Model Using a UOX Fuel.....	103
II.	The PWR Model Using a UOX Fuel	103
III.	The BWR Model Using a UOX Fuel.....	106
IV.	The PWR Separation Model Using a UOX Fuel	109
V.	The PWR Model Using a MOX Fuel	110
VI.	The PWR Model Using a MOX Fuel with Impurities.....	113
VII.	The PWR Model Using TRITON	117
VIII.	TRITON FR Models Using Actinide Fuels	120
IX.	REBUS Fast Reactor Model with Actinide Fuel and Recycle	128
	Appendix B: Graphical Verification of Model Linearity	142
	Appendix C: Results Tables for Fuel Models.....	145

List of Figures

Figure 2.1: Gaussian Distribution	19
Figure 2.2: Flux Spectra for PWR Models.	28
Figure 2.3: Flux Spectra for BWR Models.....	29
Figure 3.1: Decay heat comparison of stochastic and ESM sampling methods.	59
Figure 3.2: Radioactivity comparison of stochastic and ESM sampling methods.	59
Figure 3.3: Decay heat comparison of SCALE provided data and SAS2H updated data.	60
Figure 3.4: Radioactivity, SCALE provided data and SAS2H updated data.....	60
Figure 3.5: Decay heat comparison for BWR fuels.....	61
Figure 3.6: Radioactivity Comparison for BWR fuels.	61
Figure 3.7: Decay heat comparison of UOX and MOX fuels.....	62
Figure 3.8: Radioactivity comparison for UOX and MOX fuels.....	62
Figure 3.9: Decay heat uncertainty of key isotopes due to various sources.	63
Figure 3.10: Radioactivity uncertainty in key isotopes due to various sources.....	64
Figure 3.11: Decay heat comparison of simple ORIGEN and TRITON models.	86
Figure 3.12: Radioactivity comparison of simple ORIGEN and TRITON models.....	86
Figure 3.13: Decay heat comparison of three fast reactor fuels.	87
Figure 3.14: Radioactivity comparison for three fast reactor fuels.	87
Figure 3.15: Decay heat comparison of once through and recycled fast reactor fuels.	88
Figure 3.16: Radioactivity comparison of once through and recycled fast reactor fuels.	88
Figure 3.17: k-effective uncertainty due to recycled isotopics uncertainties only.	89
Figure 3.18: k-effective uncertainty due to cross sections and recycled isotopics uncertainties.....	89
Figure 3.19: Decay heat comparison of REBUS and TRITON Models.....	93
Figure 3.20: Radioactivity comparison of REBUS and TRITON Models.	93
Figure A.II.1: SAS2H Model, PWR, 4.5 w/o and 40 GWD/MTU	104
Figure A.II.2: ORIGEN Model, PWR, 4.5 w/o and 40 GWD/MTU	105
Figure A.III.1: SAS2H Model, BWR, 4.5 w/o and 40 GWD/MTU	107
Figure A.III.2: ORIGEN Model, BWR, 4.5 w/o and 40 GWD/MTU	108
Figure A.V.1: SAS2H Model, MOX fuel in PWR, 50 GWD/MTHM	111

Figure A.V.2: ORIGEN Model, MOX fuel in PWR, 50 GWD/MTHM	112
Figure A.VI.1: SAS2H Model, MOX with impurities fuel in PWR, 50 GWD/MTHM	114
Figure A.VI.2: ORIGEN Model, MOX with impurities fuel in PWR, 50 GWD/MTHM.....	115
Figure A.VII.1: TRITON Model, PWR, 4.5 w/o and 48 GWD/MTU	117
Figure A.VIII.1: TRITON Model, CR=1.05	121
Figure A.VIII.2: TRITON Model, CR=0.70	123
Figure A.VIII.3: TRITON Model, CR=0.25	125
Figure A.IX.1: REBUS Equilibrium Model, CR = 0.77.....	128
Figure B.1: Nuclide Output Discharge Mass Linearity	143
Figure B.1: Sampling Output Nuclide Discharge Mass Distributions.....	144

List of Tables

Table 2.1: Listing of Considered Nuclides and Reactions in SCALE Library.....	15
Table 2.2: Listing of Considered Nuclides and Reactions in REBUS Library.....	17
Table 2.3: Brief Summary of Fuel Types Examined Using SAS2H + ORIGEN.....	27
Table 2.4: Isotopes Tracked for Analysis	30
Table 2.5: Brief Summary of Fuel Types Examined Using TRITON.....	31
Table 2.6: Specific values, per nuclide, for metrics of interest.....	39
Table 3.1: Comparison of isotopic uncertainties from the two methods.	43
Table 3.2: Discharge isotopics for the PWR simplified model.	44
Table 3.3: Masses, with uncertainty, of actinides at 3 decay times.....	46
Table 3.4: Comparison of separation at 3 times vs. no separation, first 1000 years of decay.	47
Table 3.5: Comparison of separation at 3 times vs. no separation, 2500 – 10,000 years of decay.	48
Table 3.6: Discharge isotopics for typical LWR simplified model.	49
Table 3.7: Isotopics uncertainties for typical LWR simplified model.....	50
Table 3.8: Discharge isotopics for BWR fuel burned at 0% void.	51
Table 3.9: Discharge isotopics for BWR fuel burned at 35% void.	51
Table 3.10: Discharge isotopics for BWR fuel burned at 50% void.	52
Table 3.11: Discharge isotopics for BWR fuel burned at 65% void.	52
Table 3.12: Isotopics uncertainties for BWR models.	53
Table 3.13: Discharge isotopics for the "clean" MOX fuel.	55
Table 3.14: Discharge isotopics for MOX fuel with impurities.	55
Table 3.15: Isotopic uncertainties for MOX fuels.	56
Table 3.16: Comparison of isotopics between models.	66
Table 3.17: 40 GWD/MTU Discharge Isotopics	67
Table 3.18: 48 GWD/MTU Discharge Isotopics	67
Table 3.19: Resulting standard deviations from both models.....	68
Table 3.20: Change in flux as burnup increases.	71
Table 3.21: Change in 1-group cross section uncertainty due to flux change.	72
Table 3.22: Comparing discharge isotopic uncertainties for various flux updates.....	73

Table 3.23: Change in Am-243 capture cross section due to resonance treatment.	75
Table 3.24: Fuel composition data for fast reactor models.....	78
Table 3.25: Fuel geometry and power data for fast reactor models.....	78
Table 3.26: Discharge isotopics for fast reactor fuel of CR = 0.25.	79
Table 3.27: Discharge isotopics for fast reactor fuel of CR = 0.70	79
Table 3.28: Discharge isotopics for fast reactor fuel of CR = 1.05	79
Table 3.29: Relative isotopic uncertainties for fast reactor fuels.....	80
Table 3.30: Comparison of fuel composition properties for once through and recycled fuel.....	82
Table 3.31: Discharge isotopics for equilibrium recycled fuel.....	82
Table 3.32: Discharged isotopics uncertainties originating from recycled isotopics and cross sections sources of uncertainty.	83
Table 3.33: Operating Parameters for REBUS model.....	92
Table 3.34: Discharge Isotopics for REBUS model.	92
Table 3.35: Isotopic Uncertainties for REBUS model.....	92
Table A.IV.1: Isotopics of discharged UOX fuel at 5, 10, and 25 years after irradiation.	110
Table A.VIII.1: Fast Reactor Fuel Composition Data, by conversion ratio	120
Table A. VIII.2: Cladding Composition Data.....	120
Table A. VIII.3: Operating Conditions and Geometry Data.....	120
Table C.1: Results table for the PWR model using ESM for uncertainty.	146
Table C.2: Results table for PWR fuel in the simplified model.	147
Table C.3: Results table for typical LWR fuel simplified model.	148
Table C.4: Results table for BWR fuel burned at 0% void.....	149
Table C.5: Results table for BWR fuel burned at 35% void.....	150
Table C.6: Results table BWR fuel burned at 50% void.	151
Table C.7: Results table for BWR fuel burned at 65% void.....	152
Table C.8: Results table for clean MOX fuel.	153
Table C.9: Results table for MOX fuel with impurities.....	154
Table C.10: Results table for TRITON PWR model, 48 GWD/MTU.....	155
Table C.11: Results table for fast reactor fuel of CR = 0.25.	156
Table C.12: Results table for fast reactor fuel of CR = 0.70.	157

Table C.13: Results table for fast reactor fuel of CR = 1.05.	158
Table C.14: Results table for equilibrium recycled fast reactor fuel of CR = 0.70.	159
Table C.15: Results table for REBUS equilibrium recycled fast reactor fuel.	160

Nomenclature

ALWR – Advanced Light Water Reactor
BOC – Beginning of Cycle
BOL – Beginning of Life
BWR – Boiling Water Reactor
BU – Burnup
CR – Conversion Ratio
ENDF – Evaluated Nuclear Data File
EOC – End of cycle
EOL – End of Life
ESM – Efficient Subspace Method(s)
FP – Fission Product(s)
FR – Fast Reactor
GWD – Giga Watt Days
LWR – Light Water Reactor
MOX – Mixed Oxide
MTHM – Metric Ton Heavy Metal
MTIHM – Metric Ton Initial Heavy Metal
MTU – Metric Ton Uranium
PWR – Pressurized Water Reactor
TRU – Transuranic(s)
UOX – Uranium Oxide
w/o – Weight Percent

1. Introduction

1.1. *Importance to the Nuclear Fuel Cycle*

Over the next several years, policy makers will be assessing the deployment of various components of the nuclear fuel cycle, e.g. the Yucca Mountain repository, reprocessing plants, new reactors, etc. This research will be conducted in conjunction with the SINEMA (Simulation Institute for Nuclear Energy Modeling and Analysis) project headed by Idaho National Laboratory, which aims to produce a computational tool to be provided to policy makers for the assessment and comparison of various fuel cycle scenarios [1]. The objective of this work is to develop uncertainty propagation techniques to assess the affect of certain design and operation parameters on back-end fuel cycle metrics that are of key importance in various fuel cycle scenarios. Comparing two fuel cycles might be irrelevant if the uncertainty in a key metric between them overlaps.

Key metrics will hereinafter be defined as anything that is a limiting factor for the technology or facilities which are deployed in the current nuclear fuel cycle or may be deployed in future advanced fuel cycle scenarios. The nearest future deployment seems to be the spent fuel repository to be located at Yucca Mountain, Nevada. The repository's capacity is currently limited by the heat produced by the decay of the spent fuel such that the temperature between the repository tunnels remains below the local boiling temperature of water. Heat load is dominated by fission products in the first 1500 years, when peak heat production occurs and by minor actinides thereafter [2][3]. In the very distant future the waste packages are assumed to fail and the metric of concern is then what material is released, i.e. isotopic inventory and the radiotoxicity of the material released to the

biosphere. It has been suggested that implementing a so-called advanced fuel cycle that includes reprocessing of spent nuclear fuel could extend the lifetime of the repository by reusing fissile material and reclassifying inert material that would otherwise fill the repository quickly in the once through fuel cycle [4]. A good example is that greater than 95% of spent uranium oxide fuel is U-238, a low level waste that is safe enough to store somewhere other than the repository if separated out [5]. When considering the reprocessing of spent fuel for a mixed oxide fuel for a light water reactor, or an actinide fuel for a fast reactor, the concerns become radioactivity of the fuel, which facilities must contain, and the inventory of material which can be extracted from the fuel at the time of separation. Convenience of physical properties requires only the examination of the uncertainty that arises in isotopic inventories since heat, radioactivity, and radiotoxicity are linearly proportional to mass. Apart from the significant economical and political challenges of implementing advanced fuel cycles or operating a repository at all, e.g. high cost of reprocessing and poor public opinion [6], the nature of engineering requires designs to be built around safety margins which are limited by the metrics discussed above. Reducing uncertainty not only allows for a better evaluation of fuel cycles but also more economical and efficient designs of the associated infrastructure.

1.2. Cross Sections and Uncertainty

Reaction cross-sections, as part of Evaluated Nuclear Data File (ENDF) [7], provide a large amount of information that is essential to any nuclear calculation, e.g. the models that predict the behavior and operation of nuclear reactors and the resulting spent fuel. Since the aim of this work is to develop a generalized uncertainty propagation technique for nuclear

models that demand large input data sets and produce large output parameter data sets, cross-sections' uncertainty is the source that will be examined. The uncertainty cross sections contribute to the output parameters of discharged isotopic masses, decay heat load, radioactivity and radiotoxicity are the back-end nuclear fuel cycle metrics that are analyzed herein. Since the evaluation of these data is continuously being updated, emphasis is placed on their uncertainties – variances and covariances – with that data also made available in conjunction with the cross-sections themselves. The problem is augmented by the complex nature of cross-sections, measured as a function of the kinetic energy of the neutrons that are causing the reactions. Homogenization, or the averaging of a cross-section over a fixed energy range and/or spatial region, is often implemented to reduce the computational burden. The level of homogenization varies depending upon the application, ranging from hundreds of pieces of data for simple depletion, to millions of data pieces for precise in-core calculations. Considering that every material charged to, or created in, a reactor has many cross-sections for many different reaction types, even when represented by only one energy group, spatially homogenized over the entire core, the volume of uncertainty data is still large and propagating its affect on various metrics is a daunting task.

1.3. Review of Uncertainty Propagation Techniques

Uncertainty data allows uncertainty models to be applied and propagated through crucial parameters for evaluating the design system in question, such as reactor operation and the nuclear fuel cycle as a whole. “Propagating uncertainties is a non-trivial task because of the computational complexity often associated with the various modeling stages of the fuel cycles, and the size and type of different sources of uncertainties.” [8] It is also beneficial to

recognize that modeling uncertainties can be introduced through the numerical approximations that are typically found in models of complex systems, but for this study the focus is on those sources of uncertainty that are inputs to the model, particularly cross-sections input to a nuclear physics model.

The most basic analytical method is to perturb an input by some value and observe how the output is affected. While this approach efficiently arrives at a direct sensitivity of a model to an individual parameter, the investigator will usually only examine a few parameters due to the time requirements. Case in point is the work of E. Schneider [10] who introduced set perturbations into a few key cross sections and modeled the response of discharge isotopics to those perturbations. When considering huge volumes of input data such as thousands of cross-sections coupled with long CPU run-times of complex, multi-physic models, this method is very tedious and time consuming.

The classic approach to the uncertainty analysis of nuclear systems is the use of adjoint solutions that arrive at the sensitivity of a metric to all input parameters [9]. While the change in the metric to any change in that particular parameter is now known, the drawback is that m metrics will require m adjoint solutions [11]. If one follows this process to obtain sensitivity coefficients, S , for many parameters, for example R cross sections, S_R one arrives at a so-called sensitivity matrix $\overline{\overline{S_R}}$. Note that here and throughout the remainder of this document, variables shown with a single bar are assumed to be vectors and variables with a double bar are assumed to be matrices. The uncertainty matrix of a metric to this set of parameters is easily obtained by multiplying the sensitivity matrix by the covariance matrix of the parameters by the transpose of the sensitivity matrix [11][12][13], producing what is sometimes called the “sandwich” equation. This classical approach has been studied

and repeated, and consistently yields reliable and verified results. The work of H. Aliberti, et. al. uses this approach to evaluate the uncertainty of reactor and fuel cycle parameters, e.g. reactivity, decay heat, etc., in regards to cross-sections and is a valuable source with which to compare the results of this work.

The process can be very time consuming from a computational viewpoint because, every metric must have an adjoint solution and a set of sensitivity parameters evaluated. H. Abdel-Khalik of North Carolina State University has recently developed the Efficient Subspace Method (ESM) which approximates the behavior of a large, rank deficient matrix, such as the cross-section covariance matrix or the sensitivity matrix, in an effort to make computations more efficient [14]. ESM works most efficiently when the input data and the number of metrics of interest to be observed are both large. ESM also requires the problem to be ill-conditioned, as are many complex system problems. ESM can be implemented in existing models, but requires linear algebra operations to be applied via pre- and post-processors. In addition to its use for propagating cross-sections uncertainties, ESM has been harnessed for performing adaptive simulation of reactor core calculations. Adaptive simulation is an inverse theory approach that adjusts cross-sections to enhance the agreement between the measured and code-predicted core observables of interest, e.g. core power distribution, and core reactivity. Adaptive simulation is currently the focus of various research projects at NC State.

Another method of uncertainty propagation is the so-called forward perturbation method, which can either be deterministic or stochastic in nature [11]. The deterministic approach works best when the input data field is small because this method determines sensitivity by input data perturbation one piece at a time [15]. Because the input data set for

cross-sections can be very large, this approach was not considered. Alternatively, the stochastic approach can be confidently used for a larger input data set and works well when the amount of output data is large [15]. This method uses a Monte Carlo sampling (random or Latin-Hypercube [16]) of the total input data skewed by the data probability distributions. Many samples of inputs are run with existing models and probability distributions of output are determined directly from the results [11][15]. A study of the convergence of the distributions is often necessary to determine the number of samples needed to assure confidence in a specific problem.

Directly sampling the probability distribution is ideal only when the input parameters are independent [15]. In the case of covariance data for a large number of parameters input to a complex multi-scale model, two main issues arise: 1) in using random input samples to calculate outputs that are functions of many variables, some sample sets could be linearly dependent, i.e. the output could be approximated by a linear combination of previous samples, increasing the number of samples required because essentially the same sample is being repeated, and 2) covariance is defined as the expected variance of one random variable with respect to another random variable [17], which means that the probability distributions of input parameters are correlated, and that simply sampling a distribution of one parameter does not take into account its variance due to another. In the realm of linear algebra, covariances exist as the off diagonal elements of the covariance matrix and variances are the diagonal elements.

If the model is linear, both of these issues can be avoided by a single adjustment to the forward method. To account for correlations and to ensure that each set of samples is linearly independent, the covariance matrix is processed by singular value decomposition

into eigenvalues and corresponding eigenvectors. The eigenvalues which are derived from the covariance matrix are used in the probability distributions and the eigenvectors, by definition, are linearly independent. The samples used as input are a combination of samples from each of the eigen-pairs where the square root of the eigenvalue is the standard deviation of the sample [18]. When H. Kawano, et. al., used this procedure, it was applied only to the multi-group covariance matrix of the Pu-239 fission cross section. The resulting effects on criticality were subsequently examined and compared to a benchmark experiment. While fission of Pu-239 is very important for both uranium and mixed oxide fuels, as well as nuclear weapons, it is still just one reaction among many. When the covariance matrix is very sparse, this method yields another benefit for the analysis in that the eigenvectors of a sparse matrix will contain one element that is very close to 1 and the other elements will be very small. Thus, if one perturbs along only a single eigenvector at a time, the perturbation can be traced back to a single cross-section since one would have received the majority of the perturbation along that eigenvector. This is used to determine which cross-sections contribute most to the resulting uncertainty in the output.

In reviewing the methods available, both ESM and stochastic forward perturbation using the eigen-pair approach and random sampling show promise for such a problem as set forth in this work. It will be shown later that the models used in this work are nearly linear and converge after a reasonable number of samples to justify using either approach. In development of the propagation techniques in this work, the stochastic perturbation approach was used on simple LWR fuel models, namely uranium and mixed oxide fuels. Due to the fast execution time of simplified and somewhat crude models of these fuels and the linear algebra processors required for ESM, both of which will be addressed in Section 2, this

appeared a prudent choice. The benefit of this simplified model is that one can compare the traditional stochastic method to the newly developed ESM. A validation experiment for ESM, implemented within the simple model, shows that both methods produced equivalent results but that the stochastic method required less mathematical manipulation. When a much more detailed realistic fuel model is needed, however, e.g. many burnup steps in a neutron transport model using multi-group cross section data, stochastic methods become impractical and the use of the ESM becomes necessary. Such a model is the standard in practical fuel analysis and is also needed when the simplified models failed to provide needed resolution and linearity when examining fast reactor fuels. Due to the fact that the two approaches were determined to be equivalent, the move to this method, was made with confidence.

1.4. Overview of Computational Modeling Software

As already stated, the techniques developed in this work are implemented in pre-existing fuel cycle models. Computational modeling programs are cornerstones of the nuclear industry since full scale experiments are often not a pursuable approach. The pre-existing models chosen for this study are the SCALE 5.0 software package available from Oak Ridge National Laboratory, specifically, the ORIGEN depletion code, the SAS2H sequence, and the TRITON sequence; and, the REBUS 3.0 code from Argonne National Laboratory. Qualifications of the SCALE package include verified and validated models of benchmark experiments augmented by package popularity, user-friendliness, and convenient technical support from the developer [19]. Furthermore, the SCALE package also includes a pre-formatted 44-group library containing variance and covariance information for a number

of key reactions types and isotopes. The REBUS model, which has also been verified and validated, has a somewhat more difficult input structure, but was specifically designed for fast reactor models [20].

ORIGEN is a time-dependent point-depletion analysis code that can track changes in concentrations of a large number of isotopes due to nuclear transmutation and radioactive decay. The program uses the matrix exponential expansion method to solve the Bateman depletion equations for any number of discrete points in time. ORIGEN can model nuclear fuel at various stages during the fuel cycle, including irradiation, storage, transportation, etc. ORIGEN operates with various library formats, the two most common being a card image library and a binary working library. The three-group card image library must be supplied by the user in the required format and include a corresponding three group flux spectrum in the ORIGEN input deck. SCALE is distributed with a three-group card image library, and its corresponding flux spectrum that is representative of a typical light water reactor. The typical flux spectrum is also available in 44-group and 238-group representations. The library type most often used is an AMPX formatted binary library. The master libraries containing basic ENDF data in 1-, 3-, 44-, and 238- groups are included with the SCALE package. Because SCALE is a multi-physics program, there are drivers and programs that can update the master library to create a problem-specific working library that is usable in ORIGEN. When ORIGEN uses a binary library, the cross sections applied are in either one-group or three-group values that are representative of the specific problem that the working library was created for. This allows ORIGEN to execute very quickly and eliminates the need to input a specially formatted card-image library or a fuel specific flux spectrum, which is already accounted for in the new cross-sections. [21]

The SAS2H sequence uses various codes within SCALE to produce a detailed model of a fuel assembly. SAS2H is a coupled one-dimensional depletion and shielding analysis sequence. SAS2H is designed to create a 1-D model of a specific fuel type and then track various parameters -- reactivity, isotopics, dose rates in storage, etc. -- through the life of the fuel. The user supplies a fuel composition, geometry, power and decay history, and optionally, a storage cask description for disposal dose analysis. Problem specific, burnup dependent cross-sections are derived using two separate lattice cell models in a pseudo 2-D model that utilizes 1-D neutron transport modeling. The process also produces problem-dependent flux spectra in the same number and ranges of groups as the master library input to SAS2H. SAS2H uses the ORIGEN code to do all of its depletion analysis both for the in-core depletion and out-of-core decay. While SAS2H was mainly designed to model light water reactor and research reactor fuels, it can also be used to create a crude fast reactor model if given the fuel composition and geometry for such a reactor. [22]

The TRITON sequence is also another all inclusive depletion analysis, like the SAS2H routine. Unlike SAS2H, however, TRITON solves the transport equation in a 2-dimensional geometry. TRITON is particularly used for modeling single fuel assemblies or individual Wigner cells, the latter of which will be used in this work. TRITON must be given buffer region input as it does not automatically account for non-fuel holes in the lattice like SAS2H. The biggest drawback is that TRITON was developed intentionally for commercial reactors whose fuel is by standard in a square lattice. While TRITON can model any number of polygon geometries within a given domain, the outer domain is forced to be rectangular, which is effective for square unit cells but lacks the resolution and proper moderator modeling abilities for other geometries, for example, a hexagonal cell for a fast

reactor fuel. This work recognizes this shortcoming of the model and acknowledges that the results will not be absolutely accurate because of it. In its defense, TRITON is a much more detailed model than SAS2H and overcomes some modeling inadequacies of SAS2H while maintaining all the analysis abilities. [23]

REBUS is used in the latter part of this study to compare the fast reactor results from TRITON, since the fast reactor models examined were created at Argonne using this code. Also, the many group cross section library and associated covariance matrix for REBUS is based upon a sodium cooled fast reactor flux spectrum, whereas the data available in the SCALE package is based upon a light water thermal reactor flux spectrum. REBUS was used since it has the unique ability to recycle fuel, using both reprocessing plants and external sources, and iteratively find some equilibrium fuel composition to meet operating parameters and cycle energy requirements, while using the available recycle feed. As used in this study, REBUS incorporates the DIF3D diffusion theory code utilizing the finite difference option. Hexagonal-z geometry for the core is modeled, with each hexagon representing a fuel assembly with homogenized cross sections employed. The drawback to REBUS is that a few-group covariance matrix did not exist a priori as it did with the SCALE package. Thanks to the work of Dr. Masood Iqbal and Dr. Hany Abdel-Khalik, a 15-group covariance matrix [24] for key reaction types and isotopes was created specifically for REBUS at North Carolina State University using the Argonne cross section processing code MC²2 [25]. Dr. Hany Abdel-Khalik also implemented the efficient subspace method (ESM) of uncertainty propagation in REBUS.

1.5. Fuel Types and Scenarios of Interest

The most logical place to begin the analysis of uncertainty in various fuel types is to first analyze the fuel of the current reactor fleet deployed in the U.S. – low enriched uranium oxide fuel. Care is taken to select, directly or similarly from other studies, fuel types that represent an actual equilibrium cycle fuel or a fuel for a predicted equilibrium cycle, i.e. not a specialized fuel designed for start-up cores or demonstration experiments. For the current reactor designs in this study, that fuel is a 4.5 w/o uranium oxide fuel burned to 40 GWD/MTU modeled first by the typical light water reactor information provided with SCALE, and then in both a pressurized water reactor and a boiling water reactor of various void fractions as modeled by SAS2H. To consider an advanced fuel cycle in the advent of a reprocessing infrastructure being considered in the U.S., mixed oxide and fast reactor fuels are also considered. Models include an ALWR MOX containing plutonium and uranium, a mixed oxide fuel with neptunium and americium impurities, and three fast reactor fuels, of various conversion ratios, made up of spent light water reactor fuel to burn off minor actinides. Finally, an experiment is conducted to demonstrate the effects of accumulating uncertainty in the input isotopics themselves as fuel is recycled in the fast reactor case. The former single pass fast reactor models are examined in TRITON and the latter fast reactor recycle scenario will be modeled both TRITON and REBUS. The fast reactor and its corresponding fuel types are modeled after Argonne's Advanced Burner Test Reactor [26].

2. Methodology

2.1. Use of SCALE Covariance Data

The SCALE 5.0 package is distributed with two 44-group covariance libraries, based on a light water thermal reactor flux spectrum, that contain information for approximately 700 nuclide-reaction pairs for many key isotopes. A full listing of all available data is too lengthy for this document but the reader is referred to the manual describing the library [31]. Effort is taken, through assumptions and model limits, to reduce this volume of data both to fit the input needed for models and to reduce the computational effort needed to implement the chosen uncertainty propagation technique. Unexpectedly, one of the assumptions made so the data will fit the ORIGEN code, actually expands the volume of information.

The covariance library containing information for most nuclide-reaction pairs is chosen as the data source for this work. The first reduction in data is to examine only the reactions that are important to reactor calculation for depletion analysis, and the only reactions ORIGEN uses -- neutron capture and fission. Those reactions in particular are: (n,γ) , (n,p) , (n,α) , (fission), $(n,2n)$, and $(n,3n)$. The result is that covariance data for 701 nuclide-reaction pairs is reduced to 116 pairs by removing the cross-sections that are not of interest to depletion. For the simplified models, the perturbations are introduced into ORIGEN as the cross sections are read from the library, whereas with the more rigorous TRITON model, perturbations are made directly in the master cross section library before it is used by the code. When coupling a binary library to ORIGEN, generated by SAS2H as described later, the simplified model directly uses one-group cross-sections that are ideally representative of the specific problem. With this restriction on input data, the 44-group

neutron flux spectrum generated by SAS2H is used to collapse the 44-group covariance data to one-group values, instantly reducing the volume of data by a factor of 44 solely so that its affects can be applied directly to ORIGEN. With the exception of the typical library examined, which was prepared a priori by Oak Ridge, the flux spectra are generated for each simplified fuel/reactor examined in this work and the beginning of life total flux was chosen as a representative spectrum to be used for the collapse. This topic will be addressed again when discussing the TRITON results. For TRITON, perturbations obtained from the 44-group covariance library can be introduced directly into the 44-group master cross section library given as input to the code since both are of the same group structure. This eliminates all the pre-processing discussed above for the simplified models.

The covariance library contains data for ten materials in elemental form rather than the isotope specific reaction that ORIGEN uses. While this is of no consequence to TRITON which recognizes elemental forms and deals with them internally, the simplified models that use only ORIGEN for sampling need nuclide specific values. With this in mind, the data for those ten elements – magnesium, silicon, potassium, chromium, iron, nickel, copper, zirconium, hafnium and lead – is assumed to apply equally to isotopes of each element which are included in the cross section library. The result is the expansion of the data to a final value of 223 nuclide-reaction pairs that are considered in this work. Table 2.1 lists the nuclide-reaction pairs, using asterisks (*) to indicate data that were expanded from the elemental form and crosses (†) indicating pairs that have off-diagonal covariance data.

Table 2.1: Listing of Considered Nuclides and Reactions in SCALE Library.

Nuclide	Reaction(s)	Nuclide	Reaction(s)	Nuclide	Reaction(s)
H-1	(n, γ)	Co-59	(n,2n), (n, γ), (n, α)	Eu-153	(n, γ)
Li-6	(n, γ) (not used in ORIGEN)	Ni-58*	(n, γ), (n,p), (n, α) (n,2n)	Eu-154	(n, γ)
Li-7	(n, γ)	Ni-59*	(n, γ), (n,p), (n, α) (n,2n)	Eu-155	(n, γ)
B-10 [†]	(n,p)	Ni-60*	(n, γ), (n,p), (n, α) (n,2n)	Gd-154	(n, γ)
C-12	(n, γ), (n,p), (n, α)	Ni-61*	(n, γ), (n,p), (n, α) (n,2n)	Gd-155	(n, γ)
N-14	(n, γ), (n,p), (n, α)	Ni-62*	(n, γ), (n,p), (n, α) (n,2n)	Gd-156	(n, γ)
O-16	(n,p), (n, α)	Ni-63*	(n, γ), (n,p), (n, α) (n,2n)	Gd-157	(n, γ)
F-19	(n, γ), (n,p), (n, α)	Ni-64*	(n, γ), (n,p), (n, α) (n,2n)	Hf-174*	(n, γ)
Na-23	(n, γ), (n,p), (n, α) (n,2n)	Ni-65*	(n, γ), (n,p), (n, α) (n,2n)	Hf-175*	(n, γ)
Mg-24*	(n, γ)	Ni-66*	(n, γ), (n,p), (n, α) (n,2n)	Hf-176*	(n, γ)
Mg-25*	(n, γ)	Cu-63*	(n, γ)	Hf-177*	(n, γ)
Mg-26*	(n, γ)	Cu-64*	(n, γ)	Hf-178*	(n, γ)
Mg-27*	(n, γ)	Cu-65*	(n, γ)	Hf-179*	(n, γ)
Mg-28*	(n, γ)	Cu-66*	(n, γ)	Hf-180*	(n, γ)
Al-27	(n, γ), (n,p), (n, α) (n,2n)	Cu-67*	(n, γ)	Hf-181*	(n, γ)
Si-28*	(n,p), (n, α)	Zr-89*	(n, γ)	Hf-182*	(n, γ)
Si-29*	(n,p), (n, α)	Zr-90*	(n, γ)	Au-197	(n, γ)
Si-30*	(n,p), (n, α)	Zr-91*	(n, γ)	Pb-204*	(n,2n), (n,3n), (n, γ)
Si-31*	(n,p), (n, α)	Zr-92*	(n, γ)	Pb-205*	(n,2n), (n,3n), (n, γ)
Si-32*	(n,p), (n, α)	Zr-93*	(n, γ)	Pb-206*	(n,2n), (n,3n), (n, γ)
K-39*	(n, γ)	Zr-94*	(n, γ)	Pb-207*	(n,2n), (n,3n), (n, γ)
K-40*	(n, γ)	Zr-95*	(n, γ)	Pb-208*	(n,2n), (n,3n), (n, γ)
K-41*	(n, γ)	Zr-96*	(n, γ)	Pb-209*	(n,2n), (n,3n), (n, γ)
K-42*	(n, γ)	Zr-97*	(n, γ)	Th-232	(n, γ), (fission)
K-43*	(n, γ)	Mo-95	(n, γ)	U-233	(n, γ), (fission)
Cr-50*	(n, γ), (n,p), (n, α) (n,2n), (n3n)	Tc-99	(n, γ)	U-234	(n, γ), (fission)
Cr-51*	(n, γ), (n,p), (n, α) (n,2n), (n3n)	Ru-101	(n, γ)	U-235 [†]	(n, γ), (fission)
Cr-52*	(n, γ), (n,p), (n, α) (n,2n), (n3n)	Rh-103	(n, γ)	U-236	(n, γ), (fission)

Table 2.1: Continued.

Nuclide	Reaction(s)	Nuclide	Reaction(s)	Nuclide	Reaction(s)
Cr-53*	(n, γ), (n,p), (n, α) (n,2n), (n3n)	Ag-109	(n, γ)	U-238 [†]	(n, γ), (fission), (n,2n), (n3n)
Cr-54*	(n, γ), (n,p), (n, α) (n,2n), (n3n)	In-115	(n, γ)	Np-237	(fission)
Cr-55*	(n, γ), (n,p), (n, α) (n,2n), (n3n)	Cs-133	(n, γ)	Pu-238	(n, γ), (fission)
Mn-55	(n,2n)	Nd-143	(n, γ)	Pu-239 [†]	(n, γ), (fission)
Fe-54*	(n, γ), (n,p), (n, α) (n,2n)	Nd-145	(n, γ)	Pu-240 [†]	(n, γ), (fission)
Fe-55*	(n, γ), (n,p), (n, α) (n,2n)	Sm-147	(n, γ)	Pu-241 [†]	(n, γ), (fission)
Fe-56*	(n, γ), (n,p), (n, α) (n,2n)	Sm-159	(n, γ)	Pu-242 [†]	(n, γ), (fission), (n,2n), (n3n)
Fe-57*	(n, γ), (n,p), (n, α) (n,2n)	Sm-150	(n, γ)	Am-241 [†]	(n, γ), (fission)
Fe-58*	(n, γ), (n,p), (n, α) (n,2n)	Sm-151	(n, γ)	Am-243	(n, γ), (fission)
Fe-59*	(n, γ), (n,p), (n, α) (n,2n)	Sm-152	(n, γ)		

2.2. Use of REBUS Covariance Data

The fast spectrum 15-group covariance library, developed for a sodium cooled fast reactor, pertains explicitly to the 15-group cross section files which are used in the REBUS model. Due to their specific nature, and the fact that they will be directly used to create perturbations in the REBUS fast reactor models, no modification or simplifications are necessary. The library is an unofficial beta-version release compiling the work currently under development at Brookhaven National Laboratory for fast spectrum cross-section measurements [24]. While still being under development, the reported cross-section uncertainties should be representative enough of the uncertainties encountered in fast spectrum reactor calculations. The nuclides and reactions represented appear in Table 2.2.

Table 2.2: Listing of Considered Nuclides and Reactions in REBUS Library.

Nuclide	Reaction(s)	Nuclide	Reaction(s)	Nuclide	Reaction(s)
Cr-52	(n, γ), (n,el), (n,n')	Np-237	(n, γ), (fission), (n,el)	Am-242m	(n, γ), (fission), (n,el)
	(n,2n)		(n,2n), (n,n'),(v-bar)		(n,2n), (n,n'),(v-bar)
Fe-56*	(n, γ), (n,el), (n,n')	Pu-238	(n, γ), (fission), (n,el)	Am-243	(n, γ), (fission), (n,el)
	(n,2n)		(n,2n), (n,n')		(n,2n), (n,n'),(v-bar)
Ni-58*	(n, γ), (n,el), (n,n')	Pu-239	(n, γ), (fission), (n,el)	Cm-242	(n, γ), (fission), (n,el)
	(n,2n)		(n,2n), (n,n'),(v-bar)		(n,2n), (n,n')
U-234	(n, γ), (fission), (n,el)	Pu-240	(n, γ), (fission), (n,el)	Cm-243	(n, γ), (fission), (n,el)
	(n,2n), (n,n')		(n,2n), (n,n'),(v-bar)		(n,2n), (n,n')
U-235	(v-bar)	Pu-241	(n, γ), (fission), (n,el)	Cm-244	(n, γ), (fission), (n,el)
			(n,2n), (n,n'),(v-bar)		(n,2n), (n,n')
U-236	(n, γ), (fission), (n,el)	Pu-242	(n, γ), (fission), (n,el)	Cm-245	(n, γ), (fission), (n,el)
	(n,2n), (n,n')		(n,2n), (n,n')		(n,2n), (n,n')
U-238	(n, γ), (fission), (n,el)	Am-241	(n, γ), (fission), (n,el)		
	(n,2n), (n,n'),(v-bar)		(n,2n), (n,n'),(v-bar)		

2.3. Verification of Model Linearity

As stated in the introduction, before either stochastic forward perturbation or ESM methods are implemented, it is reasonable to check the linearity of the model to be used. Uncertainty propagation can be done by either a Monte Carlo sampling scheme, which can propagate all the moments of the input data, given infinite runs, to build the probability distributions, or a Moments Method, which propagates only selected moments of the

distribution [11]. Assuming that the choice between the methods depends on the nature of the probability distribution of the input data and the linearity of the model, it is reasonable to spend some time on this topic.

To illustrate this, the definition of the first and second moments are introduced as follows, assuming the probability distribution of input data y , is $p(y)$ and $p(y)dy$ is the probability that input data will be between y and $y + dy$:

$$p_1 = \int_{-\infty}^{\infty} yp(y)dy = \mu \quad (2.1)$$

$$p_2 = \int_{-\infty}^{\infty} y^2 p(y)dy = \sigma^2 + \mu^2 \Rightarrow p_2 - \mu^2 = \int_{-\infty}^{\infty} (y - \mu)^2 p(y)dy = \sigma^2 \quad (2.2)$$

where μ is the average of all possible values of the input data, i.e. the mean, and σ^2 describes the average of the squared differences between all possible values and the mean, i.e. the variance. Higher order moments exist with physical and statistical meaning, but since they will not be addressed in this work, further explanation is available in the references [11][17]. These moments are what define a probability distribution and the nature of the distribution determines how many moments are needed for its reconstruction.

The Gaussian distribution depicted in Figure 2.1 is characterized by only the first two moments, mean and variance.

$$p_{Gauss}(y) = \frac{1}{\sigma\sqrt{2\pi}} \exp\left(-\frac{(y - \mu)^2}{2\sigma^2}\right) \quad (2.3)$$

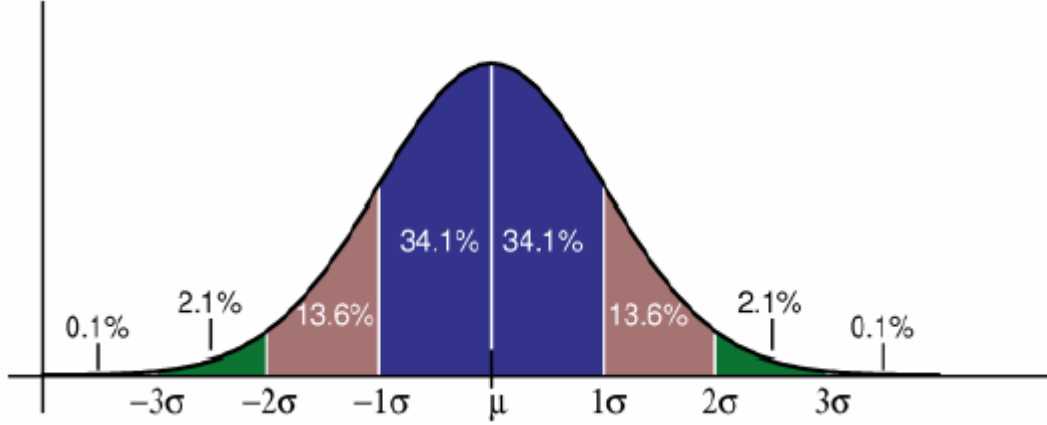


Figure 2.1: Gaussian Distribution

Further, rigorous mathematical proof shows that if a model is linear, a Gaussian input will produce a Gaussian output [23]. The first moment of the output corresponds to the reference output values calculated based on the mean input values. The second moment, variance, is obtained by re-running the model with input data perturbed by an amount proportional to the standard deviation. Most input cross-sections lack information about the second moment and no ENDF library contains information about higher order moments. For this reason it is often assumed cross-sections are normally distributed given a lack of higher order moments. Along with that assumption, this work is based on the observation that the model used, i.e. ORIGEN, which shall be discussed in detail later, is nearly linear over the range of uncertainties of interest.

To study the linearity of the model the following study is conducted. Let the model be defined by an operator, Ω ,:

$$\overline{y}_0 = \Omega(\overline{\sigma}_0) \quad (2.4)$$

where $\overline{\sigma}_0$ is a vector of input cross-sections $i = 1, \dots, N$ where subscript 0 denotes reference values, and \overline{y}_0 are calculated isotopics. The model Ω is judged linear around $\overline{\sigma}_0$ if it satisfies the condition:

Given arbitrary perturbations $\delta\bar{\sigma}_i, i = 1 \rightarrow N$
 Calculate $\delta\bar{y}_i = \Omega(\bar{\sigma}_0 + \delta\bar{\sigma}_i) - \Omega(\bar{\sigma}_0)$, for $i = 1 \rightarrow N$
 Then, $\Rightarrow \Omega(\bar{\sigma}_0 + \sum_{i=1}^N a_i \delta\bar{\sigma}_i) - \Omega(\bar{\sigma}_0) = \sum_{i=1}^N a_i \delta\bar{y}_i$ (2.5)
 for arbitrary a_i

The physical interpretation is for every cross-section perturbation, $\delta\bar{\sigma}_i$, the corresponding affect $\delta\bar{y}_i$ is obtained by running the code with the reference value and then again with cross-sections perturbed. The code can be run N times with each execution corresponding to a random cross-section perturbation, and then run with cross-sections perturbed by a linear combination of the previous N perturbations, i.e.

$$\bar{\sigma} = \bar{\sigma}_0 + \sum_{i=1}^N a_i \delta\bar{\sigma}_i \quad (2.6)$$

where a_i are arbitrary weights. If the model is linear, the perturbations should be approximately given by a linear combination of the original perturbations $\delta\bar{y}_i$, i.e.

$$\Omega\left(\bar{\sigma}_0 + \sum_{i=1}^N a_i \delta\bar{\sigma}_i\right) - \Omega(\bar{\sigma}_0) \approx \sum_{i=1}^N a_i \delta\bar{y}_i \quad (2.7)$$

The difference between the two approaches is used to qualitatively judge model linearity. It is assumed that the weights a_i summed over N equal 1.

This qualitative approach must be applied to all generated outputs. If at any time the output is judged non-linear over a range of uncertainties, in this case within 4 standard deviations of the mean, then the outputs would no longer be Gaussian. It was so determined that the ORIGEN model is nearly linear. Appendix B includes further graphical support by showing 1) linear changes in output isotopics over a range of cross section perturbations, and 2) Gaussian output of samples given Gaussian inputs.

2.4. Implementation of Stochastic Sampling Method

A linear model allows the implementation of either ESM or stochastic perturbation. Before discussing the implementation of the uncertainty propagation method, it is worthwhile to review the structure and origin of the covariance matrix, particularly as it exists in the SCALE library chosen as the data source for the majority of this work. The cross-section covariance matrix is given by:

$$\overline{\overline{C}}_{\sigma} = \begin{bmatrix} Cov(\sigma_1, \sigma_1) & Cov(\sigma_1, \sigma_2) & \cdots & Cov(\sigma_1, \sigma_n) \\ Cov(\sigma_1, \sigma_2) & Cov(\sigma_2, \sigma_2) & \cdots & \vdots \\ \vdots & \cdots & \ddots & \vdots \\ Cov(\sigma_n, \sigma_1) & \cdots & \cdots & Cov(\sigma_n, \sigma_n) \end{bmatrix} \quad (2.8)$$

where $Cov(\sigma_i, \sigma_j)$ is the absolute covariance between cross-sections i and j and is defined by:

$$Cov(\sigma_i, \sigma_j) = \int_{-\infty}^{\infty} (\sigma_i - \sigma_{i0})(\sigma_j - \sigma_{j0})p(\sigma_i, \sigma_j)d\sigma_i d\sigma_j \quad (2.9)$$

In this notation, subscripts i and j denote isotope, energy group, and reaction type dependence. Since the absolute values of the cross-sections will change for each unique problem, it is not convenient to work with this absolute covariance data. The relative covariance matrix, in which each element is between -1 and 1, will be useful for simplifying the perturbation method shown later and can be obtained by using:

$$C_{Rij} = \frac{Cov(\sigma_i, \sigma_j)}{\sigma_i \sigma_j} \quad (2.10)$$

to obtain [30]:

$$\overline{\overline{C}}_{R\sigma} = \begin{bmatrix} C_{R11} & C_{R12} & \cdots & C_{R1n} \\ C_{R21} & C_{R22} & \cdots & \vdots \\ \vdots & \cdots & \ddots & \vdots \\ C_{Rn1} & \cdots & \cdots & C_{Rnn} \end{bmatrix} \quad (2.11)$$

If given the sensitivity matrix of y with respect to σ , $\overline{\overline{S_R}}$, the uncertainty in the output parameters, $\overline{\overline{C_y}}$, can be evaluated as

$$\overline{\overline{C_y}} = \overline{\overline{S_R}} \overline{\overline{C_{R\sigma}}} \overline{\overline{S_R}}^T \quad (2.12)$$

In practice, these matrices or their products, are rarely directly constructed, but the effect of this product when using the forward perturbation with eigen-pair approach is evaluated as follows.

The singular value decomposition of $\overline{\overline{C_{R\sigma}}}$ is defined as:

$$\overline{\overline{C_{R\sigma}}} = \overline{\overline{W}} \overline{\overline{\Sigma_\sigma}} \overline{\overline{W}}^T \quad (2.13)$$

where $\overline{\overline{\Sigma_\sigma}}$ is the diagonal matrix of eigenvalues and $\overline{\overline{W}}$ the orthonormal matrix of eigenvectors where $\overline{\overline{W}} = [\overline{w_1}, \overline{w_2}, \dots, \overline{w_n}]$ and $\overline{w_i}^T \overline{w_j} = 0 \leftrightarrow i \neq j$.

Since this is a stochastic forward perturbation method, a form of Monte Carlo sampling is implemented. Each sample is a perturbation of each cross section, and that perturbation, γ_i , for cross-section i , is defined as follows [18]:

$$\gamma_i = \sum_{j=1}^n \xi_j (\overline{w_j})_i \quad (2.14)$$

where the value ξ_j is a random sample obtained from the eigenvalue Σ_{jj} having the Gaussian distribution defined as:

$$p(\xi_j)d\xi_j = \frac{1}{\sqrt{2\pi\Sigma_j}} \exp\left(\frac{-\xi_j^2}{2\Sigma_j}\right) d\xi_j \quad (2.15)$$

Finally, since the covariance data in the matrix $\overline{C_{R\sigma}}$ that was decomposed was relative data, any perturbed cross-section, σ_i , is simply:

$$\sigma_i = \sigma_{i0}(1 + \gamma_i) \quad (2.16)$$

where σ_{i0} denotes the unperturbed cross section. Perturbations are introduced thusly for all cross-sections $i = 1, \dots, n$. The matrix decomposition and creation of a set of input perturbations can be done a priori by auxiliary codes developed specifically for this purpose, thus sampling can use the model as a tool to produce perturbed results without modifying the model itself.

2.5. Implementation of the ESM

As indicated earlier, ESM methods are a favorable alternative to a stochastic forward perturbation when dealing with a large volume of input data, in this case a cross-section covariance matrix that is sparse and ill-conditioned, as required for ESM. The following section will describe the ESM method in brief but for the most detailed, rigorous, and formal definition, the reader is referred to H. Abdel-Khalik [14].

Consider n input data and m output data derived by using the model Ω . ESM states that for n inputs, at most n runs are required to fully characterize the distributions of the output, as opposed to stochastic methods which typically require a number of samples on the order of n . Define \bar{y} as the vector of m number densities calculated by:

$$\bar{y} = \bar{\Omega}(\bar{\sigma}) = \bar{y}_0 + \bar{\Omega}(\bar{\sigma} - \bar{\sigma}_0) + o\left((\bar{\sigma} - \bar{\sigma}_0)^2\right) \quad (2.17)$$

where $\bar{\sigma}$ are the n cross-section inputs. The second-order term can be ignored because of the linearity over the range of cross-section, and the matrix $\bar{\Omega}$, the Jacobi matrix, denotes the first derivatives of number density with respect to cross-cross section:

$$\left[\bar{\Omega}\right]_{ij} = \frac{\delta y_i}{\delta \sigma_j} \quad (2.18)$$

As stated before, the second moments of the input data are characterized by the covariance matrix, \bar{C}_σ , which can be decomposed as:

$$\bar{C}_\sigma = \bar{W} \bar{\Sigma}_\sigma \bar{W}^T \quad (2.19)$$

Then the second order moments of the output data are characterized by the covariance matrix

$$\bar{C}_y = \bar{\Omega} \bar{C}_\sigma \bar{\Omega}^T \quad (2.20)$$

Combing these yields:

$$\bar{C}_y = \bar{\Omega} \bar{W} \bar{\Sigma}_\sigma \bar{W}^T \bar{\Omega}^T = \bar{\Omega} \bar{W} \bar{\Sigma}_\sigma^{1/2} \left(\bar{\Omega} \bar{W} \bar{\Sigma}_\sigma^{1/2} \right)^T \quad (2.21)$$

The problem is that the matrix $\bar{\Omega}$ is not available a priori, and in practice is rarely calculated.

Stochastic methods build the values of \bar{C}_y by repeated sampling of perturbed inputs, where

as ESM directly calculates \bar{C}_y by the following:

$$\overline{\overline{C}}_y = \overline{\overline{Y}}_\Sigma \overline{\overline{Y}}_\Sigma^T \quad \text{where } \overline{\overline{Y}}_\Sigma = \begin{bmatrix} \overline{\delta y_{s1}} & \overline{\delta y_{s2}} & \dots & \overline{\delta y_{sr}} \end{bmatrix} \quad (2.22)$$

where r is the rank of the input data covariance matrix and the input perturbations are

$\overline{\delta \sigma} = s_j \overline{w_j}$, where s_j is the square root of the j^{th} diagonal element of $\overline{\overline{\Sigma}}_\sigma$, and $\overline{\delta y_{sj}}$ is given

by:

$$\overline{\delta y_{sj}} = \overline{\overline{\Omega}}(\overline{\sigma_0} + s_j \overline{w_j}) - \overline{\overline{\Omega}}(\overline{\sigma_0}), \quad j = 1, \dots, r \quad (2.23)$$

The j^{th} perturbations are along the j^{th} singular vector of the input covariance matrix and proportional to the j^{th} singular value. When repeated r times, this procedure propagates the second moments of the input data through the model, where r is the effective rank of the input covariance matrix $\overline{\overline{C}}_\sigma$, i.e. the number of singular values whose magnitudes are

considered sufficiently large to not ignore. $\overline{\overline{C}}_y$ can now be calculated directly and, if desired,

the singular value decomposition of $\overline{\overline{C}}_y$ can be obtained using $\overline{\overline{Y}}_\Sigma = \overline{\overline{U}}_\Sigma \overline{\overline{S}}_\Sigma \overline{\overline{V}}_\Sigma^T$:

$$\overline{\overline{C}}_y = \overline{\overline{Y}}_\Sigma \overline{\overline{Y}}_\Sigma^T = \overline{\overline{U}}_\Sigma \overline{\overline{S}}_\Sigma \overline{\overline{V}}_\Sigma^T \overline{\overline{V}}_\Sigma \overline{\overline{S}}_\Sigma \overline{\overline{U}}_\Sigma^T = \overline{\overline{U}}_\Sigma \overline{\overline{S}}_\Sigma^2 \overline{\overline{U}}_\Sigma^T \quad (2.24)$$

Implementing this within a pre-existing model is not impossible but requires a non-trivial effort and a mastery of both the linear algebra involved and computer code to perform those mathematic operations. The experiment which was used to validate this method within the simplified model and compare it to stochastic sampling created the set of $\overline{\delta y_{sj}}$ by elementary matrix operations executed in a separate program, using data especially for this one case. The model was then executed r times. The data was collected into matrices by an auxiliary code and then processed by MatLab 6.5 to calculate $\overline{\overline{C}}_y$ as described. The numerical results validating ESM as equivalent to the stochastic approach are presented later.

When ESM was used in the more detailed TRITON model, which operates on the 44-group cross sections, the methodology had to be formally implemented in a usable code. Mr. Matthew Jessee created a code that performs the above decomposition of the 44-group covariance library, \overline{C}_σ , provided with SCALE 5.0, and creates perturbed 44-group cross-section libraries that can be fed directly to the TRITON model. Mr. Jessee was gracious enough to provide this resource and explain its use. This code performs the singular value decomposition of the 44-group covariance matrix, block by block, where a block is considered to be the square sub-matrix containing a single nuclide-reaction pair, and also all other nuclide-reaction pairs related to it by available covariance data. In most cases, this is simply the 44 x 44 matrix for a particular nuclide and reaction combination since the covariance data is so sparse. The largest blocks occur for uranium and the transuranics, which have covariance data because their practical significance has warranted such studies. Further, those studies are of an experimental nature in which transuranics are often so dilute in the sample that their reactions are measured as ratios to the reactions of uranium, thus producing correlation data between those reactions. A simple post-processing code was then written to handle the calculation of \overline{C}_y .

2.6. Computational Models Employed for Each Method

As indicated in the introduction, this study will first use the SAS2H sequence and the ORIGEN depletion code in a simplified manner, and later the detailed TRITON sequence, all of which are available in the SCALE 5.0 package. The final model in this study uses the fast reactor code REBUS available from Argonne. For the simplified models, a particular fuel

type and geometry are modeled using the SAS2H sequence supplied with a 44-group master library provided with the SCALE package which contains cross section data along with resonance parameters, Bondarenko data, flux spectrum information, scattering matrices, specific radioactivity and decay heat constants for each isotope, etc. [30]. Table 2.3 shows a brief summary of the different fuel types used in this study. More explicit definitions will appear later in the Results section, with a more detailed description, and SAS2H and ORIGEN input decks for each of the fuels included in Appendix A.

Table 2.3: Brief Summary of Fuel Types Examined Using SAS2H + ORIGEN

Fuel Type	Reactor	Enrichment	Geometry
UOX	BWR	4.5 w/o	7 x7 square lattice
UOX	PWR	4.5 w/o	17 x 17 square lattice, 25 water holes
MOX	PWR	1.4 w/o U-235, 8 w/o Pu (65% fissile)	17 x 17 square lattice, 25 water holes
MOX	PWR	1.4 w/o U-235, 8 w/o Pu (65% fissile), 1 w/o Am, 1.5 w/o Np	17 x 17 square lattice, 25 water holes

SAS2H, when given the 44-group master library, produces 44-group flux spectra. The beginning of cycle fuel specific flux spectrum is used to collapse the 44-group covariance matrix to a 1-group covariance matrix for use in the stochastic sampling procedure described in Section 2.4. The result is a set of covariance data specific for the given fuel type being modeled. SAS2H also produces a transport updated 1-group, binary cross-section library on which the problem specific cross sections are now stored and will be used in the stand alone ORIGEN model. Note that the library for the simplified model accounts for only one representative burnup step across the life of the fuel. The following figures show the SAS2H flux spectra calculated for each of the models in Table 2.3 plotted with the typical LWR spectrum as well, where Figure 2.2 shows the PWR fuels for both

UOX and MOX, and Figure 2.3 shows the BWR fuel at various void fractions. Unlike the later TRITON model, fluxes from SAS2H are not normalized to the same fuel specific power density, but the input power applied to all materials in the model.

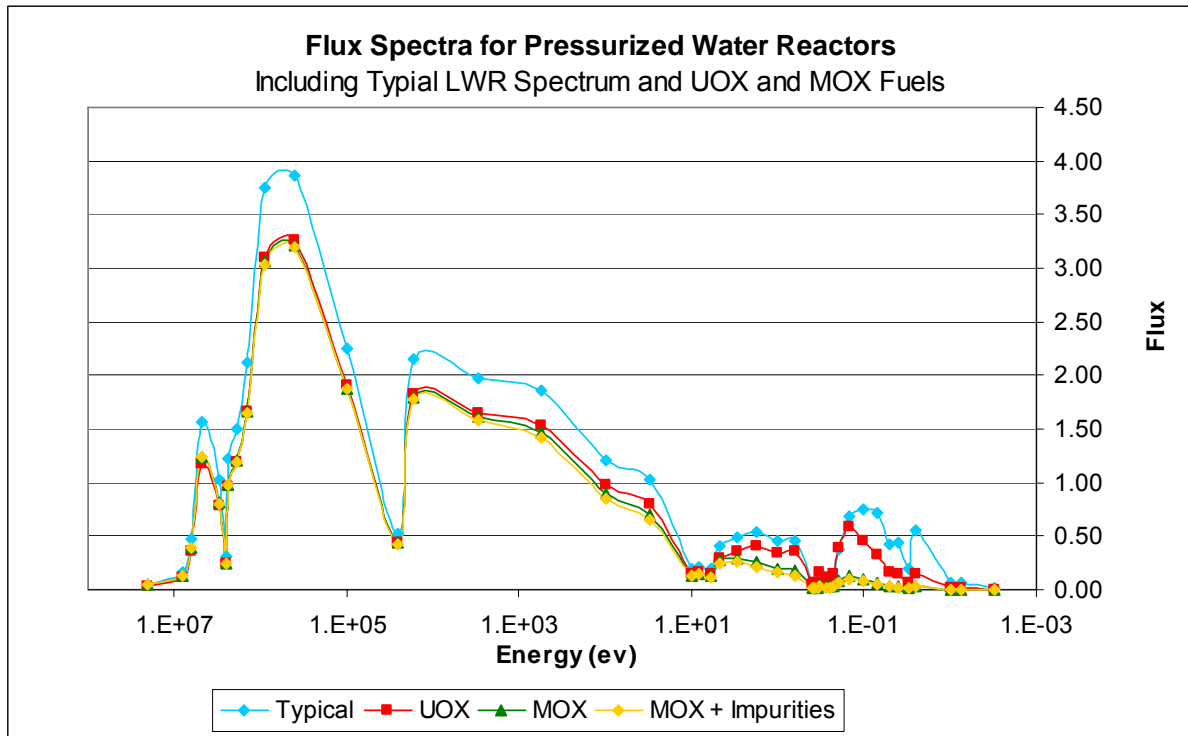


Figure 2.2: Flux Spectra for PWR Models

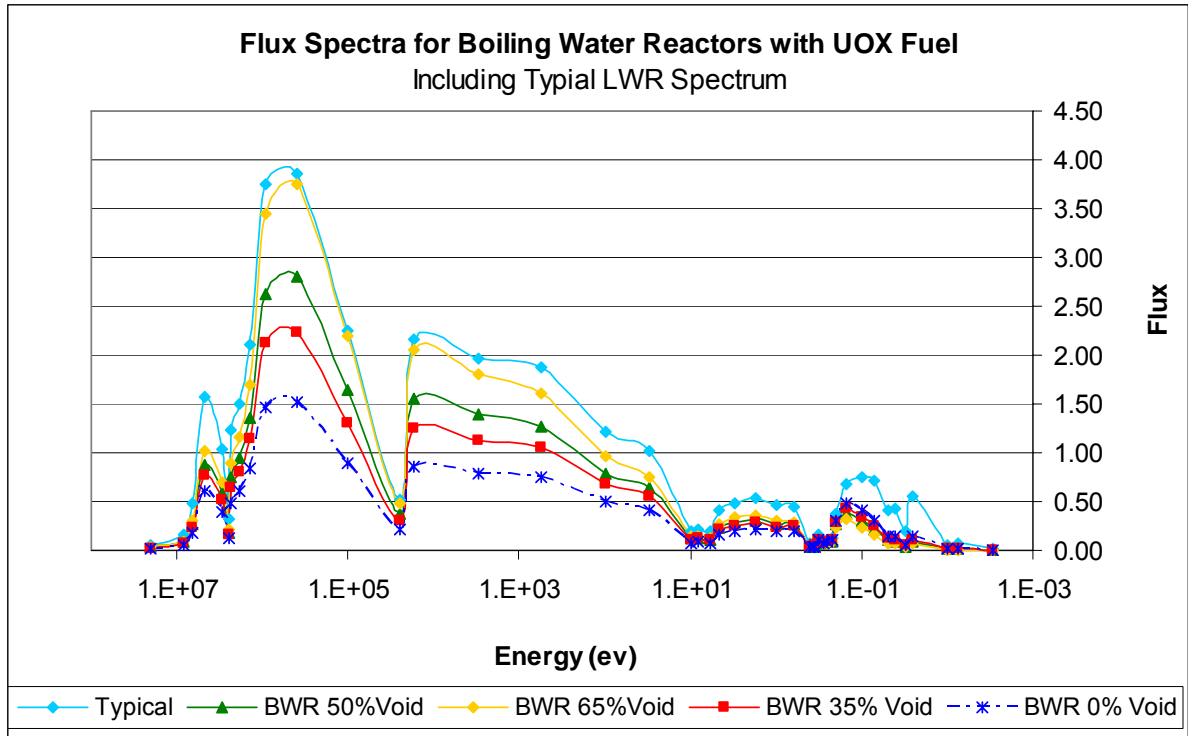


Figure 2.3: Flux Spectra for BWR Models

The stand-alone ORIGEN model is defined as 1 metric ton of the fuel modeled by SAS2H. ORIGEN depletes the model using the same power history and burnup as specified in the SAS2H model, then proceeds to decay the discharged isotopics over a series of time steps between discharge and 10,000 years, which covers the reprocessing time-frame through when waste canister failures are assumed in a waste repository. ORIGEN uses the fuel specific cross sections that were created by SAS2H for a specific fuel with a set of specific power cycle parameters. The nominal ORIGEN case, which is run with the unperturbed cross sections, creates the nominal values for the model. The nominal ORIGEN model is set to output not only the discharge isotopic masses, but also the isotopic and total values for each of the metrics of interest. Specific values for decay heat, activity, and toxicity can be obtained by dividing the metric by the mass or by directly printing the specific values from

the binary library. The ORIGEN model, into which perturbations are introduced, is set to determine only the masses, since they are all that will be needed for statistical evaluation, as will be described in the next section. One-group perturbations are created a priori for the stochastic sampling method for each fuel and for the ESM comparison experiment. The perturbations, as described in the previous sections, are then introduced directly into the cross sections as they are read into ORIGEN from the binary library by interrupting the code at that point and perturbing the cross-sections that covariance data are available for. A code was written to run ORIGEN for N samples and then acquire the number densities of the tracked nuclides from each sample (see Table 2.4) and group the results by the various decay times. The nuclides tracked are chosen mainly for their contribution to decay heat or toxicity, some of which are only chemically toxic rather than a producer of non-negligible radiation. Moreover, together the tracked nuclides represent greater than 95% of heat, radioactivity, and radiotoxicity for any time greater than 10 years for all of the fuels modeled in this work. A nominal execution of ORIGEN takes approximately eight seconds to execute on desktop PC and the sampling version that introduces perturbations takes approximately seconds to execute on the same platform.

Table 2.4: Isotopes Tracked for Analysis

Pb-210	Pa-231	U-238	Pu-240	Am-243	Se-79	Cs-134
Ra-226	U-234	Np-237	Pu-241	Cm-242	Sr-90	Cs-137
Ac-227	U-235	Np-239	Pu-242	Cm-244	Y-90	Ba-137m
Th-227	U-236	Pu-238	Am-241	Cm-245	Tc-99	
Th-230	U-237	Pu-239	Am-242m	C-14	I-129	

The TRITON model was used only for the fast reactors fuels and a validation for the pressurized water reactor fuel. For the purposes of this research, TRITON will be run as a stand-alone model using the 44-group master library as an input. The choice was made to

fully exploit TRITON's detailed modeling abilities as this was the natural progression from the cruder light water reactor models already described. For each of the fast reactor fuels modeled, and a 4.5 w/o uranium oxide fuel, detailed geometries of the unit cell and fuel composition defined by volume fractions were entered into the input. The biggest difference, besides going from simple ORIGEN depletion to a rigorous 2-D transport, was burning the fuel over 25+ smaller burnup steps with both cross-section and flux spectrum updates for each step as opposed to a single, representative step employed in the ORIGEN model with only one cross section update at mid-point of that step. At the end of the TRITON execution, the discharge number densities of the same isotopes are decayed using the same time steps as in previous models.

Table 2.5: Brief Summary of Fuel Types Examined Using TRITON

Fuel Type	Reactor	Enrichment	Geometry
UOX	PWR	4.5 w/o	17 x 17 square lattice, 25 water holes
Actinide, metal	FR, CR=0.25	59.2 w/o transuranics, 20 w/o zirconium	217 pin hexagonal lattice
Actinide, metal	FR, CR=0.70	20.6 w/o transuranics, 10 w/o zirconium	169 pin hexagonal lattice
Actinide, metal	FR, CR=1.05	16.2 w/o transuranics, 10 w/o zirconium	127 pin hexagonal lattice

Since TRITON takes approximately twenty to thirty seconds per burnup step to execute and has, in principle, 44 times as much input data, it is apparent that stochastic sampling is not a reasonable method to use with this model. Not only does TRITON take longer to execute, but it also uses the 44-group master cross section library as input and thus the 44-group covariance library as a source for perturbations. The principles of Monte Carlo sampling indicate that many thousands of samples would have to be run to properly propagate the uncertainties. In going from 1-group to 44-group covariance data the effective

rank of the covariance matrix increased from 223 to 1938, with cutoff criteria imposed on singular values with a magnitude less than 10^{-6} relative to the reference cross section. So even ESM will require the execution of the code 1938 times, but this is still far less than computationally taxing than running over 3000 samples which is on the order of the input data. For each sample set, perturbations according to the ESM method are introduced directly into the 44-group master library, using a code generously provided by Mr. Jessee, and a new perturbed library is created which is subsequently input to the TRITON model. It was concluded that the primary depletion model is nearly linear from the linearity study of ORIGEN, but in order to confidently avoid non-linearities that may arise if cross sections are perturbed outside the linear region, instead of multiplying by the square root of the eigenvalue, the perturbation is scaled by a scaling factor, $SCF = 0.07$, divided by the infinity norm of the eigenvector being used in a particular sample.

$$\bar{\sigma} = \bar{\sigma}_0 \left(I + \frac{SCF}{\|w_i\|_\infty} w_i \right) \quad (2.25)$$

The scaling factor and infinity norm are divided out in post processing, and the singular value is multiplied back into the output when computing the covariance matrix of the output.

$$\delta y_i = \left[\Omega \left(\bar{\sigma}_0 + \frac{SCF}{\|w_i\|_\infty} w_i \right) - \Omega(\bar{\sigma}_0) \right] \frac{\|w_i\|_\infty}{SCF} \quad (2.26)$$

$$\bar{C}_y = \left(\bar{Y}_\Sigma \bar{\Sigma}^{1/2} \right) \left(\bar{Y}_\Sigma \bar{\Sigma}^{1/2} \right)^T \quad (2.27)$$

The covariance matrix for output isotopics directly provides the uncertainty information needed for this study, namely the standard deviation of each isotope tracked.

The ESM sampling method was similarly implemented in REBUS by Dr. Abdel-Khalik. Both TRITON and REBUS will be used for modeling recycling of the fast reactor fuel corresponding to the conversion ratio of about 0.70. As discussed before, given material feeds and reprocessing parameters, REBUS does this automatically. A external procedure is developed and implemented for TRITON to emulate this recycling methodology. That procedure is described in the following section. The recycle procedure of taking all the fast reactor transuranics and combining them with spent LWR fuel is that which is outlined in Argonne’s ABTR Preconceptual Design Report [26].

2.7. TRITON Recycle Methodology

Having evaluated the resulting isotopic covariance matrices for once-through fuels in both thermal and fast reactors, our attention turns to a recycling scheme. The recycling scheme creates a transuranic fuel, made of spent LWR fuel, burns it in a fast reactor, and then recycles that fuel back into the fast reactor, making up part of the fuel mass by adding more spent LWR fuel to the mix. The transuranics recycled are Np-237, Np-239, Pu-238, Pu-239, Pu-240, Pu-241, Pu-242, Am-241, Am-242m, Am-243, Cm-242, Cm-244, and Cm-245. The first step is to create a nominal recycle case by taking mass $M_{FR}^{Recycle}$ from 1.5 year decayed fast reactor fuel and adding mass M_{LWR} from 10 yr decayed thermal reactor fuel (burnup of 33 GWD/MTU and an original enrichment of 3.3 w/o) and mass M_{DU} from a depleted uranium source to create a new fuel having the same volume loading as the original fuel, and thus approximately the same total heavy metal mass, given by:

$$M_{FR}^{BOL} = M_{FR}^{Recycle} + M_{LWR}^{Recycle} + M_{DU} \quad (2.28)$$

Here, an assumption about the type of reprocessing is made, e.g. UREX, perfect separation, etc. In this work, all the transuranics from the spent fast reactor fuel are added back and enrichment made up by LWR spent fuel transuranics, $M_{LWR}^{Recycle}$, with the remaining mass being depleted uranium, M_{DU} . To obtain the additional equation required to solve for $M_{LWR}^{Recycle}$ and M_{DU} , it is required that the composition of M_{FR}^{BOL} be such so as to achieve the cycle energy requirement. $M_{FR}^{Recycle}$ is therefore all the mass of the recycled fuel extracted after M_{FR}^{BOL} is burnt and reprocessed. This implies the following relationship:

$$M_{FR}^{BOL} - M_{FR}^{Recycle} = M_{LWR}^{Recycle} + M_{DU} \quad (2.29)$$

The depleted uranium is assumed to have a fixed isotopic composition of 99.8 w/o U-238 and 0.2 w/o U-235. Further, the isotopic compositions of the LWR and FR fuels are known as well, so that when the masses are combined, masses of individual isotopes add. Since the TRITON model requires input isotopics to be in w/o, M_R must be expanded in terms of its composition, completed as now explained. Treat the mass as a vector composed of isotopes

from element k : $\overline{M_{FR,k}^{BOL}}$. Convert the masses in $\overline{M_{FR,k}^{BOL}}$ to weight percents by $\frac{\overline{M_{FR,k}^{BOL}}}{\left\| \overline{M_{FR,k}^{BOL}} \right\|_1}$, where

the one-norm is the sum of the masses of all isotopes of element k . The last expression gives the isotopic data for element k that will be input to the TRITON model. This process is repeated for each element k . For this experiment, the discharged isotopics and end of life k-effective values from the initial fresh fuel TRITON input are taken to be the target values, despite k-effective being greater than 1. The output data from the unperturbed TRITON model are considered to be the nominal values for each recycle step. The k-effective values

are not only recorded for statistical analysis, but are also used to adjust the transuranic enrichment for the next recycle, in an effort to maintain the end of life k-effective value.

Next, let $\overline{\overline{C}}_{LWR}^{Re\ cycle}$ and $\overline{\overline{C}}_{FR}^{Re\ cycle}$ be the absolute isotopic covariance matrices of the once-through thermal and fast reactors, respectively, and converted, if necessary, from their relative values to units of mass. The fast reactor data are taken 1.5 years after discharge and the thermal reactor data are taken at 10 years of decay, i.e. time lapse to recycle. These matrices are 13 x 13 containing number density uncertainties for the transuranics already mentioned. These two matrices are the results of earlier work with each of these fuel types using the TRITON model with our ESM approach to propagate uncertainties due to cross-sections. We now wish to recycle the fuel characterized by these uncertainties.

The masses of each isotope of each element in each fuel stream is perturbed separately using $\overline{\overline{C}}_{LWR}^{Re\ cycle}$ and $\overline{\overline{C}}_{FR}^{Re\ cycle}$, via the ESM method. Each matrix is decomposed such that:

$$\overline{\overline{C}}^{Re\ cycle} = \overline{\overline{W}}^{Re\ cycle} \overline{\overline{\Sigma}}^{Re\ cycle} \overline{\overline{W}}^{Re\ cycle T} \quad (2.30)$$

Perturbations are introduced into the masses of the 13 isotopes in that fuel stream by scaling a singular vector by the square root of the corresponding singular value and adding this perturbation vector to the mass vector. These perturbed isotopics are then used to satisfy equation 2.29, just as the unperturbed values would be. Finally, just as in the unperturbed case, the masses of each element are converted to weight percents as required by TRITON's input structure, and a perturbed input written for the model.

Finally, uncertainty is propagated by running the model to equilibrium several times, each time choosing a subsequent singular pair to perturb with, i.e. perturbing along $w_1, w_2,$

etc. with each new run of the model. Experimentation revealed that only the first six singular pair perturbations needed to be run to effectively propagate the uncertainty, which is in accordance with the theory of ESM. The above procedure is repeated each time the fuel is recycled, thus creating a new $\overline{C_{FR}^{BOL}}$ and a new decomposition to perturb by, for each recycle step.

The resulting recycled fuel nuclei number density uncertainties are combined with the nuclei number density uncertainties due to cross-section uncertainties into a single uncertainty vector, $\overline{\sigma_{TOTAL}}$, where the elements of the vector denote different isotopes. Experience showed that nuclei number density uncertainties due to cross-section uncertainties changed little unless major compositional changes are made to the fuel (see Results section). In the following, the subscript *FR* denotes recycled fuel nuclei number density uncertainties at EOL originating from the uncertainty of the material making up the fuel independent of cross section uncertainties, and the subscript *XS* denotes fuel nuclei number density uncertainties at EOL originating from cross-section uncertainties:

$$\left(\overline{\sigma_{TOTAL}}\right)_i = \sqrt{\left(\overline{\sigma_{XS}}\right)_i^2 + \left(\overline{\sigma_{FR}}\right)_i^2 + 2\left(\overline{\sigma_{XS}}\right)_i \left(\overline{\sigma_{FR}}\right)_i \left(\rho_i\right)} \quad (2.31)$$

where ρ is a correlation between the two uncertainties. Having the total uncertainty on the recycled fuel composition at equilibrium, the mass uncertainties, and in turn the key metrics uncertainties, for any given discharged fuel that will be sent to permanent disposal can be computed. Values of operational parameters (e.g. k-effective) can be collected from the model both at equilibrium and between recycle steps, and the uncertainties on those parameters computed as well.

Since the cross section originated uncertainties on EOL isotopics affect the subsequent reload isotopics, there must be correlation. However, within the scope of this work, it is assumed that $\rho = 0$, because the only foreseeable method to obtain that correlation with the TRITON model is a posteriori calculation from the results of running the possible cross-section uncertainties with each of the possible recycle nuclei number density uncertainties, through equilibrium. This task is currently too computationally taxing as it would require execution time of (15 minutes per execution)($r_{XS} + 1$)($r_R + 1$)(6+1) times, where 1 is for the nominal case and r_{XS} and r_R are the effective ranks of the covariance matrices for cross-sections and recycled isotopics, respectively.

2.8. Statistical Analysis Performed on Results

The forward perturbation sampling process produces a large group of data for each fuel type; these raw data are in a form in which it can be processed using rudimentary statistical methods. The ESM sampling method directly calculates the covariance matrix of the isotopics in post processing, as already discussed, so much of this section applies only to the simplified ORIGEN models rather than the TRITON and REBUS models. First, the unperturbed values of the fuel sample produced by ORIGEN -- isotopics and total heat, radioactivity and radiotoxicity -- using the problem specific cross-sections provided by the SAS2H model are, by definition, the mean and most likely values for the particular model. For the thirty-three nuclides tracked, there are N samples of isotopic masses at discharge and 1, 5, 10, 50, 100, 500, 1000, 2500, 5000, and 10000 years of decay. The values at discharge and 1 year are neglected in the statistical analysis as many very-short lived isotopes present at this time contribute much of the heat load in the first 1 year or so until they die off. Thus,

the thirty three nuclides tracked would not cover greater than 95% of the heat, etc. that is of interest. This is practically justified by the fact that the fuel will be closely monitored and guarded in wet storage for at least the first five years, and this work is mainly concerned with the affects on the repository and reprocessing aspects which take place later.

Basic statistics are applicable to this data because all the metrics are linearly and directly proportional to mass, therefore each have specific values. Each isotope tracked has some specific constant for heat [W/g], activity [Ci/g], and radiotoxicity [(m³ air or water to dilute to acceptable leve) / g]. The statistical process is justified by the equation:

$$\mu_y = \left(\frac{dy}{dx} \right) \mu_x \quad (2.32)$$

which states that the uncertainty in a parameter y that is dependent upon parameter x is simply the derivative of the relationship that relates the two times the uncertainty in x [28]. For all the metrics of interest, a change in the metric is simply the change in mass times the specific value for that metric. All that is needed, therefore, are the statistics of the isotopic masses which can be translated to the metrics by means of these specific values, which are given in Table 2.6.

Table 2.6: Specific values, per nuclide, for metrics of interest.

Nuclide	Ci/Gram	Heat/Gram (W)	m³ Air/g	m³ Water/g
pb210	7.6376E+01	1.7901E-02	NA	NA
ra226	9.8912E-01	2.8565E-02	NA	NA
ac227	7.2373E+01	3.5003E-02	2.3886E+16	NA
th227	3.0749E+04	1.1235E+03	1.8412E+17	NA
th230	2.0627E-02	5.8238E-04	1.2352E+12	NA
pa231	4.7253E-02	1.4378E-03	3.9708E+12	NA
u234	6.2204E-03	1.7905E-04	3.5144E+10	1.6456E+04
u235	2.1624E-06	5.9912E-08	1.1033E+07	5.4884E+00
u236	6.4706E-05	1.7521E-06	3.3701E+08	1.6423E+02
u237	8.1658E+04	1.5809E+02	9.3110E+13	3.3604E+09
u238	3.3633E-07	8.5129E-09	1.6170E+06	8.1832E-01
np237	7.0521E-04	2.0119E-05	2.1177E+10	4.1977E+03
np239	2.3206E+05	5.8682E+02	1.3896E+14	1.0046E+10
pu238	1.7132E+01	5.6779E-01	1.1271E+15	2.1309E+08
pu239	6.2072E-02	1.9291E-03	4.4656E+12	8.3881E+05
pu240	2.2708E-01	7.0707E-03	1.6336E+13	3.0686E+06
pu241	1.0343E+02	3.2868E-03	1.4266E+14	2.6864E+07
pu242	3.9558E-03	1.1682E-04	2.6025E+11	5.1307E+04
am241	3.4309E+00	1.1448E-01	1.9718E+14	3.7091E+07
am242m	1.0481E+01	4.2370E-03	5.7904E+14	1.0760E+08
am243	1.9969E-01	6.4285E-03	1.1476E+13	2.1588E+06
cm242	3.3124E+03	1.2085E+02	1.1705E+16	2.1509E+09
cm244	8.0981E+01	2.8322E+00	2.7733E+15	5.2585E+08
cm245	1.7177E-01	5.7170E-03	1.0224E+13	1.9497E+06
c 14	4.4584E+00	1.3074E-03	1.5535E+10	NA
se 79	1.5362E-02	5.0813E-06	6.2704E+07	2.4079E+03
sr 90	1.4117E+02	1.6393E-01	1.3574E+13	2.1357E+08
tc 99	1.7114E-02	8.5821E-06	1.3370E+08	5.9217E+02
i129	1.7659E-04	8.2592E-08	1.0149E+07	1.0512E+03
cs137	8.7021E+01	9.6718E-02	2.0380E+12	6.1282E+07
ba137m	5.3801E+08	2.1138E+06	NA	5.3801E+08
y90	5.4342E+05	3.0086E+03	4.8957E+14	7.9331E+10
cs134	1.2944E+03	1.3197E+01	1.5521E+13	1.3290E+09

For each isotope tracked, the sample mean, μ_m and sample standard deviation, Σ_{SD} are calculated using the equations below [28].

$$\mu_m = \frac{1}{N} \sum_{i=1}^N x_i \quad (2.33)$$

$$\Sigma_{SD} = \sqrt{\frac{1}{N-1} \sum_{i=1}^N (x_i - \mu_m)^2} \quad (2.34)$$

The standard deviation of the isotopic masses is the key metric needed for the analysis. Thus it must be justified that the standard deviation calculated is from a reasonably accurate sample. Comparison is made between the sampled mean and the true mean in terms of the expected standard deviation of the mean, Σ_m , calculated by:

$$\Sigma_m = \frac{\Sigma_{SD}}{\sqrt{N}} \quad (2.35)$$

This is a modification of the Central Limit Theorem, where the value of the mean of the sample is expected to deviate from the true value for a finite number of samples [28]. If the difference between the sampled mean and the true mean is within two or fewer standard deviations of the mean, the sample can be said to be reasonable. Finally, the convergence of the mean and the standard deviation are examined, i.e. after how many samples do they reach a nearly constant value. Those values tended toward 200 for the mean and 220-250 for the standard deviation so $N = 300$ samples is adequate. The standard deviation of the mass translates directly into uncertainties for each of the metrics observed, i.e. +/- 5% in mass produces +/- 5% in heat, etc. Also, consider the objective of a 95% confidence interval, using the student-t distribution, the standard deviation is multiplied by 1.96 to obtain the 95% confidence interval rather than just one standard deviation which provides approximately 68% confidence [28].

Next, the affect of the uncertainty on the total values is examined. The resulting uncertainties, μ_R , are propagated by the square root of the sum of the squares [28]:

$$\mu_R = \sqrt{\sum_{i=1}^L \mu_{m,i}^2} \quad (2.36)$$

where L is the number of parameters, i.e. tracked nuclides. This equation, by definition, assumes that there is no correlation between each isotopic metric, e.g. the heat produced by plutonium does not affect the heat produced by strontium. This produces a total uncertainty in that metric as contributed by the nuclides tracked, which can be compared to the nominal value of that metric for the particular fuel type and decay time. This is done not only to see how much uncertainty is imparted to the metric by the uncertainties of these isotopes, but also to verify that in tracking the specific 33 nuclides at least 95% of the total heat, etc. for that discrete point in time is observed.

Finally, for the fast reactor fuels modeled in TRITON and REBUS, the isotopics covariance matrix was constructed using the algorithm discussed in Section 2.5. The square roots of the diagonal elements represent the standard deviations of each of the tracked nuclides, equivalent to the standard deviations calculated from stochastic sampling. Also, in the TRITON results, the sub-matrix containing the actinides Np-237 through Cm-244 is extracted to be used for uncertainty propagation when examining recycling of fast reactor fuels.

3. Numerical Results

3.1. *Simplified ORIGEN Models*

3.1.1. Equivalency of ESM and Stochastic Methods

The essential benefit of ESM is that it will produce the same results as stochastic sampling and will work efficiently in models where stochastic methods would be impractical to implement. To verify this numerically, both ESM and the full stochastic sampling are implemented for the simplified PWR model, which is simple enough to allow either method. The 1-group covariance matrix is decomposed and 223 perturbations (rank = 223) are created according to the formulas already discussed. Perturbations are introduced directly within ORIGEN, using the cross section library made by SAS2H for the PWR fuel. Considering the time required to implement this method versus the fast execution time of the simple stochastic model, ESM is not well suited to small, simple models. In more sophisticated models where the runtime increases greatly and stochastic methods are not practical, however, ESM becomes worth the time it takes to implement. Table 3.1 presents the comparison of the isotopics' uncertainties predicted by each method and Table 3.2 gives the nominal discharge isotopics for this model for reference. It is clear from these results that the two methods are producing equivalent results, as expected. A further look at the simplified PWR model is included in the next section. Note here, and in subsequent sections, only the discharge isotopics and the isotopic uncertainties for each model will be presented, as number density vs. time is calculated from the decay of the discharge isotopics. A larger, generalized results table for decay heat, radioactivity, radiotoxicity, and uncertainty

contributors is available for each model, but due to their size, have been included in Appendix C and the reader is referred to that section. The tables included there appear in the order in which models are presented in the main text.

Table 3.1: Comparison of isotopic uncertainties from the two methods.

Nuclide	% Uncertainty	
	Stochastic	ESM
pb210	1.1951	1.1477
ra226	1.3548	1.3008
ac227	0.4805	0.4575
th227	0.4805	0.4578
th230	1.4910	1.4327
pa231	0.5177	0.4957
u234	1.5787	1.5193
u235	1.3125	1.3377
u236	0.7124	0.7017
u237	2.5207	2.5509
u238	0.0775	0.0759
np237	0.6054	0.6158
np239	13.6428	13.8702
pu238	1.0497	1.0579
pu239	0.8064	0.8851
pu240	2.5656	2.7661
pu241	2.5207	2.5509
pu242	2.5983	2.6248
am241	2.5016	2.5345
am242m	2.1720	2.2293
am243	13.6428	13.8698
cm242	2.1717	2.2289
cm244	11.3402	11.6702
cm245	10.2508	10.5995
c 14	0.4523	0.4900
se 79	0.3663	0.3825
sr 90	0.3748	0.3853
tc 99	1.9704	1.8803
i129	0.4186	0.4487
cs137	0.3822	0.3986
ba137m	0.3822	0.3988
y90	0.3748	0.3857
cs134	1.1380	1.2094

Table 3.2: Discharge isotopics for the PWR simplified model.

Discharge Isotopics, grams / MTHM					
pb210	2.415E-11	np237	5.538E+02	cm244	3.215E+01
ra226	1.628E-08	np239	8.925E+01	cm245	1.208E+00
ac227	3.443E-09	pu238	1.791E+02	c 14	3.335E-03
th227	1.014E-11	pu239	5.466E+03	se 79	5.817E+00
th230	1.140E-03	pu240	1.887E+03	sr 90	6.899E+02
pa231	3.116E-04	pu241	1.575E+03	tc 99	9.577E+02
u234	1.530E+02	pu242	5.576E+02	i129	1.741E+02
u235	1.233E+04	am241	4.302E+01	cs137	1.485E+03
u236	5.524E+03	am242m	9.197E-01	ba137m	2.283E-04
u237	1.346E+01	am243	1.162E+02	y90	1.866E-01
u238	9.298E+05	cm242	1.346E+01	cs134	1.439E+02

3.1.2. PWR Model with UOX Fuel

The following data are for a representative UOX fuel that is burned in a pressurized water reactor. An updated cross-section library is created using SAS2H for one representative burnup step, and the resulting 1-group working library used with ORIGEN. The 44-group covariance library is collapsed to 1-group using the beginning of cycle flux spectrum for this fuel, and stochastic sampling is implemented. The UOX fuel is 4.5 w/o and burned to 40 GWD/MTU in a single cycle representative of a once-through fuel. The geometry is a 17x17 Westinghouse fuel assembly with no burnable poison elements and 25 water holes with one being an instrumentation hole; adapted from Gauld [21]. See Appendix A for a more detailed description of this model. Since the discharge isotopics and the isotopic uncertainties for this model have already been presented in the previous section, and the results table is available in Appendix C, the discussion moves on to the separation study of this fuel.

This simple experiment examines the affect of decay heat uncertainties in the process of UOX fuel separation, a key aspect of fuel reprocessing. The simple model 4.5 w/o UOX that was burned to 40 GWD/MTU is decayed in three separate cases for 5, 10 and 25 years

(Table 3.3). At each individual time the uranium, plutonium, neptunium, americium, and curium were separated out by elemental species (henceforth referred to as lumps) with assumed 100% separation efficiency. The lumps were then decayed over the 10,000 year time, regardless of the lump's separation time or decay products. The heat load of each of these lumps is compared with the heat load of the total fuel assembly over the same decay time. The same process is then repeated for the masses plus one standard deviation of the isotopic uncertainties which propagates the uncertainty associated with each separation time. Table 3.4 shows these decays heat loads for the first 1000 years and Table 3.5 shows 2,500 to 10,000 years (see the Appendix A for a more detailed description of this model). As data shows, the majority of the long term heat load resides with the decaying of actinides. If these can be burned off in some reprocessing scheme, margin to the taxing heat limits on the repository could be realized. This experiment provides some insight for the more rigorous experiment of uncertainty propagation in recycled fast reactor fuel.

Table 3.3: Masses, with uncertainty, of actinides at 3 decay times.

Nuclide	Mass at 5 Years		Mass at 10 Years		Mass at 25 Years	
	Grams	+/-	Grams	+/-	Grams	+/-
u234	1.60E+02	2.53E+00	1.67E+02	2.64E+00	1.87E+02	2.96E+00
u235	1.23E+04	1.62E+02	1.23E+04	1.62E+02	1.23E+04	1.62E+02
u236	5.53E+03	3.94E+01	5.53E+03	3.94E+01	5.53E+03	3.94E+01
u237	3.75E-05	9.45E-07	2.95E-05	7.42E-07	1.43E-05	3.60E-07
u238	9.30E+05	7.21E+02	9.30E+05	7.21E+02	9.30E+05	7.21E+02
np237	5.69E+02	3.44E+00	5.73E+02	3.47E+00	5.95E+02	3.60E+00
np239	1.00E-04	1.37E-05	1.00E-04	1.37E-05	9.99E-05	1.36E-05
pu238	1.87E+02	1.96E+00	1.80E+02	1.88E+00	1.60E+02	1.67E+00
pu239	5.56E+03	4.48E+01	5.55E+03	4.48E+01	5.55E+03	4.48E+01
pu240	1.89E+03	4.85E+01	1.90E+03	4.86E+01	1.90E+03	4.88E+01
pu241	1.24E+03	3.12E+01	9.72E+02	2.45E+01	4.71E+02	1.19E+01
pu242	5.58E+02	1.45E+01	5.58E+02	1.45E+01	5.58E+02	1.45E+01
am241	3.79E+02	9.49E+00	6.41E+02	1.60E+01	1.12E+03	2.80E+01
am242m	8.97E-01	1.95E-02	8.76E-01	1.90E-02	8.13E-01	1.77E-02
am243	1.16E+02	1.59E+01	1.16E+02	1.59E+01	1.16E+02	1.58E+01
cm242	8.07E-03	1.75E-04	2.28E-03	4.96E-05	2.12E-03	4.60E-05
cm244	2.66E+01	3.02E+00	2.20E+01	2.49E+00	1.24E+01	1.40E+00
cm245	1.21E+00	1.24E-01	1.21E+00	1.24E-01	1.21E+00	1.24E-01

Table 3.4: Comparison of separation at 3 times vs. no separation, first 1000 years of decay.

Element	If Separated At 5 Years After Discharge, a 4.5 w/o Burned for 40 GWD/MTU, (Note: times below are after separation)							
	50 (55) Years		100 (105) Years		500 (505) Years		1000 (1005) Years	
	W	+/- W'	W	+/- W'	W	+/- W'	W	+/- W'
U	0.049	0.001	0.049	0.001	0.049	0.001	0.049	0.001
Np	0.012	0.000	0.012	0.000	0.012	0.000	0.013	0.000
Pu	218.010	4.235	195.781	4.025	91.127	2.085	52.097	1.136
Am	41.217	1.102	38.110	1.026	20.348	0.589	9.513	0.319
Cm	11.264	0.310	1.823	0.050	0.186	0.005	0.179	0.005

Element	If Separated At 10 Years After Discharge, a 4.5 w/o Burned for 40 GWD/MTU, (Note: times below are after separation)							
	50 (60) Years		100 (110) Years		500 (510) Years		1000 (1010) Years	
	W	+/- W'	W	+/- W'	W	+/- W'	W	+/- W'
U	0.050	0.001	0.050	0.001	0.050	0.001	0.051	0.001
Np	0.013	0.000	0.013	0.000	0.013	0.000	0.013	0.000
Pu	188.917	3.590	167.357	3.374	76.953	1.739	45.779	0.981
Am	68.819	1.792	63.588	1.662	33.770	0.925	15.538	0.471
Cm	9.302	1.033	1.506	0.167	0.156	0.016	0.149	0.015

Element	If Separated At 25 Years After Discharge, a 4.5 w/o Burned for 40 GWD/MTU, (Note: times below are after separation)							
	50 (75) Years		100 (125) Years		500 (525) Years		1000 (1025) Years	
	W	+/- W'	W	+/- W'	W	+/- W'	W	+/- W'
U	0.054	0.001	0.054	0.001	0.054	0.001	0.054	0.001
Np	0.013	0.000	0.013	0.000	0.013	0.000	0.013	0.000
Pu	131.727	1.327	112.187	1.425	50.156	1.033	33.859	0.677
Am	119.336	3.064	110.214	2.835	58.356	1.542	26.584	0.747
Cm	5.274	0.516	0.857	0.083	0.093	0.008	0.090	0.008

Element	1MT of Fuel After Discharge, a 4.5 w/o FA Burned for 40 GWD/MTU, (Note: times below are after irradiation)							
	50 Years		100 Years		500 Years		1000 Years	
	W	+/- W'	W	+/- W'	W	+/- W'	W	+/- W'
FUEL	662.820	19.380	356.663	8.038	112.558	4.262	62.215	1.999

Table 3.5: Comparison of separation at 3 times vs. no separation, 2500 – 10,000 years of decay.

Element	If Separated At 5 Years After Discharge, a 4.5 w/o FA Burned for 40 GWD/MTU, (Note: times below are after separation)					
	2500 (2505) Years		5000 (5005) Years		10000 (10005) Years	
	W	+/- W'	W	+/- W'	W	+/- W'
U	0.051	0.001	0.056	0.001	0.065	0.001
Np	0.013	0.000	0.013	0.000	0.014	0.000
Pu	23.033	0.413	17.347	0.281	12.833	0.187
Am	1.481	0.112	0.604	0.079	0.439	0.059
Cm	0.154	0.004	0.119	0.003	0.071	0.002

Element	If Separated At 10 Years After Discharge, a 4.5 w/o FA Burned for 40 GWD/MTU, (Note: times below are after separation)					
	2500 (2510) Years		5000 (5010) Years		10000 (10010) Years	
	W	+/- W'	W	+/- W'	W	+/- W'
U	0.053	0.001	0.057	0.001	0.067	0.001
Np	0.013	0.000	0.013	0.000	0.014	0.000
Pu	22.472	0.399	17.343	0.280	12.833	0.187
Am	2.029	0.128	0.619	0.081	0.444	0.060
Cm	0.129	0.013	0.100	0.010	0.060	0.006

Element	If Separated At 25 Years After Discharge, a 4.5 w/o FA Burned for 40 GWD/MTU, (Note: times below are after separation)					
	2500 (2525) Years		5000 (5025) Years		10000 (10025) Years	
	W	+/- W'	W	+/- W'	W	+/- W'
U	0.056	0.001	0.061	0.001	0.072	0.001
Np	0.013	0.000	0.014	0.000	0.015	0.000
Pu	21.410	0.372	17.332	0.280	12.828	0.186
Am	3.037	0.151	0.647	0.081	0.456	0.059
Cm	0.078	0.007	0.061	0.005	0.036	0.003

	1MT of Fuel After Discharge, a 4.5 w/o FA Burned for 40 GWD/MTU, (Note: times below are after irradiation)					
	2500 Years		5000 Years		10000 Years	
	W	+/- W'	W	+/- W'	W	+/- W'
FUEL	24.808	0.594	18.184	0.446	13.460	0.281

3.1.3. Typical LWR with UOX Fuel

The SCALE package comes with a prepared “test” card-image cross-section library that is ideally representative of a typical LWR. The following data depict a uranium oxide fuel depleted, with stochastic sampling, in ORIGEN using this typical LWR cross section library provided with SCALE, and the typical LWR flux spectrum (also provided) to collapse the 44-group covariance library. The UOX fuel is 4.5 w/o and burned to 40 GWD/MTU in a single representative burnup step divided into depletion intervals by default in ORIGEN (see the Appendix A for a more detailed description of these models). While in terms of isotopics, the model produced similar results to the PWR model as expected (Table 3.6), the uncertainties using the typical flux spectrum tended to over predict those obtained from the PWR model (Table 3.7).

Table 3.6: Discharge isotopics for typical LWR simplified model.

Discharge Isotopics, grams / MTHM					
pb210	2.113E-11	np237	4.696E+02	cm244	1.930E+01
ra226	1.641E-08	np239	8.942E+01	cm245	7.951E-01
ac227	3.114E-09	pu238	1.343E+02	c 14	3.343E-03
th227	8.370E-12	pu239	4.863E+03	se 79	5.895E+00
th230	1.164E-03	pu240	2.193E+03	sr 90	7.127E+02
pa231	3.159E-04	pu241	1.245E+03	tc 99	9.754E+02
u234	1.049E+04	pu242	4.435E+02	i129	1.690E+02
u235	1.547E+02	am241	3.190E+01	cs137	1.488E+03
u236	5.641E+03	am242m	5.701E-01	ba137m	2.285E-04
u237	1.202E+01	am243	8.028E+01	y90	1.939E-01
u238	9.323E+05	cm242	1.000E+01	cs134	1.506E+02

Table 3.7: Isotopics uncertainties for typical LWR simplified model.

Isotopic Uncertainties (% St. Dev.)					
Nuclide	Uncertainty	Nuclide	Uncertainty	Nuclide	Uncertainty
pb210	1.1518	np237	1.0320	cm244	11.4636
ra226	1.3188	np239	12.6984	cm245	11.2314
ac227	0.8004	pu238	2.4674	c 14	0.6833
th227	0.8007	pu239	2.2019	se 79	0.4147
th230	1.4124	pu240	2.8370	sr 90	0.7126
pa231	1.3595	pu241	3.7081	tc 99	1.6437
u234	1.4532	pu242	3.9948	i129	0.5690
u235	6.1838	am241	3.6751	cs137	0.3347
u236	1.3642	am242m	3.1688	ba137m	0.3347
u237	3.7081	am243	12.6985	y 90	0.7126
u238	0.0894	cm242	3.1693	cs134	1.9556

3.1.4. BWR Models with UOX Fuel

The following data are for a representative UOX fuel burned in a boiling water reactor. An updated cross-section library is created using SAS2H for one representative burnup step, and the 1-group working library used with ORIGEN. The 44-group covariance library is collapsed to 1-group using the beginning of cycle flux spectrum for this fuel, and stochastic sampling is implemented. The UOX fuel is 4.5 w/o and burned to 40 GWD/MTU in a single cycle representative of a once-through fuel. The geometry is a 7x7 General Electric fuel assembly homogenized to 4.5 w/o, with no burnable poison elements; adapted from Hermann [32]. The experiment is repeated for void fractions of 0%, 35%, 50%, and 65% by modifying the average density of the coolant (see the Appendix A for a more detailed description of this model). Table 3.8 – Table 3.11 show the discharge isotopics for each of the voids, and Table 3.12 gives a listing of the isotopics uncertainties for each void. The key observation to take away from these data, as will be stressed again later, that for UOX fuels in a LWR (be it PWR or BWR), the uncertainties are on the same order of magnitude. Across the range of voids, uncertainties do change by a factor of 1.1 to 1.7. The

top of the fuel is typically at 70-80% void while the bottom is always at 0% void, resulting in an average operating void in the 40% - 50% range. This indicates that the isotopics and their uncertainties will be a function of not only burnup but also void history, both dependent upon not only the fuel assembly, but axial position within the assembly. The BWR results in that voided region are similar to the PWR results. In fact the PWR uncertainties fall within the uncertainties of the 50% void and 65% BWR void results.

Table 3.8: Discharge isotopics for BWR fuel burned at 0% void.

Discharge Isotopics, grams / MTHM					
pb210	1.338E-11	np237	3.433E+02	cm244	9.658E+00
ra226	1.793E-08	np239	8.156E+01	cm245	1.883E-01
ac227	1.680E-09	pu238	8.692E+01	c 14	3.165E-03
th227	4.465E-12	pu239	3.294E+03	se 79	5.966E+00
th230	1.380E-03	pu240	1.848E+03	sr 90	7.468E+02
pa231	1.941E-04	pu241	8.414E+02	tc 99	1.001E+03
u234	1.675E+02	pu242	4.334E+02	i129	1.602E+02
u235	8.102E+03	am241	1.936E+01	cs137	1.491E+03
u236	5.706E+03	am242m	3.008E-01	ba137m	2.290E-04
u237	9.736E+00	am243	5.414E+01	y90	2.063E-01
u238	9.370E+05	cm242	7.232E+00	cs134	1.141E+02

Table 3.9: Discharge isotopics for BWR fuel burned at 35% void.

Discharge Isotopics, grams / MTHM					
pb210	1.692E-11	np237	4.265E+02	cm244	1.668E+01
ra226	1.728E-08	np239	8.489E+01	cm245	4.522E-01
ac227	2.391E-09	pu238	1.202E+02	c 14	3.247E-03
th227	6.618E-12	pu239	4.161E+03	se 79	5.911E+00
th230	1.274E-03	pu240	1.922E+03	sr 90	7.234E+02
pa231	2.459E-04	pu241	1.112E+03	tc 99	9.833E+02
u234	1.613E+02	pu242	4.859E+02	i129	1.663E+02
u235	9.843E+03	am241	2.770E+01	cs137	1.489E+03
u236	5.640E+03	am242m	4.901E-01	ba137m	2.288E-04
u237	1.124E+01	am243	7.594E+01	y90	1.977E-01
u238	9.340E+05	cm242	9.467E+00	cs134	1.268E+02

Table 3.10: Discharge isotopics for BWR fuel burned at 50% void.

Discharge Isotopics, grams / MTHM					
pb210	2.010E-11	np237	4.842E+02	cm244	2.278E+01
ra226	1.671E-08	np239	8.780E+01	cm245	7.550E-01
ac227	2.958E-09	pu238	1.474E+02	c 14	3.306E-03
th227	8.384E-12	pu239	4.905E+03	se 79	5.867E+00
th230	1.195E-03	pu240	1.990E+03	sr 90	7.060E+02
pa231	2.839E-04	pu241	1.334E+03	tc 99	9.685E+02
u234	1.564E+02	pu242	5.166E+02	i129	1.705E+02
u235	1.109E+04	am241	3.478E+01	cs137	1.487E+03
u236	5.621E+03	am242m	6.776E-01	ba137m	2.286E-04
u237	1.223E+01	am243	9.138E+01	y90	1.918E-01
u238	9.317E+05	cm242	1.122E+01	cs134	1.359E+02

Table 3.11: Discharge isotopics for BWR fuel burned at 65% void.

Discharge Isotopics, grams / MTHM					
pb210	2.601E-11	np237	5.685E+02	cm244	3.264E+01
ra226	1.570E-08	np239	9.288E+01	cm245	1.398E+00
ac227	3.847E-09	pu238	1.934E+02	c 14	3.392E-03
th227	1.126E-11	pu239	6.262E+03	se 79	5.797E+00
th230	1.073E-03	pu240	2.119E+03	sr 90	6.803E+02
pa231	3.400E-04	pu241	1.704E+03	tc 99	9.429E+02
u234	1.487E+02	pu242	5.478E+02	i129	1.764E+02
u235	1.290E+04	am241	4.697E+01	cs137	1.483E+03
u236	5.638E+03	am242m	1.058E+00	ba137m	2.281E-04
u237	1.363E+01	am243	1.118E+02	y90	1.837E-01
u238	9.280E+05	cm242	1.392E+01	cs134	1.488E+02

Table 3.12: Isotopics uncertainties for BWR models.

Isotopic Uncertainties (% St. Dev.)				
Nuclide	Uncertainty			
	0% Void	35% Void	50% Void	65% Void
pb210	0.798	1.056	1.126	1.388
ra226	0.902	1.193	1.274	1.575
ac227	0.335	0.429	0.477	0.548
th227	0.335	0.429	0.477	0.548
th230	1.022	1.335	1.415	1.725
pa231	0.424	0.504	0.570	0.594
u234	1.146	1.462	1.526	1.809
u235	1.360	1.472	1.757	1.677
u236	0.481	0.608	0.731	0.839
u237	2.105	2.390	2.492	2.479
u238	0.055	0.065	0.069	0.079
np237	0.541	0.593	0.638	0.697
np239	8.910	11.086	12.685	14.483
pu238	1.102	1.101	1.147	1.172
pu239	0.817	0.867	0.874	0.920
pu240	2.157	2.381	2.637	2.536
pu241	2.105	2.390	2.492	2.479
pu242	2.011	2.252	2.437	2.531
am241	2.089	2.372	2.474	2.462
am242m	1.807	2.071	2.156	2.154
am243	8.910	11.086	12.685	14.483
cm242	1.806	2.070	2.155	2.153
cm244	7.416	9.233	10.618	12.041
cm245	6.816	8.431	9.687	10.851
c 14	0.392	0.441	0.483	0.544
se 79	0.316	0.363	0.408	0.465
sr 90	0.322	0.381	0.436	0.496
tc 99	1.309	1.609	1.864	2.238
i129	0.362	0.408	0.444	0.502
cs137	0.326	0.374	0.413	0.473
ba137m	0.326	0.374	0.413	0.473
y 90	0.322	0.381	0.436	0.496
cs134	0.962	1.063	1.166	1.305

3.1.5. PWR Models with MOX Fuels

The following data is for two representative MOX fuels burned in a pressurized water reactor, adapted from fuel compositions in Bathke [4]. An updated cross-section library is

created using SAS2H for one representative burnup step and the 1-group binary library used with ORIGEN. The 44-group covariance library is collapsed to 1-group using the beginning of cycle flux spectrum for each fuel, and stochastic sampling is implemented. The first, clean MOX fuel is 91.903 w/o uranium with the following composition: 1.40 w/o U-235, 98.572 w/o U-238, 0.028 w/o U-234, and 8.097 w/o plutonium. The plutonium has the composition: 1.655 w/o Pu-238, 61.751 w/o Pu-239, 24.701 w/o Pu-240, 3.248 w/o Pu-241, 8.645 w/o Pu-242. The second MOX fuel is representative of imperfect separation techniques and includes only 89.403 w/o uranium and impurities of 1 w/o Np-237 and 1.5 w/o Am-241. The geometry of both fuels is that of a 17x17 Westinghouse-type fuel assembly with 25 water holes and they are each burned to 50 GWD/MTHM (see the Appendix A for a more detailed description of these models). Table 3.13 and Table 3.14 show the discharge isotopics for the two MOX fuels, and Table 3.15 presents the isotopic uncertainties for the two fuels. It can be seen from these data that making a significant change in the fuel composition will result in a change in the uncertainties.

Table 3.13: Discharge isotopics for the "clean" MOX fuel.

Discharge Isotopics, grams / MTHM					
pb210	1.310E-10	np237	3.290E+02	cm244	9.958E+02
ra226	1.840E-08	np239	9.836E+01	cm245	9.472E+01
ac227	6.215E-09	pu238	4.530E+03	c 14	5.611E-03
th227	3.415E-11	pu239	2.384E+04	se 79	6.108E+00
th230	1.292E-03	pu240	1.549E+04	sr 90	4.569E+02
pa231	4.894E-04	pu241	9.475E+03	tc 99	1.127E+03
u234	2.299E+02	pu242	6.822E+03	i129	3.038E+02
u235	7.081E+03	am241	6.046E+02	cs137	1.864E+03
u236	1.503E+03	am242m	1.961E+01	ba137m	2.872E-04
u237	7.047E+00	am243	1.851E+03	y90	1.218E-01
u238	8.759E+05	cm242	1.355E+02	cs134	2.055E+02

Table 3.14: Discharge isotopics for MOX fuel with impurities.

Discharge Isotopics, grams / MTHM					
pb210	1.442E-09	np237	5.422E+03	cm244	1.075E+03
ra226	1.928E-08	np239	9.590E+01	cm245	1.075E+02
ac227	6.988E-09	pu238	1.328E+04	c 14	5.300E-03
th227	2.498E-10	pu239	2.816E+04	se 79	6.053E+00
th230	1.441E-03	pu240	1.593E+04	sr 90	4.491E+02
pa231	5.488E-04	pu241	9.545E+03	tc 99	1.105E+03
u234	3.133E+02	pu242	7.792E+03	i129	3.039E+02
u235	7.406E+03	am241	4.880E+03	cs137	1.843E+03
u236	1.501E+03	am242m	2.003E+02	ba137m	2.842E-04
u237	6.927E+00	am243	2.130E+03	y90	1.196E-01
u238	8.501E+05	cm242	1.304E+03	cs134	1.993E+02

Table 3.15: Isotopic uncertainties for MOX fuels.

Isotopic Uncertainties (% St. Dev.)			
Nuclide	Uncertainty		
	"Clean MOX		MOX w/ Impurities
pb210	1.0641		0.6387
ra226	1.2235		0.8533
ac227	0.6231		0.6575
th227	0.6231		0.6575
th230	1.1831		0.7945
pa231	0.6028		0.6460
u234	1.1110		0.7477
u235	1.3668		1.3539
u236	1.0367		1.0588
u237	1.9287		1.8627
u238	0.0918		0.0963
np237	0.7904		0.3727
np239	24.9776		23.0736
pu238	1.3121		0.7914
pu239	1.3840		1.3535
pu240	2.3612		2.2987
pu241	1.9287		1.8627
pu242	2.5902		2.3931
am241	1.8381		1.1829
am242m	1.2130		1.1621
am243	24.9775		23.0737
cm242	1.2128		1.1618
cm244	17.6375		16.1298
cm245	14.4246		13.1267
c 14	0.8374		0.9462
se 79	0.7336		0.8164
sr 90	0.6899		0.7637
tc 99	2.5609		2.9419
i129	0.7641		0.8277
cs137	0.7591		0.8189
ba137m	0.7591		0.8189
y 90	0.6899		0.7637
cs134	1.6727		1.6825

3.1.6. Comparison of Results, Simplified ORIGEN Models

In the following pages, the two most commonly examined metrics for repository performance and reprocessing are graphically compared: decay heat and radioactivity, spanning 10 to 10,000 years of decay time. These data are depicted as plots of the isotopic

uncertainty information from the simplified ORIGEN models as propagated to these two key metrics. For additional information about each model, please refer to the previous sections. Attention is again drawn to the observation that, by experience, it is shown that major changes in the fuel composition, e.g. from UOX to MOX, cause changes to the distribution of isotopic uncertainties. Comparing the PWR UOX and PWR MOX fuels, which have the same geometry and are burned in the same reactor type, exemplifies this by showing a drop in uncertainties for plutonium isotopes, increase in americium and curium isotopic uncertainties, and fission product uncertainties more than doubling. This is quite dissimilar from when the BWR (in the 50-65% void region) and PWR results are compared. Even with two different reactor types and two different geometries, those results are similar due to their fuel type and burnup.

Following the order in which the models were presented, the first comparison made is of the ORIGEN model representing a PWR, using both the stochastic method and the ESM approach for the same model. The nominal information is the same for each since it is the same model, only analyzed with different uncertainty analysis methods. Both the decay heat uncertainty (Figure 3.1) and the radioactivity uncertainty (Figure 3.2) were nearly identical between the two models, showing graphically that ESM yields the same results as forward perturbation.

Next, comparison is made between the metrics for the PWR model using the SAS2H updated flux spectrum and cross sections versus using the typical LWR spectrum and cross sections provided with the SCALE package for decay heat (Figure 3.3) and for radioactivity (Figure 3.4). While nominal decay performance was nearly the same, indicating similar

isotopics results, the typical values tended to over-estimate decay heat uncertainty and underestimate radioactivity uncertainty after the first one hundred years.

The BWR models at various void fractions are compared next. In terms of nominal values, the different voids produced nearly the same short term decay heat (Figure 3.5) and radioactivity (Figure 3.6), but the variance can be seen in the later decay times. This variance in longer term performance is due to slightly different actinide buildup, which can be seen in the discharge isotopics presented in Section 3.1.4. The uncertainties which are shown to vary between different voids models do so due to a different flux spectrum used to collapse the covariance matrix with each different void. It is also observed that the magnitude of the relative uncertainties for the BWR is similar to that of the PWR, which uses the same UOX fuel. One notices a trend in the UOX fuels, that as time increases, the uncertainty tends to increase, typically around 100-500 years. This is due to low uncertainty, high contributing fission products decaying away, leaving higher uncertainty, long lived actinides to decay.

Finally, the PWR model with UOX fuel is compared to the two PWR models using MOX fuels – both clean and with impurities – that were examined in this study. MOX fuels maintain higher heat load (Figure 3.7) and radioactivity (Figure 3.8) for a longer span of time than the PWR fuel due to the build up of long-lived actinides in the MOX fuel. Also, the MOX uncertainty is higher than that of the PWR UOX fuel due to the presence of higher quantities of actinides initially, longer burnup, and different operating conditions.

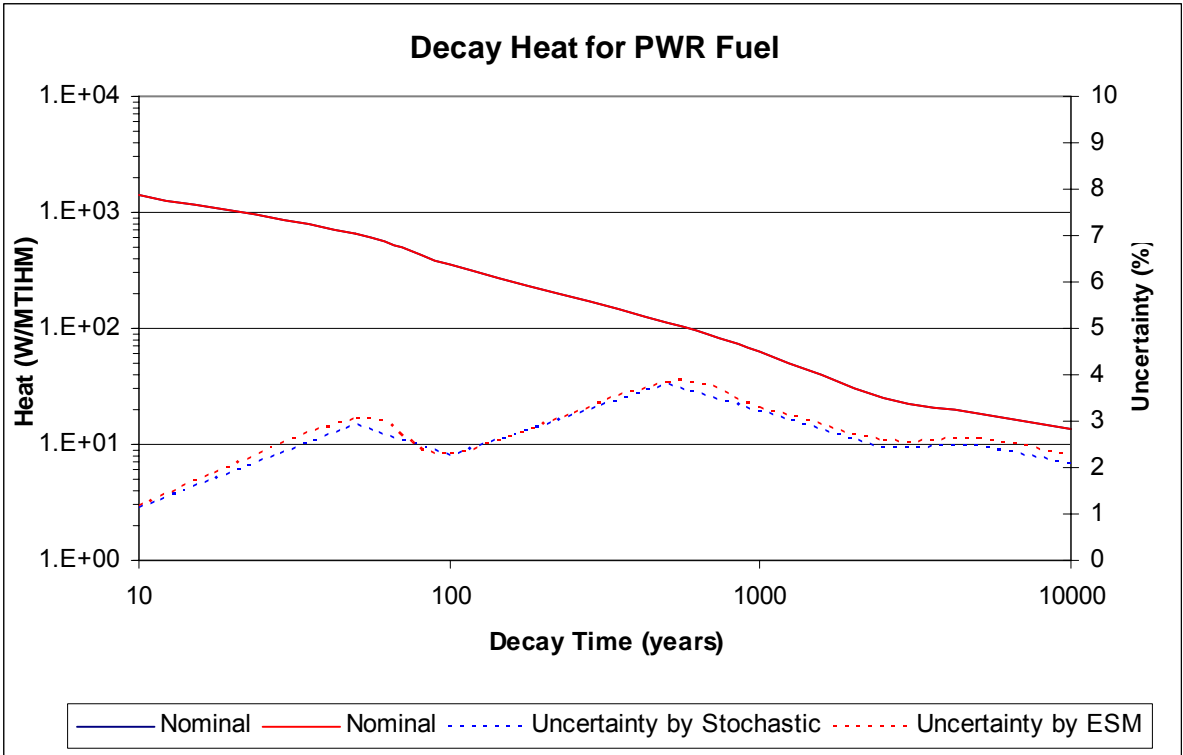


Figure 3.1: Decay heat comparison of stochastic and ESM sampling methods.

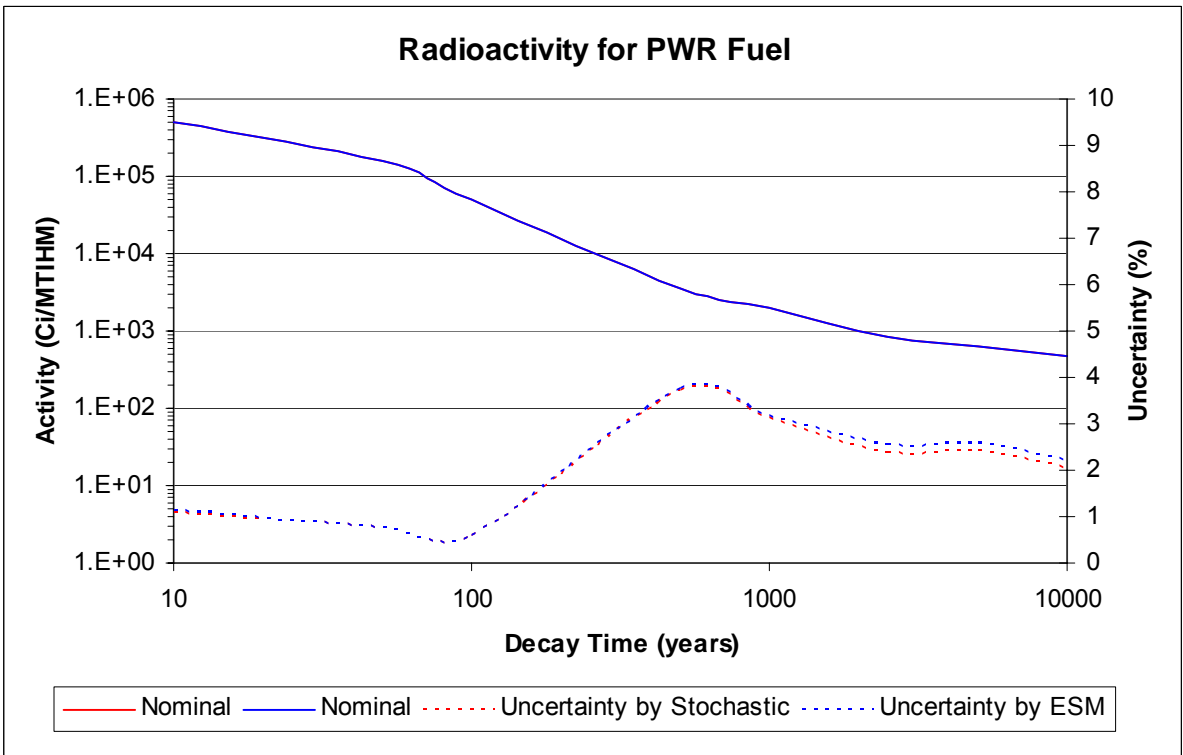


Figure 3.2: Radioactivity comparison of stochastic and ESM sampling methods.

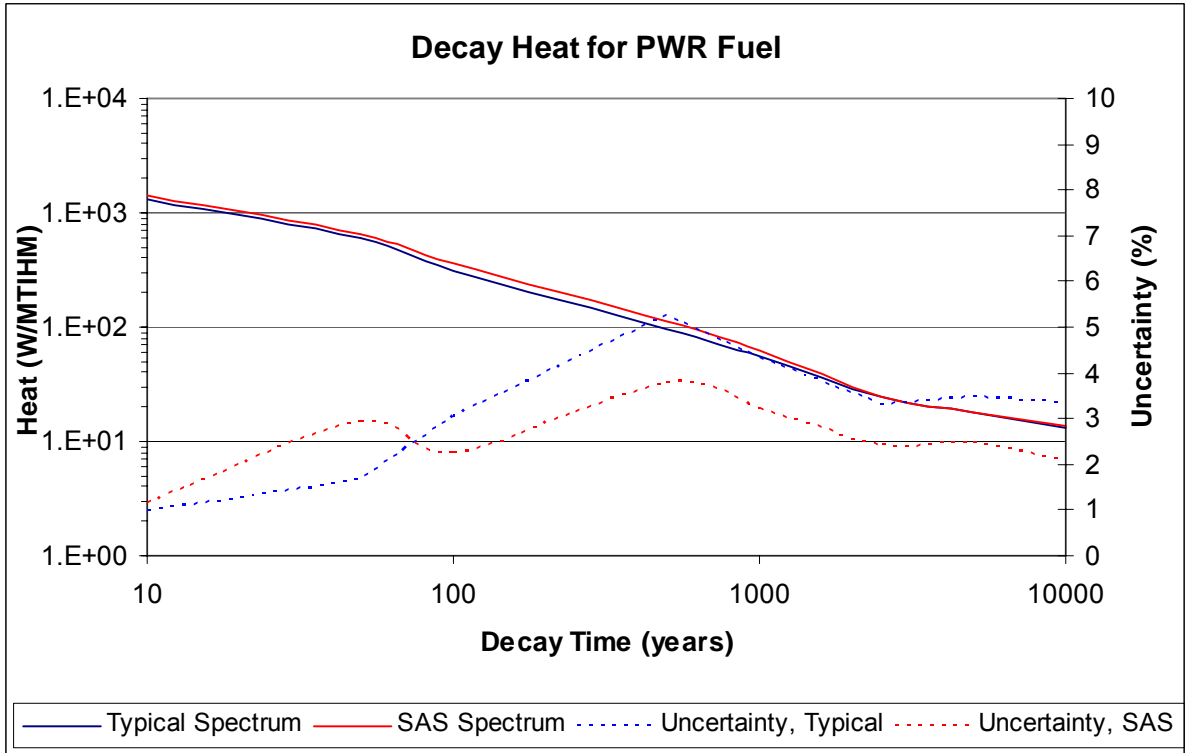


Figure 3.3: Decay heat comparison of SCALE provided data and SAS2H updated data.

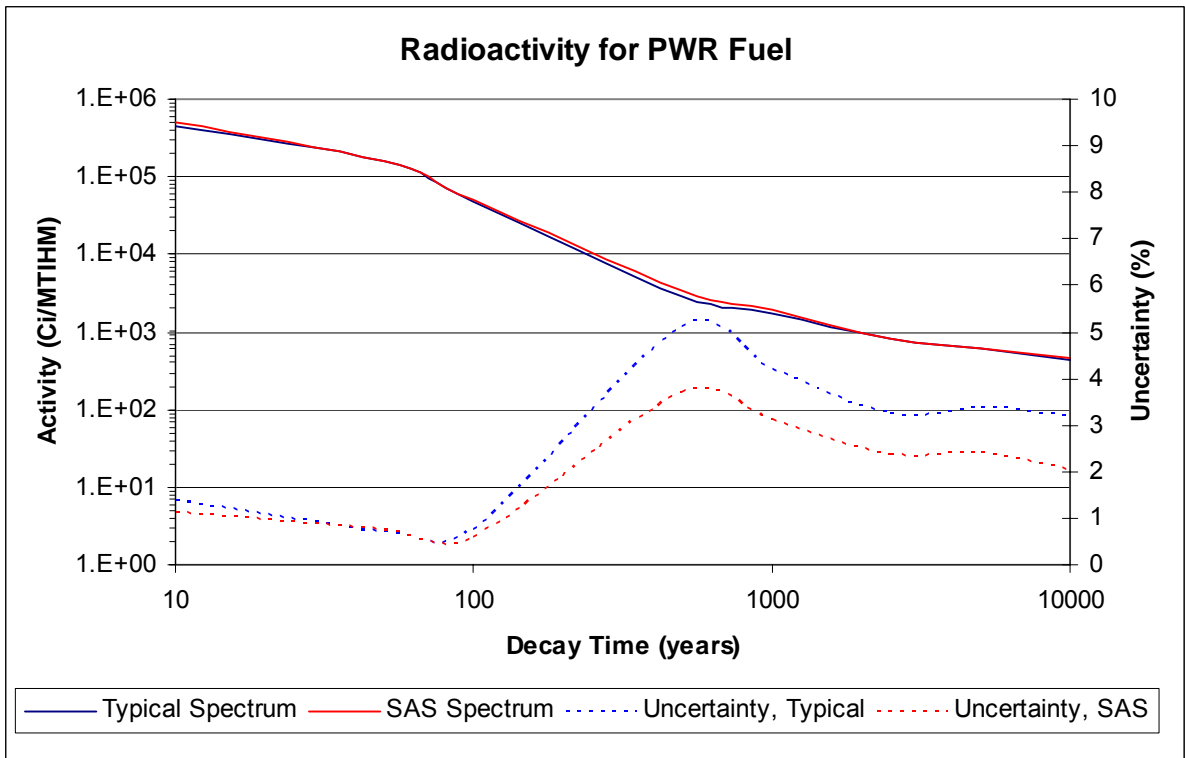


Figure 3.4: Radioactivity, SCALE provided data and SAS2H updated data.

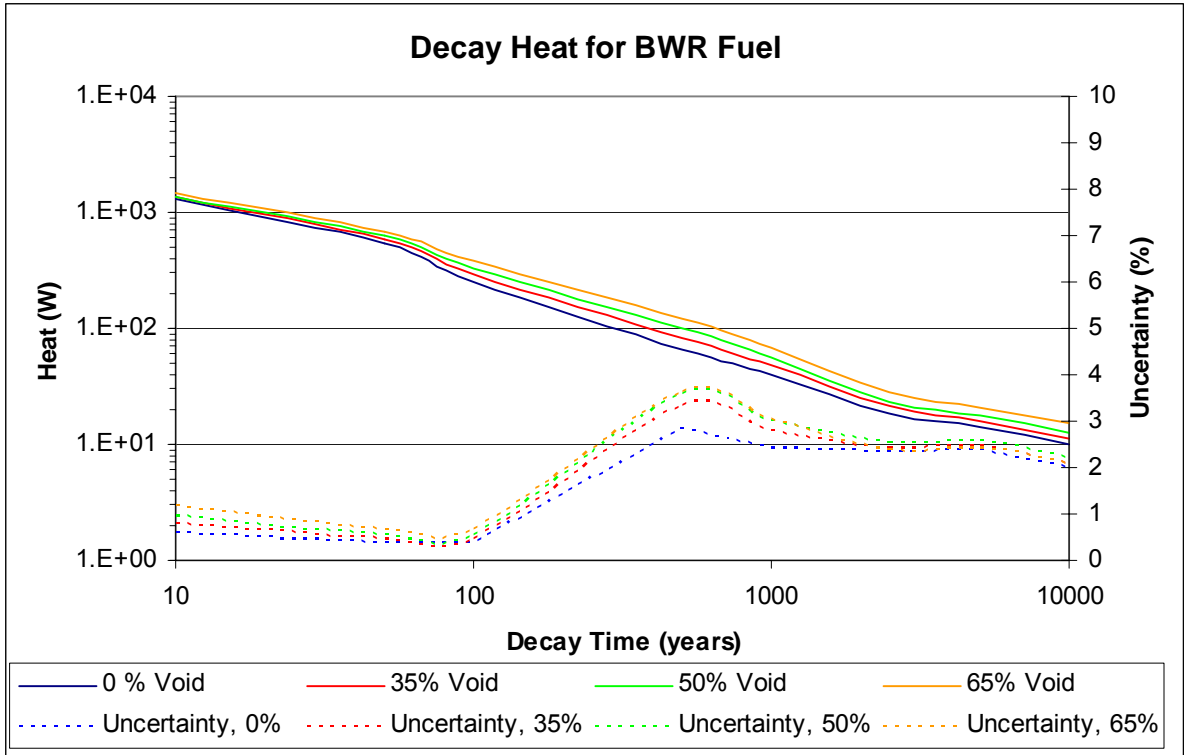


Figure 3.5: Decay heat comparison for BWR fuels.

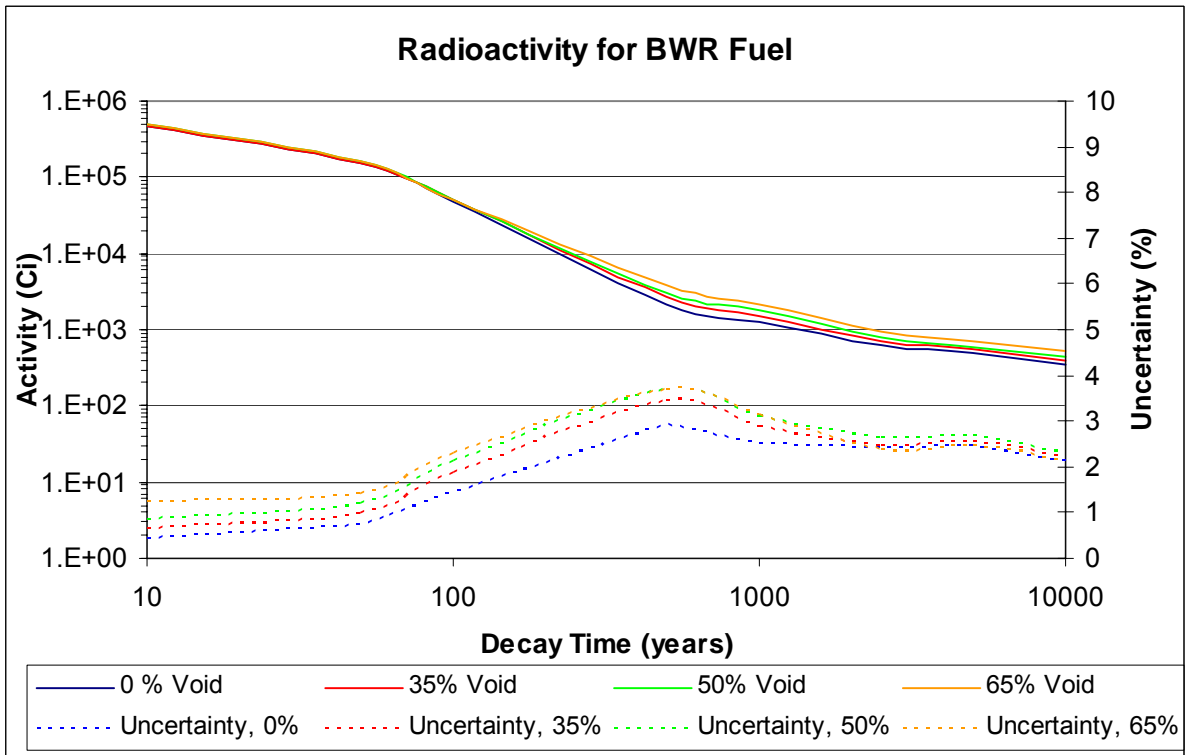


Figure 3.6: Radioactivity Comparison for BWR fuels.

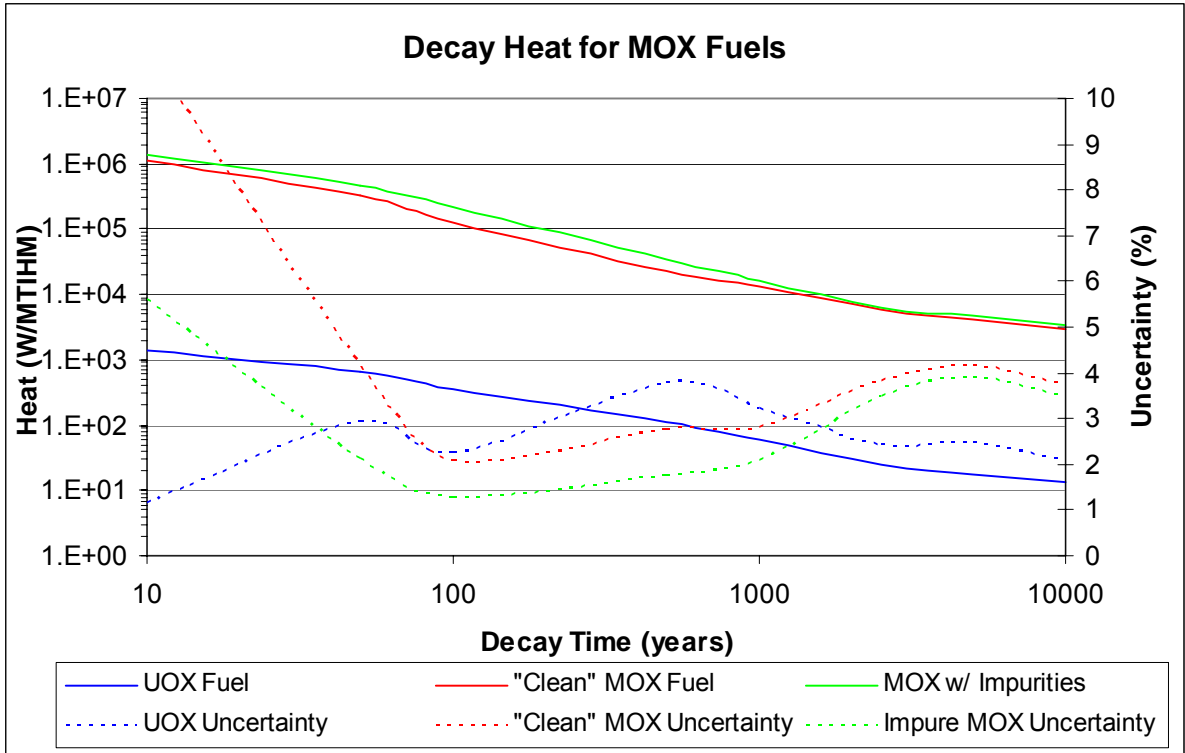


Figure 3.7: Decay heat comparison of UOX and MOX fuels.

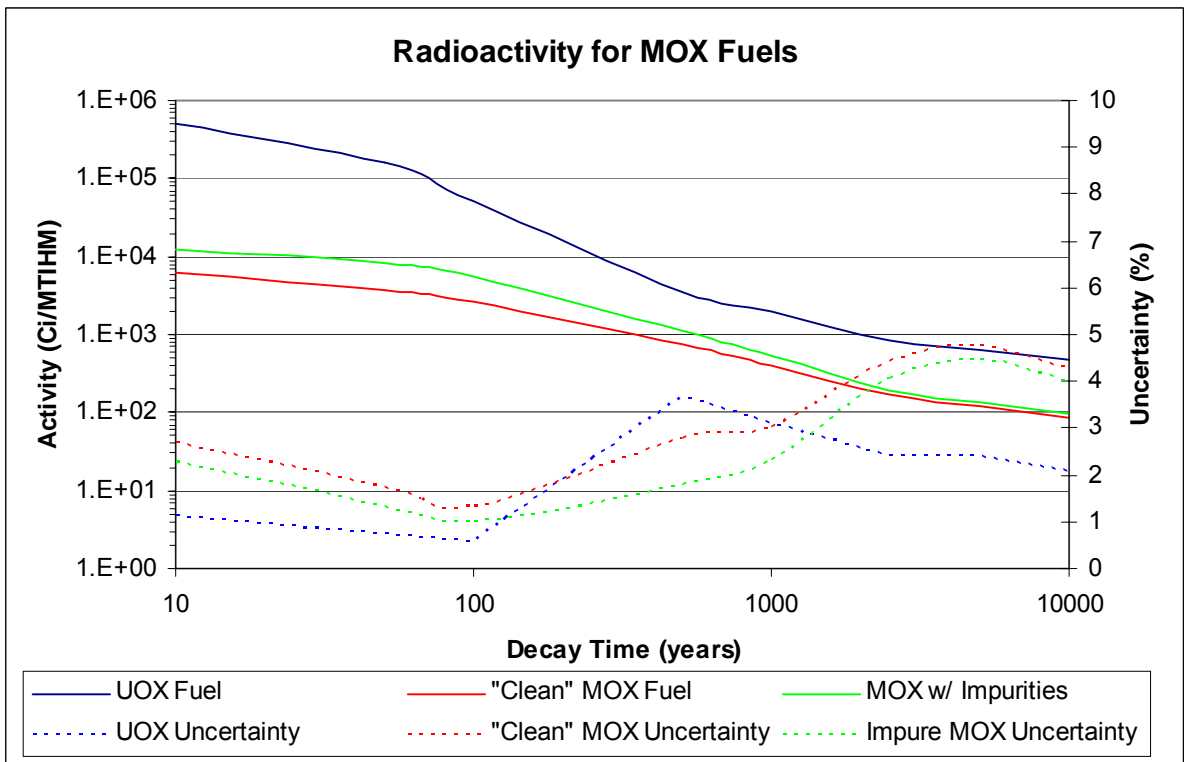


Figure 3.8: Radioactivity comparison for UOX and MOX fuels.

3.1.7. A Brief Experiment with Operational Uncertainties

Since cross section uncertainties have shown almost negligible affects on the metrics of interest that have been examined in this study, whether operational parameters could outweigh these small cross section induced uncertainties was examined. A simple experiment was performed to test this hypothesis. The simplified, unperturbed PWR model in ORIGIN as discussed in Section 3.1.2 was depleted adjusting the following parameters: +/- 2 GWD/MTU burnup (a reasonable measurement uncertainty, [33]), and varied power history between 90 and 105% of full power over the life of the fuel. Data are presented for several key isotopes that are primary contributors to decay heat (Figure 3.9) and radioactivity (Figure 3.10), taken at a time of one hundred years after decay. In examining the following figures, operational uncertainties can clearly be seen to have a much greater impact on the metrics of interest than cross-section uncertainty.

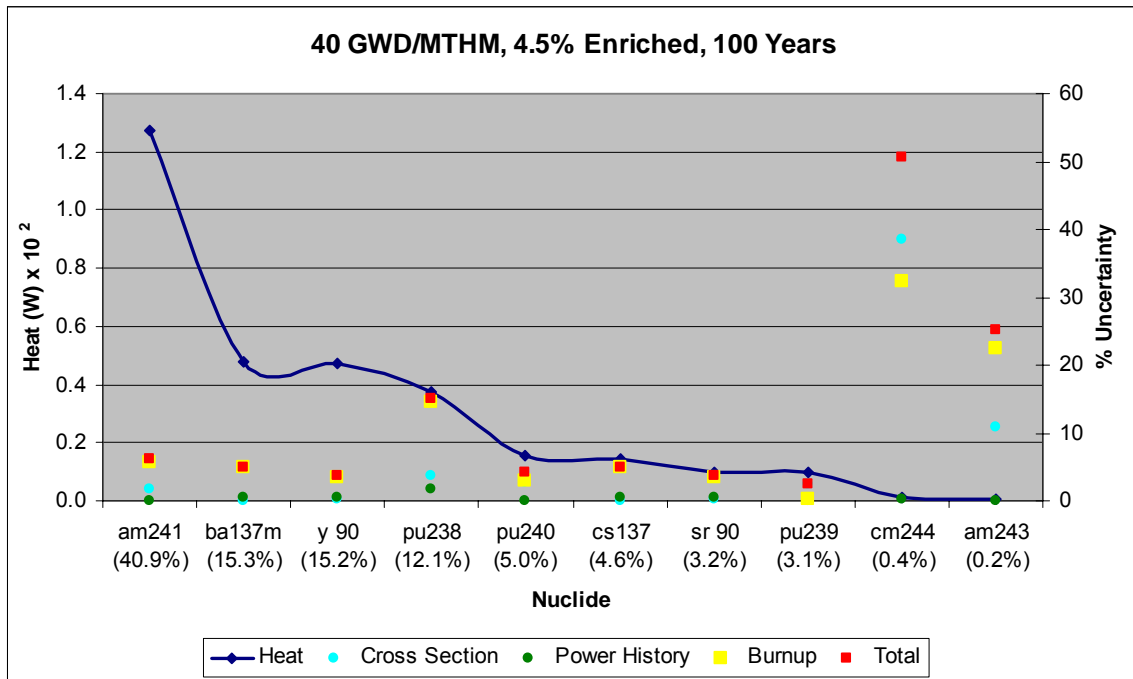


Figure 3.9: Decay heat uncertainty of key isotopes due to various sources.

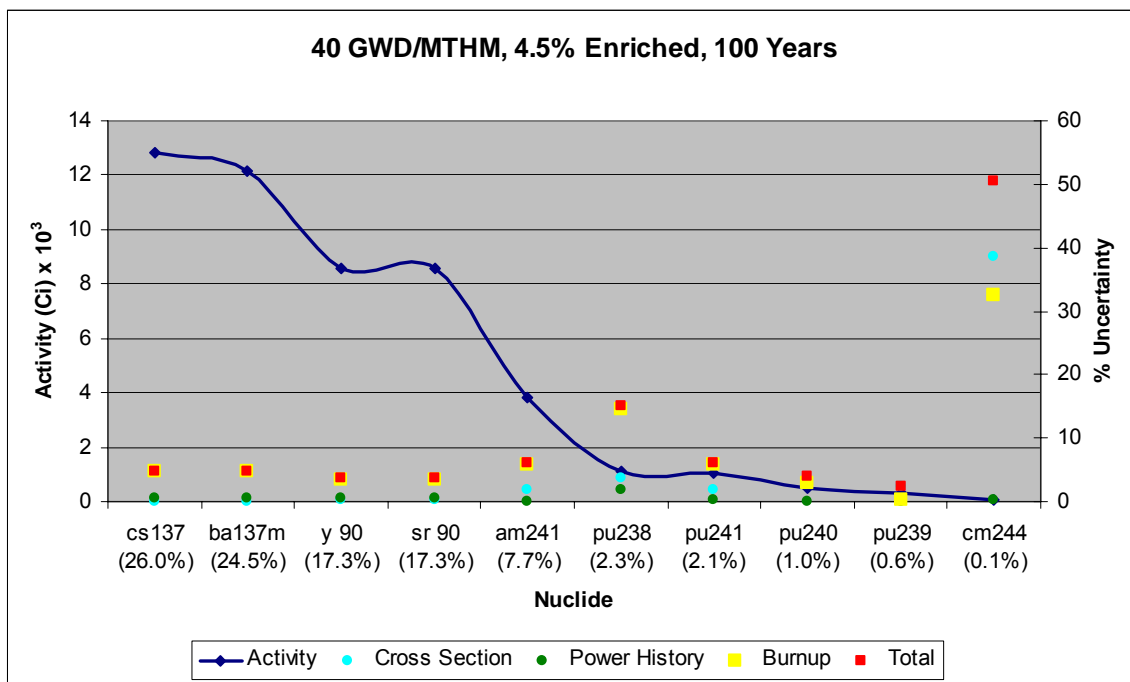


Figure 3.10: Radioactivity uncertainty in key isotopes due to various sources.

3.2. TRITON Models

3.2.1. PWR Model in TRITON with UOX Fuel

The choice to move the analysis to using TRITON for the remaining fuel types has been discussed previously. The PWR model was reconstructed in the more rigorous TRITON sequence to 1) validate the uncertainty propagation approach of using ESM in TRITON, 2) compare to the SAS2H/ORIGEN model, 3) use a more detailed and finer model which is a procedure closer to standard fuel analysis, and 4) provide an isotopic covariance matrix for the spent PWR fuel that will be used in the recycling experiment. If TRITON, using only the Wigner cell, is given the same geometry, isotopics, and power history -- using one burnup step -- as SAS2H it will produce equivalent results (Table 3.16). Results are not identical due to different transport solutions, but the differences are statistically insignificant. Note that if more burnup steps are used or the buffer region equivalent to water holes is neglected in TRITON the results are no longer equivalent (Table 3.16). The model, using 4.5 w/o UOX fuel, was first burned to 40 GWD/MTU to match the SAS2H model, and then the burnup was extended to 48 GWD/MTU so as to provide a more realistic end of life k-effective value. The 40 GWD model used 26 burnup steps while the 48 GWD model had 30. The discharge isotopics of the 48 GWD/MTU model are given in Table 3.18, and it is these values to which uncertainty is propagated in later discussion and comparison. For completeness, the 40 GWD/MTU discharge isotopics are presented in Table 3.17 and the reader can see how an additional 8 GWD/MTU changes the fuel composition.

Table 3.16: Comparison of isotopics between models.

Nuclide	Number Density at 10 Years Decay, (g)			
	ORIGEN with 1 SAS2H Updated BU Step	TRITON with 1 BU Step	TRITON with 1 BU Step without Buffer	TRITON with 4 BU Steps
pb210	5.054E-10	5.369E-10	5.193E-10	5.357E-10
ra226	3.165E-07	3.369E-07	3.239E-07	3.353E-07
ac227	6.941E-08	7.115E-08	7.796E-08	7.326E-08
th227	1.613E-10	1.653E-10	1.812E-10	1.702E-10
th230	5.585E-03	5.951E-03	5.766E-03	5.921E-03
pa231	4.323E-04	4.412E-04	4.806E-04	4.537E-04
u234	1.675E+02	1.781E+02	1.754E+02	1.771E+02
u235	1.234E+04	1.252E+04	1.315E+04	1.252E+04
u236	5.526E+03	5.526E+03	5.570E+03	5.555E+03
u237	2.945E-05	2.978E-05	3.463E-05	2.603E-05
u238	9.298E+05	9.293E+05	9.265E+05	9.292E+05
np237	5.730E+02	5.668E+02	6.277E+02	5.489E+02
np239	1.001E-04	1.012E-04	1.187E-04	9.312E-05
pu238	1.796E+02	1.771E+02	2.088E+02	1.725E+02
pu239	5.555E+03	5.619E+03	6.484E+03	5.796E+03
pu240	1.895E+03	1.899E+03	2.002E+03	2.278E+03
pu241	9.717E+02	9.824E+02	1.143E+03	8.589E+02
pu242	5.576E+02	5.571E+02	5.976E+02	5.123E+02
am241	6.407E+02	6.533E+02	7.596E+02	5.690E+02
am242m	8.756E-01	9.965E-01	1.237E+00	7.995E-01
am243	1.163E+02	1.176E+02	1.380E+02	1.082E+02
cm242	2.284E-03	2.599E-03	3.226E-03	2.086E-03
cm244	2.200E+01	2.204E+01	2.826E+01	2.087E+01
cm245	1.207E+00	1.218E+00	1.773E+00	1.213E+00
c 14	3.331E-03	3.327E-03	3.461E-03	3.324E-03
se 79	5.817E+00	5.804E+00	5.878E+00	5.796E+00
sr 90	5.393E+02	5.363E+02	5.342E+02	5.366E+02
tc 99	9.622E+02	9.603E+02	9.705E+02	9.585E+02
i129	1.760E+02	1.762E+02	1.839E+02	1.755E+02
cs137	1.179E+03	1.175E+03	1.199E+03	1.173E+03
ba137m	1.801E-04	1.794E-04	1.831E-04	1.791E-04
y90	1.401E-01	1.394E-01	1.388E-01	1.394E-01
cs134	4.990E+00	4.749E+00	5.162E+00	4.751E+00

Table 3.17: 40 GWD/MTU Discharge Isotopics.

Discharge Isotopics, grams / MTHM					
pb210	3.068E-11	np237	5.327E+02	cm244	2.989E+01
ra226	2.051E-08	np239	8.249E+01	cm245	1.188E+00
ac227	4.409E-09	pu238	1.743E+02	c 14	3.337E-03
th227	1.286E-11	pu239	5.745E+03	se 79	5.807E+00
th230	1.311E-03	pu240	2.342E+03	sr 90	6.853E+02
pa231	3.637E-04	pu241	1.362E+03	tc 99	9.752E+02
u234	1.630E+02	pu242	5.071E+02	i129	1.741E+02
u235	1.248E+04	am241	4.344E+01	cs137	1.476E+03
u236	5.563E+03	am242m	8.884E-01	ba137m	2.268E-04
u237	1.108E+01	am243	1.062E+02	y90	1.844E-01
u238	9.291E+05	cm242	1.277E+01	cs134	1.346E+02

Table 3.18: 48 GWD/MTU Discharge Isotopics.

Discharge Isotopics, grams / MTHM					
pb210	5.772E-11	np237	6.646E+02	cm244	6.780E+01
ra226	2.667E-08	np239	8.826E+01	cm245	3.088E+00
ac227	5.433E-09	pu238	2.678E+02	c 14	4.127E-03
th227	1.827E-11	pu239	5.746E+03	se 79	6.827E+00
th230	1.370E-03	pu240	2.716E+03	sr 90	7.807E+02
pa231	4.338E-04	pu241	1.566E+03	tc 99	1.135E+03
u234	1.436E+02	pu242	7.621E+02	i129	2.141E+02
u235	8.934E+03	am241	5.407E+01	cs137	1.757E+03
u236	5.989E+03	am242m	1.111E+00	ba137m	2.700E-04
u237	1.240E+01	am243	1.883E+02	y90	2.112E-01
u238	9.228E+05	cm242	1.912E+01	cs134	1.824E+02

The ESM approach was implemented in TRITON using the eigenvalues and eigenvectors of the 44-group covariance matrix for selected reactions to perturb the 44-group master cross section library input to the code. A total of 1938 samples were run as this number was the effective rank of this covariance matrix obtained by limiting perturbations to those corresponding to eigenvalues greater than 10^{-6} relative to the reference cross section. Results for uncertainty of the 33 tracked nuclides are presented in Table 3.19, along with the

uncertainty results from the simple ORIGEN 1-group model using the direct perturbation method. Appendix C present further details.

Table 3.19: Resulting standard deviations from both models.

Nuclide	% Standard Deviation	
	TRITON	ORIGEN
pb210	0.152	1.195
ra226	0.185	1.355
ac227	0.231	0.480
th227	0.233	0.480
th230	0.185	1.491
pa231	0.253	0.518
u234	0.173	1.579
u235	0.583	1.312
u236	1.048	0.712
u237	2.053	2.521
u238	0.015	0.078
np237	1.602	0.605
np239	3.910	13.643
pu238	1.751	1.050
pu239	1.045	0.806
pu240	2.490	2.566
pu241	2.053	2.521
pu242	3.907	2.598
am241	2.053	2.502
am242m	2.104	2.172
am243	3.908	13.643
cm242	2.107	2.172
cm244	4.345	11.340
cm245	4.680	10.251
c 14	0.379	0.452
se 79	0.088	0.366
sr 90	0.117	0.375
tc 99	0.075	1.970
i129	0.241	0.419
cs137	0.032	0.382
ba137m	0.032	0.382
y 90	0.107	0.375
cs134	0.300	1.138

At first glance, one is likely to say that the models are not equivalent. Rigorous and thorough search for the difference, however, yielded an explanation of these differences.

Both a primary and a secondary reason for the differences were discovered. Discussed first will be the secondary cause, as it has more tangible data. Consider carefully what terms of the uncertainty are being propagated in each model. Let the result, \bar{y} , of a perturbed model be defined as:

$$\bar{y} = \Omega \left[\overline{\sigma_0^T \phi_0} + \overline{\Delta \sigma^T \phi_0} + \overline{\sigma_0^T \Delta \phi} + \overline{\Delta \sigma^T \Delta \phi} \right] \quad (3.1)$$

where $\|\overline{\phi_0} + \overline{\Delta \phi}\|_1 = 1$. $\overline{\sigma_0^T \phi_0}$ is the cross sections collapsed using the BOL, unchanged flux, $\overline{\Delta \sigma^T \phi_0}$ is the perturbation added by a cross section perturbations, $\overline{\sigma_0^T \Delta \phi}$ is the perturbation added by an updated burnup dependent flux spectrum, and $\overline{\Delta \sigma^T \Delta \phi}$ is the second order perturbation added by both sources, which is assumed to be negligible. A nominal run of ORIGEN inputs $\overline{\sigma_0^T \phi_0}$. When making perturbations only in the ORIGEN input via the collapsed covariance data only the term $\overline{\Delta \sigma^T \phi_0}$ is captured. When using a sequence such as TRITON that performs a transport update of flux and applies it to the master library, however, the term $\overline{\sigma_0^T \Delta \phi}$ is also captured. Table 3.20 contains 44-group fluxes that have been normalized to the 1-group BOL flux, i.e. the sum of the BOL column of fluxes is equal to 1. As can be seen in Table 3.20, as fuel depletes with burnup, the groups from (0.1 – 3.0) ev tend to have the group fluxes decrease in value. Even though the flux is normalized by ORIGEN to keep the same power density, the overall shape of the flux changes. The energy spectra shift causes the term $\overline{\sigma_0^T \Delta \phi}$ to be negative and reduces the overall uncertainty. A numerical experiment of this is shown in Table 3.21 where the 44-group variance was collapsed using both averaged and burnup averaged flux changes from Table 3.20. Since the

1-group variances are collapsed from the 44-group using the flux, this directly affects the magnitude of the 1-group covariance values. More explicitly, the change in the 1-group covariance, $\overline{\overline{\Delta COV(\sigma)}}$, due to a change in the 44-group flux, $\overline{\Delta\phi}$, is:

$$\overline{\overline{\Delta COV(\sigma)}} = \overline{\phi_0}^T \overline{\overline{COV(\sigma)}} \overline{\Delta\phi} + \overline{\Delta\phi}^T \overline{\overline{COV(\sigma)}} \overline{\phi_0} \quad (3.2)$$

where $\|\overline{\phi_0} + \overline{\Delta\phi}\|_1 = 1$. As shown in Table 3.22, the reduced covariance data cause output uncertainties to be reduced. These affects can account for at most about 20% of the difference between the two models.

Table 3.20: Change in flux as burnup increases.

ENERGY (ev)	BOL FLUX	Flux at Various Burnups (MWD/MTU)			
		2000	14000	26000	38000
2.00E+07	1.5651E-03	1.5763E-03	1.6394E-03	1.6954E-03	1.7454E-03
8.19E+06	4.4291E-03	4.4524E-03	4.5744E-03	4.6727E-03	4.7564E-03
6.43E+06	1.3934E-02	1.3987E-02	1.4250E-02	1.4445E-02	1.4606E-02
4.80E+06	4.6375E-02	4.6501E-02	4.7090E-02	4.7490E-02	4.7804E-02
3.00E+06	3.0549E-02	3.0614E-02	3.0917E-02	3.1119E-02	3.1279E-02
2.48E+06	9.2170E-03	9.2356E-03	9.3223E-03	9.3810E-03	9.4283E-03
2.35E+06	3.7375E-02	3.7434E-02	3.7707E-02	3.7891E-02	3.8038E-02
1.85E+06	4.6158E-02	4.6211E-02	4.6462E-02	4.6639E-02	4.6788E-02
1.40E+06	6.4489E-02	6.4525E-02	6.4697E-02	6.4832E-02	6.4951E-02
9.00E+05	1.1652E-01	1.1653E-01	1.1664E-01	1.1676E-01	1.1687E-01
4.00E+05	1.1869E-01	1.1872E-01	1.1885E-01	1.1900E-01	1.1915E-01
1.00E+05	6.7525E-02	6.7549E-02	6.7674E-02	6.7801E-02	6.7913E-02
2.50E+04	1.5345E-02	1.5351E-02	1.5386E-02	1.5420E-02	1.5450E-02
1.70E+04	6.3885E-02	6.3925E-02	6.4125E-02	6.4312E-02	6.4473E-02
3.00E+03	5.7312E-02	5.7371E-02	5.7669E-02	5.7936E-02	5.8161E-02
5.50E+02	5.3043E-02	5.3131E-02	5.3575E-02	5.3974E-02	5.4312E-02
1.00E+02	3.3399E-02	3.3474E-02	3.3846E-02	3.4203E-02	3.4521E-02
3.00E+01	2.7654E-02	2.7687E-02	2.7868E-02	2.8123E-02	2.8389E-02
1.00E+01	5.0899E-03	5.1134E-03	5.2116E-03	5.2966E-03	5.3718E-03
8.10E+00	5.0429E-03	5.0502E-03	5.0835E-03	5.1301E-03	5.1791E-03
6.00E+00	5.2123E-03	5.1352E-03	4.7772E-03	4.5935E-03	4.4920E-03
4.75E+00	1.1050E-02	1.1047E-02	1.1012E-02	1.1009E-02	1.1022E-02
3.00E+00	1.3506E-02	1.3511E-02	1.3504E-02	1.3459E-02	1.3353E-02
1.77E+00	1.4724E-02	1.4636E-02	1.3081E-02	1.2225E-02	1.1719E-02
1.00E+00	1.2651E-02	1.2620E-02	1.1948E-02	1.1464E-02	1.1130E-02
6.25E-01	1.2905E-02	1.2795E-02	1.2113E-02	1.1786E-02	1.1611E-02
4.00E-01	1.9535E-03	1.9051E-03	1.7194E-03	1.6557E-03	1.6395E-03
3.75E-01	2.1397E-03	2.0608E-03	1.7892E-03	1.7019E-03	1.6831E-03
3.50E-01	2.3695E-03	2.2414E-03	1.8389E-03	1.7169E-03	1.6920E-03
3.25E-01	5.7177E-03	5.2816E-03	4.0465E-03	3.6950E-03	3.6285E-03
2.75E-01	3.6375E-03	3.3722E-03	2.6589E-03	2.4553E-03	2.4277E-03
2.50E-01	4.4406E-03	4.1571E-03	3.4519E-03	3.2579E-03	3.2562E-03
2.25E-01	5.4824E-03	5.1577E-03	4.4577E-03	4.2966E-03	4.3487E-03
2.00E-01	1.5222E-02	1.4320E-02	1.2882E-02	1.2742E-02	1.3134E-02
1.50E-01	2.2839E-02	2.1257E-02	1.9756E-02	2.0051E-02	2.1107E-02
1.00E-01	1.7676E-02	1.6305E-02	1.5454E-02	1.5962E-02	1.7058E-02
7.00E-02	1.2312E-02	1.1381E-02	1.0939E-02	1.1434E-02	1.2344E-02
5.00E-02	5.7830E-03	5.3621E-03	5.2021E-03	5.4819E-03	5.9593E-03
4.00E-02	5.1278E-03	4.7654E-03	4.6568E-03	4.9395E-03	5.4003E-03
3.00E-02	2.0759E-03	1.9324E-03	1.8998E-03	2.0264E-03	2.2263E-03
2.53E-02	4.7235E-03	4.4056E-03	4.3795E-03	4.7204E-03	5.2342E-03
1.00E-02	4.0214E-04	3.7567E-04	3.7910E-04	4.1461E-04	4.6586E-04
7.50E-03	4.0006E-04	3.7390E-04	3.8150E-04	4.2187E-04	4.7886E-04
3.00E-03	5.5627E-05	5.1989E-05	5.4307E-05	6.1555E-05	7.1549E-05

Table 3.21: Change in 1-group cross section uncertainty due to flux change.

Nuclide	Reaction Type	Relative Variance for BOL Flux	Relative Variance for Averaged Flux	Relative Variance for BU Averaged Flux
92235	(Fission)	2.479E-05	2.327E-05	2.341E-05
92235	(n, γ)	1.343E-03	1.332E-03	1.335E-03
92236	(Fission)	3.619E-04	3.413E-04	3.373E-04
92236	(n, γ)	2.469E-03	2.271E-03	2.233E-03
92238	(n,2n)	7.371E-03	8.136E-03	8.366E-03
92238	(n,3n)	1.442E-02	1.627E-02	1.684E-02
92238	(Fission)	4.245E-04	4.365E-04	4.398E-04
92238	(n, γ)	9.982E-04	1.024E-03	1.033E-03
93237	(Fission)	8.608E-03	8.764E-03	8.807E-03
94238	(Fission)	8.105E-03	8.151E-03	8.205E-03
94238	(n, γ)	8.151E-04	7.013E-04	7.182E-04
94239	(Fission)	6.927E-05	4.575E-05	4.275E-05
94239	(n, γ)	6.489E-04	3.999E-04	3.659E-04
94240	(Fission)	2.087E-03	1.962E-03	1.928E-03
94240	(n, γ)	1.008E-03	7.567E-04	6.873E-04
94241	(Fission)	6.947E-05	5.915E-05	5.859E-05
94241	(n, γ)	1.668E-03	1.233E-03	1.210E-03
94242	(n,2n)	5.685E-02	6.301E-02	6.487E-02
94242	(n,3n)	2.474E-01	2.791E-01	2.889E-01
94242	(Fission)	1.529E-03	1.562E-03	1.571E-03
94242	(n, γ)	5.200E-03	5.168E-03	5.147E-03
95241	(n,2n)	9.176E-01	1.023E+00	1.056E+00
95241	(n,3n)	9.938E-01	1.121E+00	1.160E+00
95241	(Fission)	4.635E-04	4.583E-04	4.573E-04
95241	(n, γ)	5.538E-05	4.694E-05	4.486E-05
95243	(Fission)	3.918E-03	3.987E-03	4.007E-03
95243	(n, γ)	4.273E-01	3.207E-01	2.913E-01

Table 3.22: Comparing discharge isotopic uncertainties for various flux updates.

Nuclide	% Standard Deviation			
	ORIGEN	ORIGEN Averaged	ORIGEN - BU Averaged	TRITON
pb210	1.195	1.115	1.106	0.152
ra226	1.355	1.262	1.252	0.185
ac227	0.480	0.453	0.454	0.231
th227	0.480	0.453	0.454	0.233
th230	1.491	1.394	1.384	0.185
pa231	0.518	0.490	0.494	0.253
u234	1.579	1.484	1.474	0.173
u235	1.312	1.316	1.339	0.583
u236	0.712	0.622	0.642	1.048
u237	2.521	2.154	2.248	2.053
u238	0.078	0.077	0.077	0.015
np237	0.605	0.566	0.544	1.602
np239	13.643	11.240	10.889	3.910
pu238	1.050	1.014	0.955	1.751
pu239	0.806	0.651	0.614	1.045
pu240	2.566	2.263	2.298	2.490
pu241	2.521	2.154	2.248	2.053
pu242	2.598	2.450	2.426	3.907
am241	2.502	2.137	2.233	2.053
am242m	2.172	1.855	1.968	2.104
am243	13.643	11.240	10.889	3.908
cm242	2.172	1.854	1.968	2.107
cm244	11.340	9.238	9.015	4.345
cm245	10.251	8.297	8.138	4.680
c 14	0.452	0.446	0.411	0.379
se 79	0.366	0.355	0.344	0.088
sr 90	0.375	0.362	0.359	0.117
tc 99	1.970	1.903	1.847	0.075
i129	0.419	0.413	0.388	0.241
cs137	0.382	0.371	0.354	0.032
ba137m	0.382	0.371	0.354	0.032
y 90	0.375	0.362	0.359	0.107
cs134	1.138	1.204	1.105	0.300

The primary cause is due to the intrinsic methodology within TRITON itself, making this cause less tangible than the previous data. When working with the simplified ORIGEN models, the cross section library used and perturbed was a working library that had already been updated by SAS2H. What occurs in updating is that the reference cross sections of the

master library are subjected to resonance self-shielding analysis and updated based on those procedures. Consider Table 3.23 which shows the infinitely dilute, 44-group Am-243 capture cross section and the same 44-group cross section after resonance treatment is applied. Notice in the fast region, for example, some cross sections have changed by up to two orders of magnitude, while thermal energy groups show almost no change. The cross sections in the working library used by the lattice physics codes consisted of two parts: the reference component and the resonance self-shielded component in the resolved resonance energy range. When introducing perturbations into the cross sections in the master library, only the reference cross sections are perturbed. In the thermal energy range and unresolved resonances energy ranges, this perturbation is picked up because cross sections in these energy ranges were not considered in the resonance self-shielding analysis. However in the resonance regions, perturbations in the reference cross sections are easily overwhelmed by the magnitude of the resonance updates. This accounts for the smaller values of uncertainty seen in the TRITON models. This in turn forces the assumption that the resonances are not perturbed at all which means they are assumed to be perfectly known. This assumption can lead to under-estimated uncertainties, e.g. plutonium is highly affected by low-lying resonances in the U-238 absorption cross section. Further study into this matter was beyond the scope of this work.

Table 3.23: Change in Am-243 capture cross section due to resonance treatment.

Energy	Master Cross Section	Treated Cross Section
2.00E+07	1.10580996E-02	2.51107000E+00
8.19E+06	1.15339998E-02	2.44640000E+00
6.43E+06	1.23779997E-02	1.80170000E+00
4.80E+06	1.90602001E-02	1.58490000E+00
3.00E+06	3.09389997E-02	1.57700000E+00
2.48E+06	3.72469984E-02	1.57860000E+00
2.35E+06	4.79950011E-02	1.66690000E+00
1.85E+06	7.02812970E-02	1.63750000E+00
1.40E+06	1.07110001E-01	1.45130000E+00
9.00E+05	2.26100996E-01	4.88705000E-01
4.00E+05	5.77825010E-01	5.96831000E-01
1.00E+05	1.56948996E+00	1.58408000E+00
2.50E+04	2.11269999E+00	2.12890000E+00
1.70E+04	3.18284011E+00	3.19814000E+00
3.00E+03	8.80949974E+00	8.81098000E+00
5.50E+02	2.44122009E+01	2.44834000E+01
1.00E+02	4.30122986E+01	4.36353000E+01
3.00E+01	1.03167999E+02	1.02405000E+02
1.00E+01	3.96268997E+01	4.01052000E+01
8.10E+00	2.73347992E+02	2.98206000E+02
6.00E+00	1.06544998E+02	1.05959000E+02
4.75E+00	1.19114998E+02	1.19325000E+02
3.00E+00	9.09586029E+01	1.03057000E+02
1.77E+00	2.30728003E+03	2.27778000E+03
1.00E+00	1.05037003E+02	1.04765000E+02
6.25E-01	4.81402016E+01	4.75895000E+01
4.00E-01	5.20870018E+01	5.45036000E+01
3.75E-01	3.81459999E+01	3.93748000E+01
3.50E-01	3.39099998E+01	3.42099000E+01
3.25E-01	3.19234009E+01	3.19722000E+01
2.75E-01	3.14440002E+01	3.14953000E+01
2.50E-01	3.16469994E+01	3.16905000E+01
2.25E-01	3.21749992E+01	3.21896000E+01
2.00E-01	3.37787018E+01	3.34703000E+01
1.50E-01	3.78905983E+01	3.79820000E+01
1.00E-01	4.37220001E+01	4.38877000E+01
7.00E-02	5.05588989E+01	5.06487000E+01
5.00E-02	5.72869987E+01	5.72870000E+01
4.00E-02	6.43789978E+01	6.43790000E+01
3.00E-02	7.17419968E+01	7.17420000E+01
2.53E-02	9.00500031E+01	9.00490000E+01
1.00E-02	1.25260002E+02	1.25260000E+02
7.50E-03	1.60410004E+02	1.60868000E+02
3.00E-03	2.79713013E+02	2.85547000E+02

3.2.2. Fast Reactor Models with Transuranic Fuels

Before discussing the fast reactor models, it is important to take an objective look at the capabilities of TRITON, and to recognize how these may limit the results. TRITON is part of SCALE, which, for the most part was designed with current LWR's in mind. The most restrictive issue is with TRITON's cell domain restrictions. While any polygon can be modeled inside the cell, the cell itself is required to be rectangular, and the remaining space must be filled with moderator. For BWR and PWR square assemblies this is fine – one can model the exact dimensions of either the Wigner cell or the entire assembly. However if one tries to input a hexagonal cell, like the ones in the following models, the exact dimensions cannot be modeled. Essentially one ends up with a hexagonal peg in a square hole, which is filled with additional coolant, which yields an over moderated cell, which in turn affects flux which, in turn affects isotopic depletion. Another restriction is that we are using the 44-group cross-section library which has a corresponding 44-group covariance library. These cross-sections were generated for a thermal reactor, i.e. about 50% of the data is in the thermal groups. There are only a few, broad fast energy groups, whose cross-sections are the reactions which drive the fast reactor. So, this over moderated cell and lack of fine data in the region where most reactions occur forces one to question the results obtained using this method. Further, it was early noted that the uncertainty of the resonances could not be treated. While the results do clearly demonstrate the methodology developed in this work, the actual numerical values can only be taken as plausible, rather than absolutely accurate. To provide comparison, Argonne's REBUS fast reactor code was used to further examine one of the fast reactor models. The fuel design corresponding to a conversion ratio of 0.70 is

modeled in REBUS and those results are presented in a subsequent section following the TRITON models.

Three distinctly different fast reactor models were examined in TRITON. Physically, they differ in terms of composition and operating conditions, but those parameters cause a difference in another key property of the fuel – conversion ratio or CR. For this study, the fuels examined have CRs equal to 0.25, 0.70 and 1.05, the latter being a so called breeder reactor and the two former being burner reactors. A description of basic composition (Table 3.24) and geometry and operating conditions (Table 3.25) of each is presented below, but the reader is referred to Appendix A where more detailed model data are provided. Table 3.26 through Table 3.28 show the discharge isotopics and Table 3.29 presents the isotopic relative standard deviations for each fuel type, in order of ascending conversion ratio. The reader will observe that U-235 content does not monotonically change between conversion ratios as do other isotopics. This anomalous behavior is noted but the source could not be identified within this work. The reader will also observe that uncertainty increases with conversion ratio. Increasing conversion ratio requires increasing uranium content and the relative fissile fraction of TRU. In observing the values in the SCALE covariance library, the largest sources of uncertainty are the fission and absorption reactions of the fissile minor actinides, which are often correlated to U-235. It follows that the increase in uranium and fissile TRU fraction serve to magnify these uncertainties, thus uncertainty should increase as conversion ratio increases, which is the observed behavior.

Table 3.24: Fuel composition data for fast reactor models.

Nuclide / Conversion Ratio:	Weight Percent in TRU		
	0.25	0.7	1.05
Np-237	18.635	7.334	9.907
Pu-238	0.855	1.253	0.000
Pu-239	32.764	48.058	72.150
Pu-240	14.983	21.973	4.469
Pu-241	4.936	7.241	0.250
Pu-242	2.956	4.335	0.000
Am-241	20.579	8.100	10.941
Am-242m	0.041	0.016	0.022
Am-243	3.565	1.403	1.895
Cm-244	0.689	0.271	0.366
Cm-245	0.041	0.016	0.022
Fissile Fraction, %	37.7	55.30	72.40
TRU Enrichment, %	59.2	20.6	16.2
Zr w/o	20	10	10
Depleted U, w/o	20.8	69.4	73.8

Table 3.25: Fuel geometry and power data for fast reactor models.

Conversion Ration	0.25	0.70	1.05
Specific Power of active core, MW/MT	114.8	47.7	41.2
Discharge Burnup, GWD.MT	94.3	78.4	67.7
Height, cm	80	80	80
Number of pins per assembly	217	169	127
Assembly lattice pitch, cm	14.834	14.834	14.834
Inter-assembly gap, mm	4.45	4.0	4.0
Duct thickness, mm	4.45	3.0	3.0
Pin pitch-to-diameter ratio	1.29	1.11	1.10
Cladding thickness, mm	0.75	0.41	0.41

Table 3.26: Discharge isotopics for fast reactor fuel of CR = 0.25.

Discharge Isotopics, grams / MTHM					
pb210	4.950E-10	np237	9.563E+03	cm244	1.268E+04
ra226	4.002E-09	np239	1.147E+02	cm245	3.075E+03
ac227	1.967E-09	pu238	2.691E+04	c 14	9.454E-03
th227	2.759E-11	pu239	1.367E+05	se 79	1.023E+01
th230	4.585E-04	pu240	1.934E+05	sr 90	7.015E+02
pa231	4.248E-04	pu241	3.548E+04	tc 99	2.454E+03
u234	4.204E+02	pu242	5.692E+04	i129	5.747E+02
u235	5.135E+02	am241	2.383E+04	cs137	3.582E+03
u236	1.228E+02	am242m	1.908E+03	ba137m	5.560E-04
u237	9.338E-01	am243	1.807E+04	y90	2.008E-01
u238	3.789E+05	cm242	2.045E+03	cs134	1.694E+02

Table 3.27: Discharge isotopics for fast reactor fuel of CR = 0.70

Discharge Isotopics, grams / MTHM					
pb210	3.200E-10	np237	1.895E+03	cm244	2.249E+03
ra226	3.978E-09	np239	1.288E+02	cm245	5.264E+02
ac227	1.573E-09	pu238	5.555E+03	c 14	9.724E-03
th227	1.118E-11	pu239	9.083E+04	se 79	8.726E+00
th230	2.281E-04	pu240	6.292E+04	sr 90	6.166E+02
pa231	2.595E-04	pu241	9.851E+03	tc 99	2.040E+03
u234	1.632E+02	pu242	1.066E+04	i129	4.561E+02
u235	6.758E+02	am241	4.796E+03	cs137	2.878E+03
u236	2.213E+02	am242m	3.738E+02	ba137m	4.465E-04
u237	1.576E+00	am243	3.234E+03	y90	1.751E-01
u238	7.246E+05	cm242	3.251E+02	cs134	1.704E+02

Table 3.28: Discharge isotopics for fast reactor fuel of CR = 1.05.

Discharge Isotopics, grams / MTHM					
pb210	8.775E-11	np237	5.698E+02	cm244	2.776E+02
ra226	1.135E-09	np239	1.438E+02	cm245	6.964E+01
ac227	4.121E-10	pu238	1.370E+03	c 14	1.071E-02
th227	2.723E-12	pu239	8.565E+04	se 79	8.740E+00
th230	5.873E-05	pu240	3.916E+04	sr 90	6.242E+02
pa231	6.911E-05	pu241	5.607E+03	tc 99	2.013E+03
u234	4.292E+01	pu242	2.129E+03	i129	4.408E+02
u235	5.982E+02	am241	1.414E+03	cs137	2.814E+03
u236	2.533E+02	am242m	9.679E+01	ba137m	4.372E-04
u237	1.674E+00	am243	4.754E+02	y90	1.776E-01
u238	7.826E+05	cm242	9.319E+01	cs134	1.890E+02

Table 3.29: Relative isotopic uncertainties for fast reactor fuels.

Nuclide	Conversion Ratio		
	0.25	0.7	1.05
pb210	2.190	2.668	3.029
ra225	2.770	3.760	4.214
ac227	1.229	2.415	2.992
th227	1.227	2.415	2.990
th230	2.935	3.999	4.431
pa231	1.222	2.384	2.900
u234	3.129	4.317	4.723
u235	1.490	2.587	3.267
u236	1.795	4.793	5.535
u237	2.764	3.832	4.247
u238	0.205	0.230	0.255
np237	1.114	1.680	2.828
np239	10.752	15.475	15.989
pu238	3.371	4.824	5.204
pu239	1.468	2.406	2.800
pu240	0.906	1.992	3.066
pu241	2.764	3.833	4.246
pu242	0.548	1.150	3.141
am241	1.341	2.369	3.271
am242m	1.434	1.836	1.972
am243	10.752	15.475	15.989
cm242	1.434	1.837	1.972
cm244	13.025	16.925	19.875
cm245	4.344	9.295	11.948
c 14	1.655	0.962	0.708
se 79	1.137	0.627	0.544
sr 90	0.348	0.180	0.159
tc 99	0.319	0.472	0.554
i129	0.412	0.460	0.494
cs137	0.094	0.098	0.099
ba137m	0.094	0.092	0.099
y 90	0.348	0.181	0.158
cs134	2.553	2.250	2.214

3.2.3. Fast Reactor Model with Transuranic Fuel and Recycling

The principles of the recycling methodology have already been discussed, and it suffices to say that the model used in this experiment is the same as the CR = 0.70 model discussed in the previous section, save for the fact that the model burnup will be adjusted to give the end of cycle burnup of 41.4 GWD/MTHM rather than the end of life burnup

modeled in the previous section. This is done so that the target k-effective will be the one for end of cycle, which is what would be a real world objective of the reactor operator and fuel designer. Also, as indicated previously, the method of choice is the UREX process in which transuranics are separated as a stream and combined with depleted uranium to make up the new recycled fuel; however one could use any separation scheme with the methodology described. The model was run to an equilibrium state at 6 recycles and, in addition to typical uncertainty data, the beginning of cycle and end of cycle k-effective values, and their uncertainties, were also collected in output data. The values for end of cycle k-effective were also used to adjust transuranics loading with each recycle to maintain cycle energy production. Since the composition is defined by elemental weight percents and volume fractions, those are compared in Table 3.30. Table 3.31 gives the discharge isotopics of the equilibrium model and Table 3.32 shows discharge isotopics uncertainties originating due to cross sections, recycled isotopics, and total combined uncertainties. As can easily be seen from just the isotopics uncertainties, recycled isotopics originated uncertainties add to the cross-sections originated uncertainties to give almost a two-fold increase in total discharge isotopics uncertainties. A simple study (not shown) was conducted where it is assumed that the recycled fast reactor composition is known. When only the uncertainties of the LWR fuel were applied, this being a small fraction of the fuel in this particular TRITON model and possessing small uncertainties, the uncertainties originating from recycled isotopics in this case were negligible, (which is why they were not presented). In reality the reprocessing engineer knows fairly accurately the composition of the spent fast reactor and LWR fuels via performing mass spectroscopy. Knowing these compositions, the mass fractions of recycled fast reactor fuel, thermal reactor fuel, and depleted uranium would be altered to assure the

target EOC k-effective value is predicted to be achieved based upon cross section values which have inaccuracies.

Table 3.30: Comparison of fuel composition properties for once through and recycled fuel.

Fuel Composition Properties			No Recycle	Equilibrium
Uranium Volume Fraction:			0.5682	0.5594
U-235	(w/o)		0.200	0.200
U-238	(w/o)		99.800	99.800
Neptunium Volume Fraction:			0.0023	0.001
Np-237	(w/o)		100.000	100.000
Plutonium Volume Fraction:			0.1283	0.1380
Pu-238	(w/o)		1.512	2.972
Pu-239	(w/o)		57.999	47.048
Pu-240	(w/o)		26.518	37.937
Pu-241	(w/o)		8.739	5.715
Pu-242	(w/o)		5.232	6.929
Americium Volume Fraction:			0.0109	0.0108
Am-241	(w/o)		85.092	63.995
Am-242m	(w/o)		0.168	3.574
Am-243	(w/o)		14.740	32.431
Curium Volume Fraction:			0.0022	0.0031
Cm-242	(w/o)		0.000	1.170
Cm-244	(w/o)		94.444	76.878
Cm-245	(w/o)		5.556	21.952
Cm-246	(w/o)		0.000	1.170

Table 3.31: Discharge isotopics for equilibrium recycled fuel.

Discharge Isotopics, grams / MTHM					
pb210	7.407E-11	np237	1.172E+03	cm244	2.593E+03
ra226	1.074E-09	np239	1.264E+02	cm245	7.121E+02
ac227	5.675E-10	pu238	5.574E+03	c 14	4.817E-03
th227	5.309E-12	pu239	8.999E+04	se 79	4.781E+00
th230	1.214E-04	pu240	7.586E+04	sr 90	3.318E+02
pa231	1.061E-04	pu241	1.201E+04	tc 99	1.093E+03
u234	9.651E+01	pu242	1.257E+04	i129	2.591E+02
u235	9.771E+02	am241	5.878E+03	cs137	1.560E+03
u236	1.451E+02	am242m	3.963E+02	ba137m	2.418E-04
u237	1.475E+00	am243	3.506E+03	y90	9.372E-02
u238	7.452E+05	cm242	3.720E+02	cs134	5.866E+01

Table 3.32: Discharged isotopics uncertainties originating from recycled isotopics and cross sections sources of uncertainty.

Nuclide	Recycled Isotopics Originated (At Equilibrium)	Cross Sections Originated	Total
pb210	12.450	2.668	12.732
ra225	12.931	3.760	13.466
ac227	14.025	2.415	14.231
th227	14.026	2.415	14.232
th230	12.681	3.999	13.296
pa231	13.465	2.384	13.674
u234	12.364	4.317	13.096
u235	1.121	2.587	2.819
u236	3.189	4.793	5.757
u237	5.460	3.832	6.671
u238	0.120	0.230	0.260
np237	11.311	1.680	11.435
np239	44.021	15.475	46.662
pu238	11.931	4.824	12.869
pu239	4.296	2.406	4.924
pu240	5.107	1.992	5.482
pu241	5.460	3.833	6.671
pu242	6.325	1.150	6.429
am241	6.846	2.369	7.244
am242m	9.100	1.836	9.284
am243	44.021	15.475	46.662
cm242	9.100	1.837	9.284
cm244	9.202	16.925	19.265
cm245	12.163	9.295	15.308
c 14	2.886	0.962	3.042
se 79	1.415	0.627	1.548
sr 90	0.369	0.180	0.410
tc 99	0.204	0.472	0.514
i129	0.719	0.460	0.854
cs137	0.106	0.098	0.144
ba137m	0.106	0.092	0.140
y 90	0.369	0.181	0.410
cs134	1.932	2.250	2.966

3.2.4. Comparison of Results, TRITON Models

As with the simplified models, the two most commonly examined metrics for repository performance or reprocessing – decay heat and radioactivity spanning 10 to 10,000 years of decay time, are graphically presented. These data are plots of the numerical values of the metrics, propagated from number density uncertainties presented in the previous sections for the TRITON models, including once through and the recycling method.

The first plots compare the uncertainty between the PWR models for the simplified ORIGEN method and the TRITON method (decay heat in Figure 3.11 and radioactivity in Figure 3.12). While, in terms of isotopics, the two methods deliver different uncertainties for reasons already discussed, as can clearly be seen, the long term affect on the metrics of interest is generally the same. This occurs mainly because the uncertainty on the long term heat contributors, e.g. plutonium, is on the same order of magnitude between the two models.

Next, the fast reactor models, three different compositions and conversion ratios, are compared with each other for the no recycle case. Since these are three different fuel types with different operating and composition parameters, comparison just provides a look at the three possibilities. While decay heat (Figure 3.13) and radioactivity (Figure 3.14) were higher for the low conversion ratio fuel, its long term uncertainty was the lowest. This is an interesting consideration for planning a fuel scenario regarding what one wants to dispose of and what one wants to recycle.

Finally, comparison is drawn between once-through faster reactor fuel and recycled fast reactor fuel, adding to it a stream of spent light water reactor fuel. As one would expect, uncertainty in both decay heat (Figure 3.15) and radioactivity (Figure 3.16) is higher in the

recycled fuel than in the once-through, and these figures give a visual comparison of that difference. In general, recycling nearly doubled the amount of uncertainty on the metrics examined, though the nominal long term performance is nearly identical for the two cases. Also, the k-effective study shows that the uncertainties originating from cross sections are the greatest contributor to k-effective uncertainty in that method (Figure 3.18), but uncertainties originating from recycled isotopic uncertainties scheme (recycling uncertainties alone in Figure 3.17) add a noticeable increase to that uncertainty (Figure 3.18). As can be seen from these figures, uncertainty from recycling seems to increase to some saturation as equilibrium is reached.

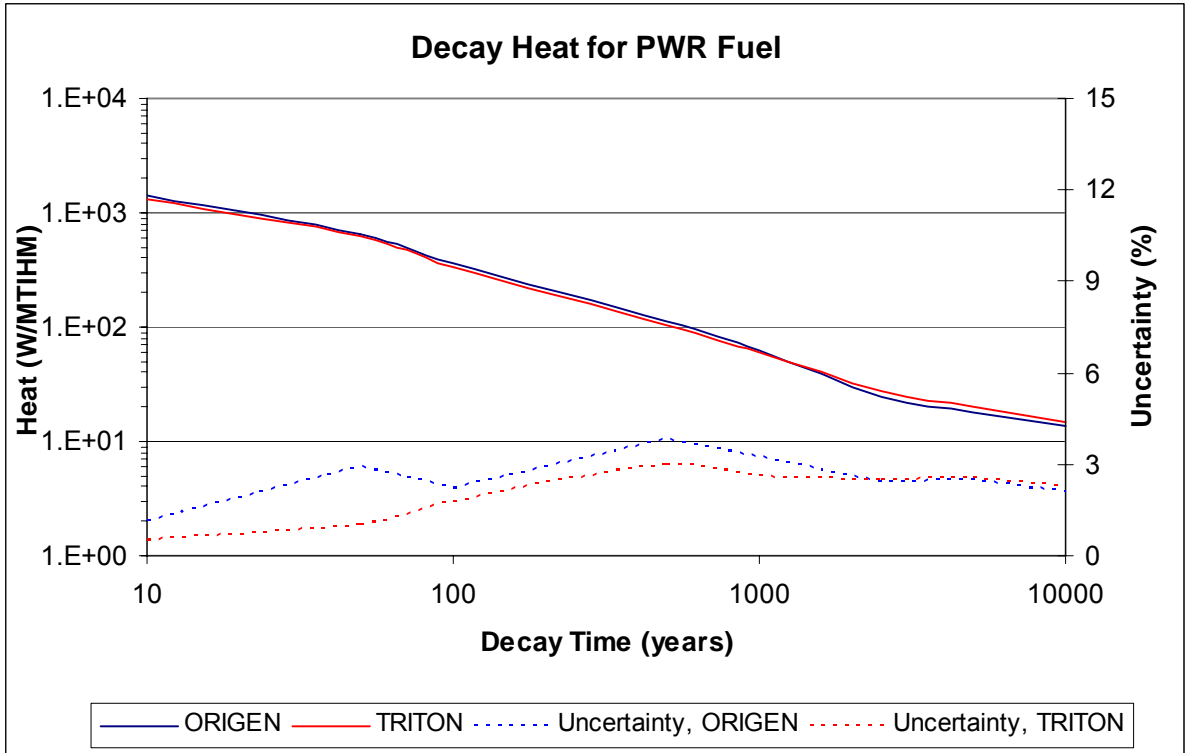


Figure 3.11: Decay heat comparison of simple ORIGEN and TRITON models.

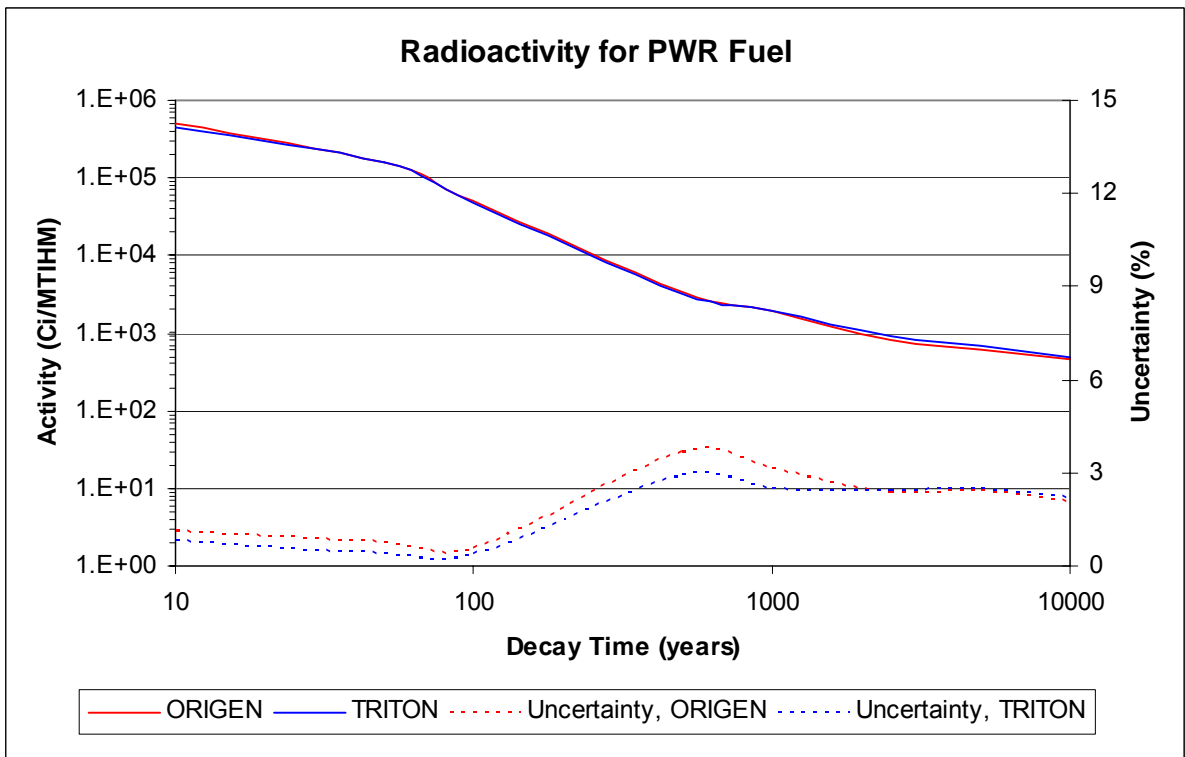


Figure 3.12: Radioactivity comparison of simple ORIGEN and TRITON models.

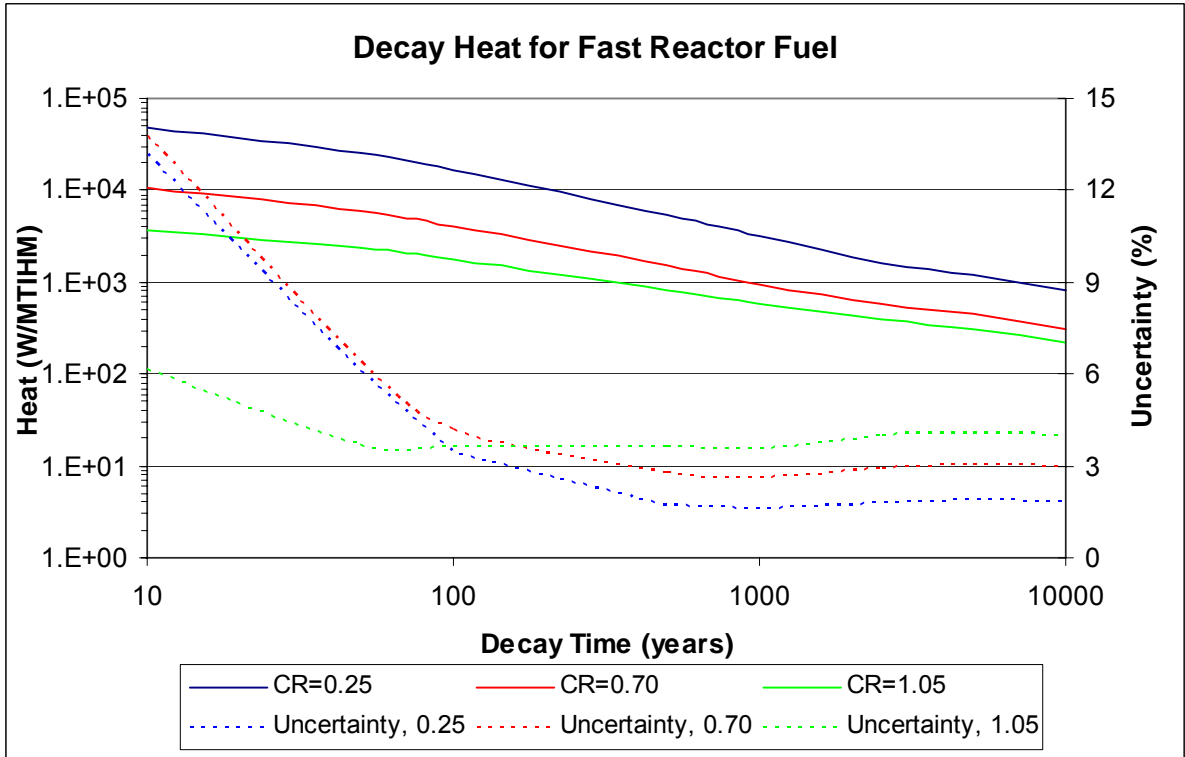


Figure 3.13: Decay heat comparison of three fast reactor fuels.

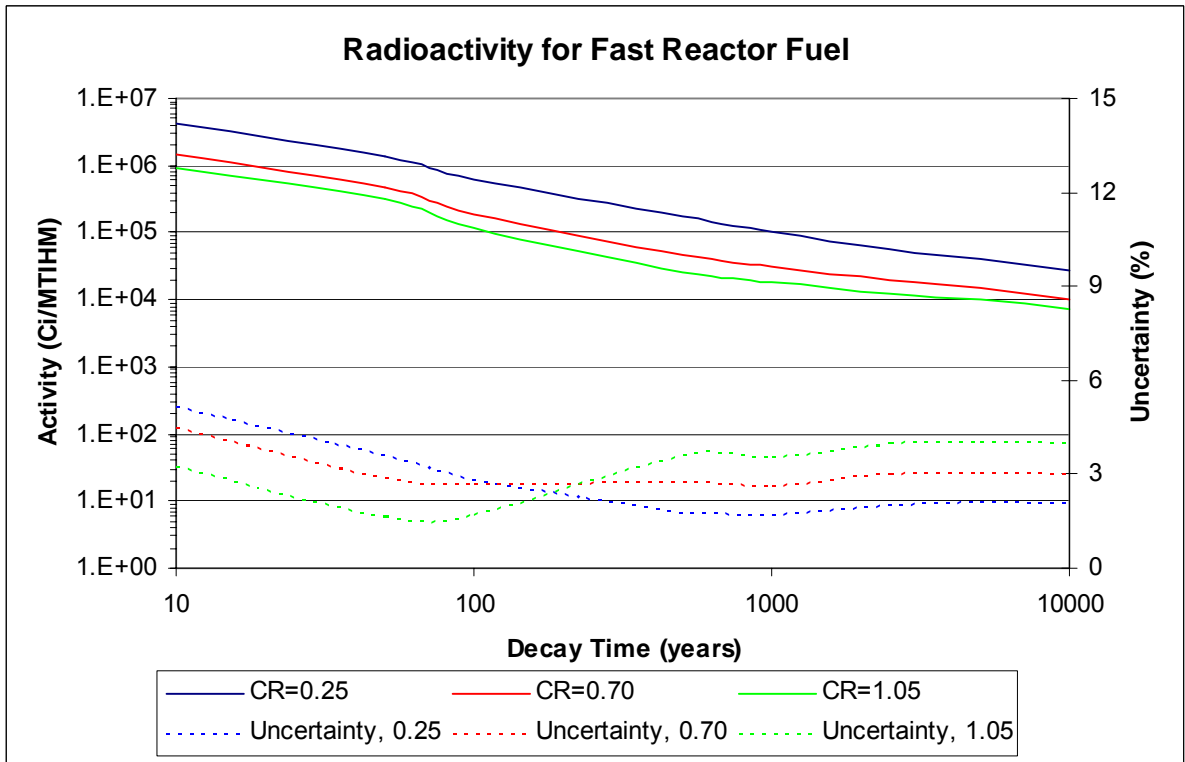


Figure 3.14: Radioactivity comparison for three fast reactor fuels.

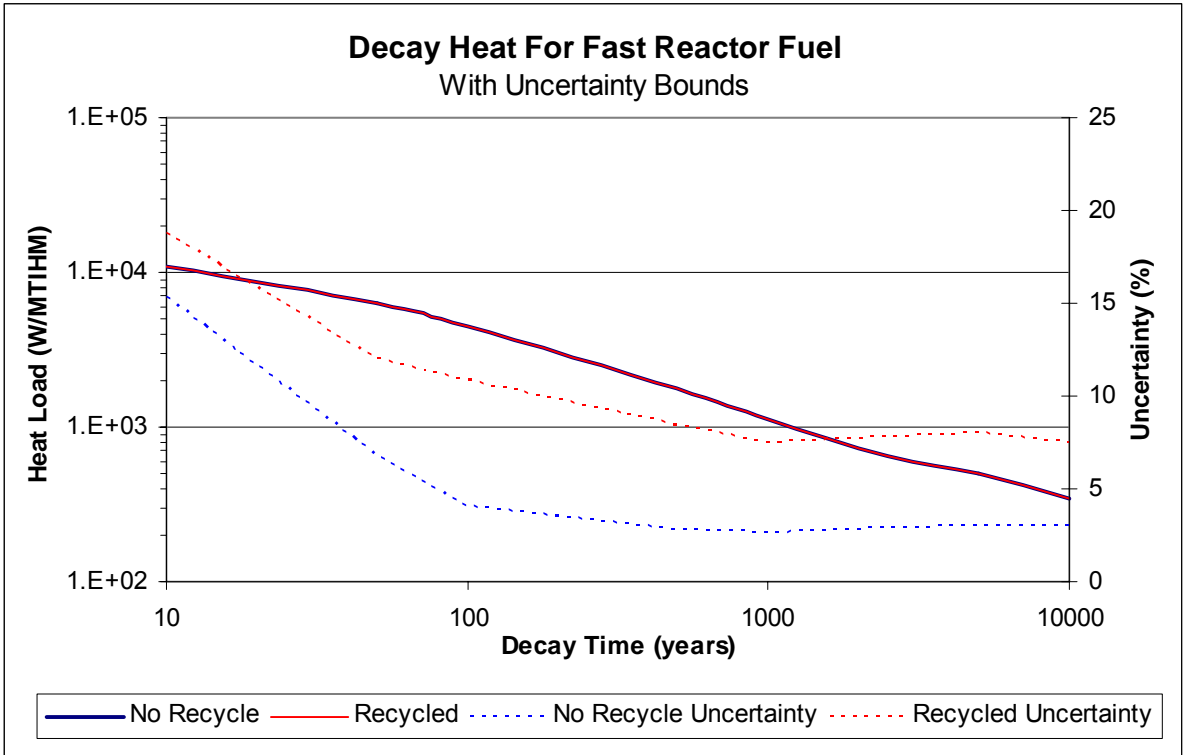


Figure 3.15: Decay heat comparison of once through and recycled fast reactor fuels.

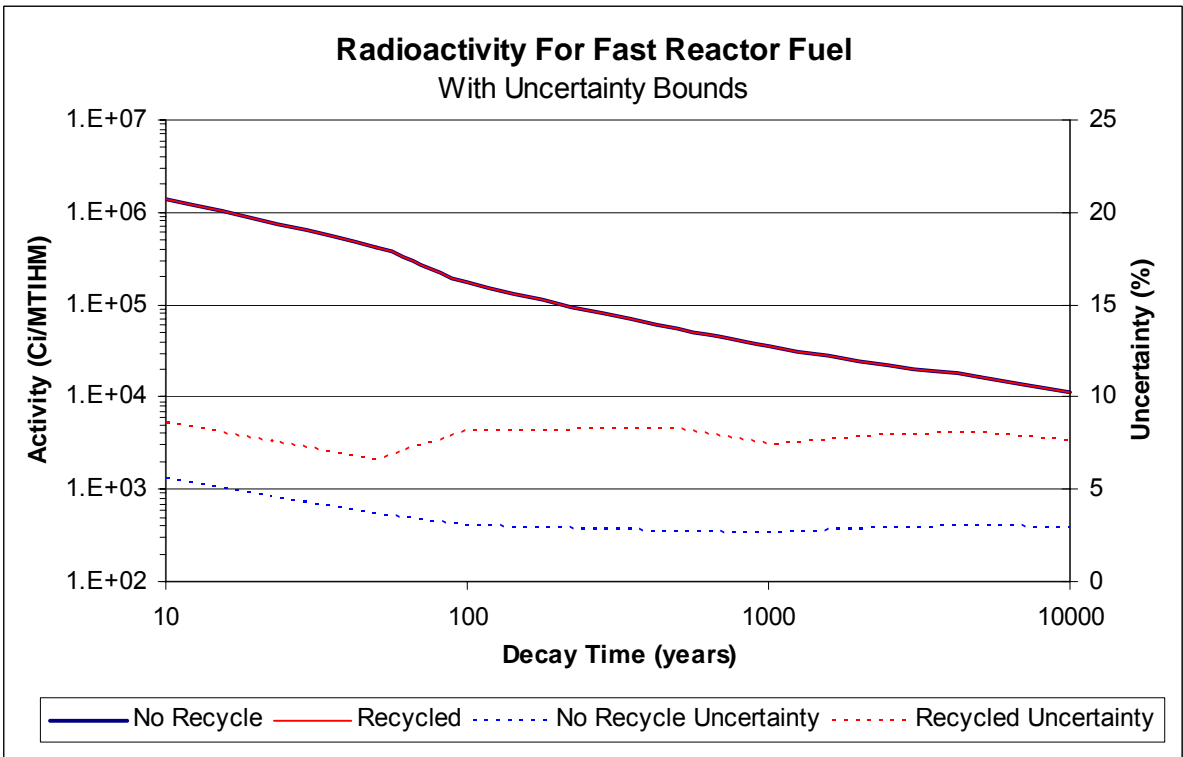


Figure 3.16: Radioactivity comparison of once through and recycled fast reactor fuels.

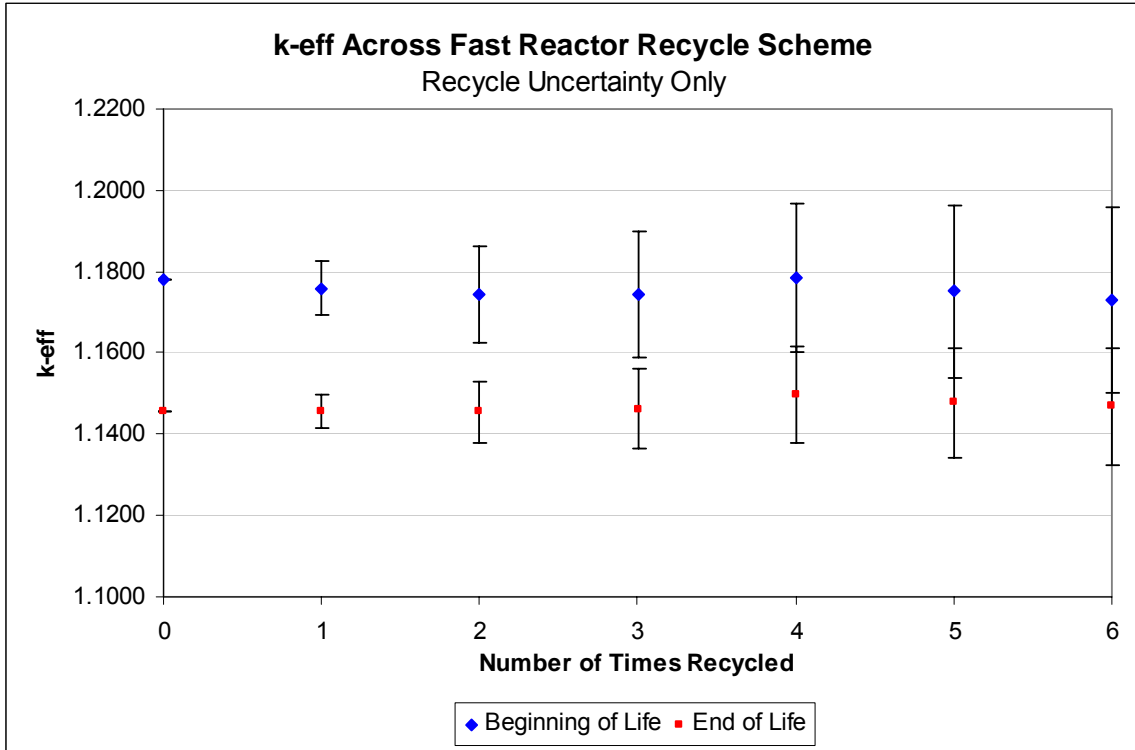


Figure 3.17: k-effective uncertainty due to recycled isotopes uncertainties only.

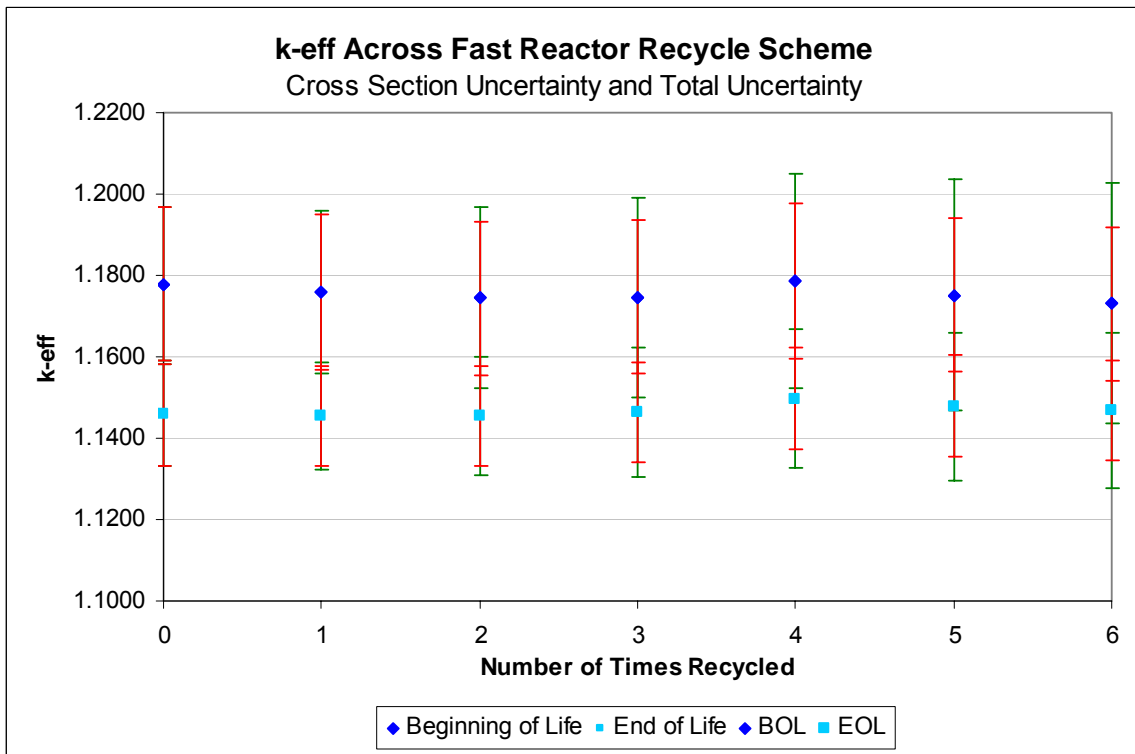


Figure 3.18: k-effective uncertainty due to cross sections and recycled isotopes.

3.3. REBUS Fast Reactor Equilibrium Model

With the TRITON sequence producing questionable results for the fast reactor models examined, REBUS was used to examine a fast reactor fuel with uncertainty. The code REBUS, developed by Argonne National Laboratory, is similar to TRITON in that it takes a fuel composition, simulates operating a reactor with that fuel and performs depletion analysis and returns reactor operating parameters (e.g. burnup, k-effective, etc.) REBUS's capability to automatically perform a recycling analysis, brining the fuel to an equilibrium recycling scenario, is exploited here unlike in TRITON where this process was done externally. Further REBUS was able to easily model a 1/3 reactor core with all the heterogeneities as opposed to TRITON's one smeared cell, implying a more reliable model. One draw-back of REBUS is that it can only specifically track the actinide number densities, unlike the SCALE codes which track almost every isotope. For this reason, information from REBUS about amounts of fission and decay products present in the spent fuel is not available. The REBUS k-effective results are closer to expected values than those of the TRITON model, implying a more likely flux spectrum, and thus more likely isotopic composition and fuel depletion. The k-effective for EOC, along with EOC conversion ratio, are provided in Table 3.33 with uncertainty. All results are for the equilibrium composition.

Cross-section uncertainty propagation, using ESM, was implemented in the REBUS code by Dr. Hany Abdel-Khalik. Developed as part of the work reported here was an equilibrium model in REBUS for the fast reactor with a conversion ratio of ~ 0.77 , using the same recycling specifications given for the recycle scenario using TRITON. The model was executed using Dr. Abdel-Khalik's modified version of REBUS.

Table 3.34 gives the discharge isotopics, here EOC core composition normalized to 1 MTHM, and Table 3.35 presents the isotopic uncertainties. Figure 3.19 - Figure 3.20 show the heat load and radioactivity, respectively, with the uncertainty for the REBUS model compared to the TRITON recycle model. Uncertainties on the LWR recycled isotopics were considered, accomplished by perturbing the LWR isotopics in each input deck via the ESM approach and then determining the uncertainties produced by these, which were very small. The results presented include these perturbations as well as the uncertainty induced by cross section uncertainties. A drawback in REBUS is that correlations between the cross section induced uncertainties and the recycled LWR isotopics induced uncertainties must be assumed to be zero. That is the cross section uncertainties that lead to producing the recycled isotopics uncertainties during LWR operations are not consistently carried forward to the REBUS model of FR operations. To do this, a singlet set of cross sections and their perturbations would need to be employed by the models representing LWR and FR operations. In examining the results, note that these values are much closer to those indicated by the ABTR report [26], in isotopics as well as conversion ratio and k-effective, than are the TRITON results. As discussed before, uncertainties are available only for the actinides and are considerable higher than those predicted by TRITON. With the exception of the initial decay heat uncertainty, the REBUS results had uncertainties more than twice as high as the TRITON model. The higher results are due to a different cross section library, covariance library, and model – all specialized for the fast reactor. The assumptions forced by the resonance treatment in TRITON were recognized to be missing uncertainty components, thus the uncertainties likely underestimated. The REBUS 15-group structure has very little dependence on thermal energies, with 14 of the 15 groups spanning fast and

resonance energies. Since the structure was designed for the fast reactor, the associated uncertainties are more indicative of the fast system and less restricted by the issues in TRITON.

Table 3.33: Operating Parameters for REBUS model.

Operational Parameter	Nominal Value	Uncertainty (%)
EOC k-effective	0.99925	0.2180
EOC Core Conversion Ratio	0.7695	1.7147

Table 3.34: Discharge Isotopics for REBUS model.

Discharge Isotopics, grams / MTHM					
pb210	--	np237	3.644E+03	cm244	1.836E+03
ra226	--	np239	--	cm245	4.324E+02
ac227	--	pu238	6.074E+03	c 14	--
th227	--	pu239	1.030E+05	se 79	--
th230	--	pu240	6.228E+04	sr 90	--
pa231	--	pu241	8.259E+03	tc 99	--
u234	1.088E+02	pu242	1.230E+04	i129	--
u235	1.213E+03	am241	7.936E+03	cs137	--
u236	9.393E+01	am242m	5.665E+02	ba137m	--
u237	--	am243	3.968E+03	y90	--
u238	7.878E+05	cm242	2.355E+02	cs134	--

Table 3.35: Isotop Uncertainties for REBUS model.

Isotopics Uncertainties, grams / MTHM					
pb210	--	np237	7.344	cm244	20.387
ra226	--	np239	--	cm245	38.508
ac227	--	pu238	18.616	c 14	--
th227	--	pu239	1.336	se 79	--
th230	--	pu240	7.463	sr 90	--
pa231	--	pu241	10.570	tc 99	--
u234	18.383	pu242	18.769	i129	--
u235	0.809	am241	10.163	cs137	--
u236	2.034	am242m	14.836	ba137m	--
u237	--	am243	17.986	y90	--
u238	0.950	cm242	8.856	cs134	--

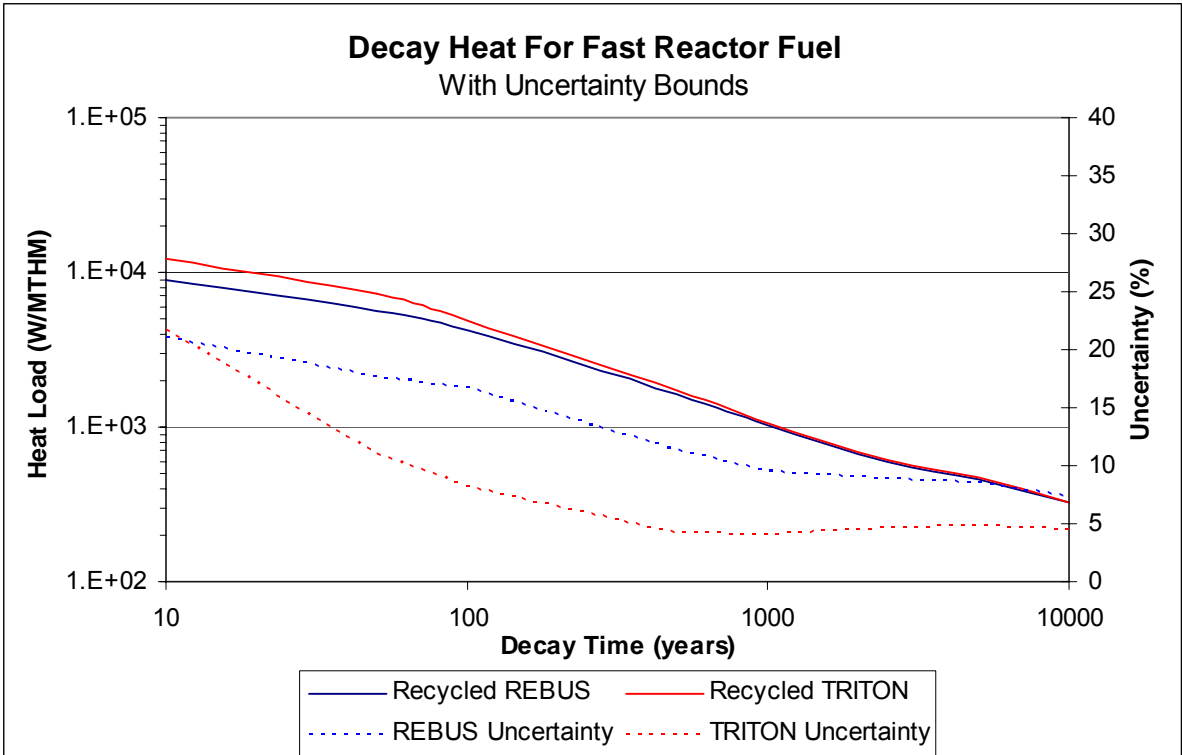


Figure 3.19: Decay heat comparison of REBUS and TRITON Models.

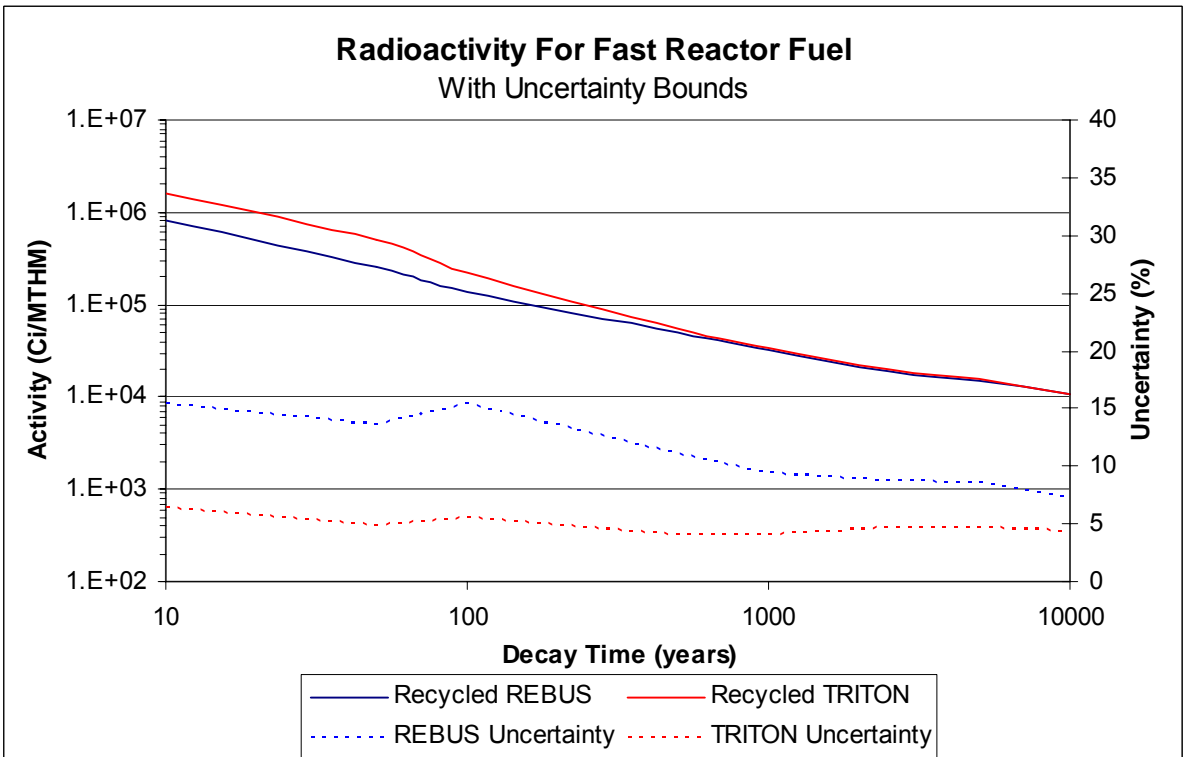


Figure 3.20: Radioactivity comparison of REBUS and TRITON Models.

4. Discussion and Conclusions

4.1. Discussion of the Use of ESM in this Study

The Efficient Subspace Method (ESM) has been demonstrated to produce results equivalent to those of traditional stochastic sampling methods. While this provides an alternative to these methods in any case where stochastic sampling could be used, it is most beneficial in models where stochastic methods would not be practical. For the case of the TRITON and REBUS models, where perturbed input data numbered in thousands, stochastic sampling would have taken at least twice as long as using ESM. In most multi-scale, multi-physics codes, such as the TRITON sequence in SCALE, input data do number in the thousands, if not orders of magnitude higher. For example, the core simulator FORMOSA developed at North Carolina State University has millions of input data, and, if perturbed, would have thousands of millions of perturbations. With growing reliance on computer simulation in many industries, including nuclear, these large, complex models are becoming more popular and necessary. Thus, having a method to quickly and efficiently propagate uncertainties becomes a much desired capability. Since one goal of this study was to demonstrate the capability of ESM to perform in this manner, it can be concluded that ESM can be successfully used on large, complex models while producing results that are equivalent to traditional sampling methods.

4.2. Discussion Concerning the Results of the Models

The other objective of this study was to determine how cross section uncertainties affect back-end fuel cycle metrics such as decay heat, radioactivity, and radiotoxicity.

Essentially, this implies determining how cross section uncertainty affects the composition of what is discharged from the reactor, since all other metrics are directly proportional to isotopic masses. For the UOX fuels, in both the simplified and detailed models, uncertainty on these metrics was 1-2 % for the first 100 years and then 3-5% thereafter. Short term uncertainty is dominated by low-uncertainty fission products that make up the majority of the heat load and activity in the first 100 years. The constant uncertainty in the long term is due to a few long lived actinides, mainly plutonium and americium isotopes. When looking at the simplified MOX fuels, the uncertainty increases in the short term, especially for the decay heat, due to uncertainty in fission products and short lived actinides caused by the uncertainties on the fission and absorption cross sections of the minor actinides, which are now present in greater quantities. However, the long term uncertainty is still about 5%, stemming from long lived actinides with similar uncertainties to those for the same isotopes in the UOX fuel.

Considerable differences between the short term uncertainties for the PWR models were discovered between the simplified ORIGEN model and the TRITON model. An evaluation concluded this was the result of the resonance treatment applied in the TRITON sequence. In the simple ORIGEN models, prepared 1-group cross sections were perturbed just before the depletion calculation. However in TRITON, only the reference 44-group cross sections were perturbed, and the resonance component in the resolved resonance regions missed, which diminished the affect of the perturbations. Further study on this topic was beyond the scope of the current work.

The fast reactor TRITON models, though the short-comings of the model are recognized, showed considerably higher values for heat load and radioactivity than those of

the PWR model. This was expected because of the nature of the fuel, that being a large weight percent of transuranics which contribute to the longevity and magnitude of these metrics. The increasing activity and decay heat with respect to decreasing conversion ratio is the result of increasing the transuranic enrichment and extending the burnup to reach the clad fluence limit, therefore building up more of products contributing to these metrics. The increasing uncertainty with increasing conversion ratio results from the increase of uranium content and fissile fraction of the TRU, which have large, highly correlated uncertainties. Still the over all long term uncertainty of these fuels is about 3-5 %.

The TRITON recycling models show the expected result of increasing uncertainty as fuel is recycled to an equilibrium. While this process nearly doubles the uncertainty, long term uncertainties are still on the order of 5% but short term uncertainties could increase from 10 to 20%, which would result in more conservative handling and processing in the near term. The main concern of recycling would appear to be the uncertain compositions being used as fuel for the reactor, but this is easily eliminated by measuring the isotopic masses prior to refabrication. Recycling isotopics uncertainties add a non-negligible amount to the already present cross-section uncertainty on k-effective values.

The REBUS equilibrium recycling model was nominally comparable to the TRITON model in terms of long term heat load and radioactivity. However the nominal REBUS results are regarded as more indicative of the properties of the spent fuel in consideration, since that model very nearly matched the one in the Argonne report after which it was designed, both in isotopics and operating conditions. The uncertainty displayed by the REBUS model was, however, considerable different than that of the TRITON model, in some instances up to 7 times greater. This indicates that, as stated in the discussion on

resonance treatment, that the TRITON model was underestimating the uncertainty on the isotopics, which propagated to the metrics examined. Also the 11% uncertainty on the conversion ratio implies that reactor operation may or may not destroy the desired amount of actinides, which is essentially the job of this type of reactor. So, for this equilibrium fuel cycle, judging from the REBUS results, the fuel that is discharged from the reactor needs to be carefully measured in terms of isotopics before refabrication or would have to be treated very conservatively if immediately disposed of. Thankfully there would not be much of it to dispose of if widespread use of fast reactors destroyed much of the spent LWR fuel.

If one is simply disposing of UOX or even MOX fuel that was burned in a LWR, uncertainties due to cross sections seem to be of little concern. This is especially true when one considers the highly restrictive geological uncertainties, waste package material uncertainties, and even reactor operation uncertainties, which can easily overwhelm the low uncertainties seen for these models. However, when one considers reprocessing, cross-section uncertainties become more important. High short term uncertainties on decay heat and activity would result in more conservative handling of fuels for reprocessing. Isotopic uncertainties for fuel mainly impact composition changes during irradiation and design of the repository, since isotopics can be measured prior to refabrication. The decrease in repository loading due to fast reactor operation likely will outweigh the uncertainty associated with that fuel, but further study on such margins is needed. Concluding from these results, cross section uncertainty would need to be reduced to better the operation of fast reactors and dispose of their reprocessed fuel.

4.3. Recommendations and Future Work

The immediate future work is to develop the uncertainty propagation methodology in this work into a model that is usable within SINEMA's primary software, GENIUS. In keeping with the GENIUS format, this will be a series of tables from which to interpolate data concerning uncertainties, given a fuel composition and discharge burnup, for each reactor type. Further development should be implemented in the TRITON sequence to improve the treatment of resonance uncertainties.

Beyond the cross section uncertainties propagated into the isotopics, which is all that was considered in this work, reprocessing includes chemical reaction rates and uncertainties, plant efficiencies, separation time, storage and transport time, etc. All of these can play a role in the composition of the fuel that is fabricated. Also, as shown in a very simple experiment for an LWR, operational uncertainties can add much more to the uncertainties seen in the discharged isotopics than the cross sections do, so they warrant further study. Finally, the metrics considered herein were rather simplistic metrics, directly related to isotopics masses and instantaneous in nature. The uncertainty margins on more thorough, integral metrics (e.g. long-term heat integral, or dose calculations) would also be of interest, especially for disposal purposes. For the recycling cases, further study should be conducted to include correlations between recycled isotopics uncertainties and cross sections uncertainties, which were assumed uncorrelated in this work. Finally the cut-off value for the choice of samples to run could be adjusted, as the value used in this work was a very conservative. Removing unused cross sections and working with absolute values rather than relative values could help the user to better select which samples to run. In this work, an

unimportant cross section may have a high relative uncertainty and that sample would be kept when it does not actually need to be run.

References

- [1] Official Site of the Simulation Institute for Nuclear Energy Analysis. 2006-2007. 1 June 2006. <<http://thesinema.org>>.
- [2] Wigeland, R., et. al. "Repository Impact of LWR MOX and Fast Reactor Recycling Options". ANS Topical Meeting. New Orleans, LA 2003.
- [3] Yacout, A., et. al. "Dynamic Analysis of the AFCI Scenarios". Proceedings of the PHYSOR 2004: The Physics of Fuel Cycles and Advanced Nuclear Systems - Global Developments 2004: 785-794
- [4] Bathke, C., et. al. "Report of LANL Advanced Fuel Cycle Systems Analyses for FY 2003". Los Alamos National Laboratory. 2004.
- [5] J. Saling. Radioactive Waste Management, 2nd Edition. Taylor and Francis, 2001.
- [6] Bunn, M., et. al. "Economics of Reprocessing vs. Direct Disposal of Spent Nuclear Fuel". Harvard University, 2003
- [7] Rose, P. F. and C. L. Dunford. "ENDF-102: Data Formats and Procedures for the Evaluated Nuclear Data File ENDF-6". Brookhaven National Laboratory. 1990.
- [8] Turinsky, P., H. Abdel-Khalik, and T.E. Stover. "Development of Uncertainty Analysis Capabilities for the SINEMA Project, FY 2006 Report". North Carolina State University. 2006.
- [9] Duderstadt, J., and L. Hamilton. Nuclear Reactor Analysis. Hoboken, NJ. John Wiley & Sons, Inc., 1976.
- [10] Schneider, E., and C. Bathke, "Sensitivity of Fuel Cycle Performance Metrics to Perturbations in Cross-Sections". Transactions of the American Nuclear Society v 92, 2005.
- [11] Ronen, Yigal. Uncertainty Analysis. Boca Raton, FL. CRC Press Inc., 1988.
- [12] Aliberti, G., et. al. "Nuclear data sensitivity, uncertainty and target accuracy assessment for future nuclear systems". Annals of Nuclear Energy, 33(8), 2006: 700-733.
- [13] Aliberti, G., et al. "Impact of Nuclear Data Uncertainties on Transmutation of Actinides in Accelerator-Driven Assemblies," Nuclear Science and Engineering v 146, 2004: 13-50.
- [14] H. Abdel-Khalik, "Adaptive Core Simulation". Ph.D. Dissertation. North Carolina State University, 2004.
- [15] Cacuci, Dan. Sensitivity and Uncertainty Analysis, Volume I. Chapman & Hall/CRC Press, 2005.
- [16] Olsson, A., and G. Sandberg, "Latin Hypercube Sampling for Stochastic Finite Element Analysis". Journal of Engineering Mechanics January 2002.
- [17] Bendat, J., and A. Piersol. Random Data: Analysis and Measurement Procedures. 2nd Ed. Hoboken, NJ. John Wiley & Sons, Inc., 1986.

- [18] Kawano, T., et. al. “Evaluations and Propagation of the Pu-239 Fission Cross-Section Uncertainties Using a Monte Carlo Technique”. Nuclear Science and Engineering v 153, n 1, May 2006: 1-7.
- [19] Oak Ridge National Laboratory. SCALE: A Modular Code System for Performing Standardized Computer Analyses for Licensing Evaluations. ORNL/TM-2005/39, Version 5, Vols. I–III, 2005.
- [20] Argonne National Laboratory. REBUS-3/Variant 8.0: Code System for Analysis of Fast Reactor Fuel Cycles. CCC-653, REBUS-3, Variant 8.0, 2001.
- [21] Gauld, I. C., et. al. “ORIGEN-S: Scale System Module to Calculate Fuel Depletion, Actinide Transmutation, Fission Product Buildup and Decay, and Associated Radiation Source Terms”. Oak Ridge National Laboratory. ORNL/NUREG/CSD-2/V2/R7, 2004
- [22] Gauld, I.C., and O. Hermann “SAS2: A Coupled One-Dimensional Depletion and Shielding Analysis Module”. Oak Ridge National Laboratory. ORNL/TM-2005/39 Version 5 Vol. I, Book 3, Sect. S2, 2005.
- [23] DeHart, M.D. “TRITON: A Two-Dimensional Depletion Sequence for Characterization of Spent Nuclear Fuel”. Oak Ridge National Laboratory. ORNL/TM-2005/39 Version 5 Vol. I, Book 3, Sect. T1, 2005.
- [24] Rochman, D., et. al. “Preliminary Cross Section and $\bar{\nu}$ -bar Covariances for WPEC Subgroup 26”. National Nuclear Data Center. Brookhaven National Laboratory. BNL-77407-2007-IR, 2007
- [25] Argonne National Laboratory. MC² - 2: Code System for Calculating Fast Neutron Spectra and Multigroup Cross-Sections. PSR-350, MC² – 2, 2000.
- [26] Chang, Y.I., et. al. “Advanced Burner Test Reactor, Preconceptual Design Report”. Argonne National Laboratory. ANL-AFCI-173, 2006.
- [27] Tarantola, A., Inverse Problem Theory: Methods for Data Fitting and Model Parameter Estimation. Elsevier Science Publishers B. V., 1987.
- [28] Figliola, F., and D. Beasley. Theory and Design for Mechanical Measurements. 3rd Ed. Hoboken, NJ. John Wiley & Sons, Inc., 2000.
- [29] Tong, Y.L. Multivariate Normal Distribution. New York, NY. Springer-Verlag, 1990.
- [30] Jordan, W., et. al. “SCALE Cross-Section Libraries”. Oak Ridge National Laboratory. ORNL/TM-2005/39 Version 5 Vol. III, Sect. M4, 2005.
- [31] Rearden, B. “Sensitivity Utility Modules”. Oak Ridge National Laboratory. ORNL/TM-2005/39 Version 5 Vol. III, Sect. M18, 2005.
- [32] Hermann, O., and M. DeHart. “Validation of SCALE (SAS2H) Isotopic Predictions for BWR Spent Fuel”. Oak Ridge National Laboratory. ORNL/TM-13315, 1998.
- [33] Cochran, R., and N. Tsoulfanidis. Nuclear Fuel Cycle: Analysis and Management. 2nd Ed. Washington D.C. American Nuclear Society, 2002.

Appendices

Appendix A: Fuel Models

I. The Typical LWR Model Using a UOX Fuel

For use in base cases and general examples, SCALE is distributed with a flux spectrum and three-group card image cross-section library that are representative of a typical LWR. The first sampling routine was implemented with this resource. The input library can be used in its three-group form along with the flux spectrum supplied directly to ORIGEN or the library may be collapsed to a one-group binary library. This model was taken directly from the ORIGEN users manual and changed only in the enrichment of U-235 to 4.5 w/o rather than the 3.3 w/o of the original example problem so the reader is referred to the ORIGEN users manual [21].

II. The PWR Model Using a UOX Fuel

The PWR model used in this study is based on the example provided with the SCALE 5.0 SAS2H User's Manual, that being a Westinghouse type PWR fuel assembly (Figure A.II.1). The assembly is 17 pins by 17 pins with 25 water holes and an active fuel length of 12 feet (365.76 cm) in a square pitch design. Fuel rods have a pitch of 1.25984 cm and an outside diameter of 0.83566 cm (no gap in this model). The fuel itself is UO₂ containing 461.4 kg of uranium in the proportions 4.50 w/o U-235, 95.472 w/o U-238 and 0.028 w/o U-234 and is volume fraction weighted (VF=0.90182) for the given fuel assembly based on the volume weighting method described in the SAS2H user's manual, i.e. VF depends on mass of fuel and volume of fuel assembly. Cladding is zirc2 (versus actual zirc4) and the moderator is water. Operating temperatures are 811, 570 and 570 degrees Fahrenheit for the

fuel, clad and moderator respectively with the moderator density at 0.733 g/cm³. The SAS2H model is burned at a specific power of 18.456 MW/assembly for 1000 days giving a total burnup of 40 GWD/MTU.

The corresponding ORIGEN model (Figure A.II.2), from which sampling is conducted, is one metric ton of the 4.5 w/o UOX fuel with approximately 271 kg of zirc2 cladding. The ORIGEN model is set to deplete the fuel using the binary cross section library generated from the fuel specific SAS2H model. Note: cross section perturbations are introduced directly into this binary working library during the sampling procedure. Fuel specific power density is 40 MW/MTU for a cycle length of 1000 days giving the same 40GWD/MTU burnup as the SAS2H Model. The ORIGEN model is set to “burn” the fuel for 10 equal time steps at 100% power and then print out decay isotopics at charge, discharge, 1, 5, 10, 50, 100, 500, 1000, 2500, 5000, and 10000 year times. ORIGEN also has the availability to print the decay heat, activity, and radiotoxicity for these times.

```
=sas2 parm='skipcellwt'
sas2 LWR UOX: 40 mwd/kgHM, 17*17 pin, pwr, 1 cyc
44groupndf5 latticecell
'-----
' FUEL COMPOSITION
'-----
uo2  1 0.90182 811 92234 0.028 92235 4.5 92238 95.472 end
'-----
' CLADDING
'-----
zirc2 2 1 620 end
'-----
' MODERATOR / COOLANT
'-----
h2o 3 den=0.733 1 570 end
end comp
'-----
' FUEL-PIN GEOMETRY
'-----
squarepitch 1.25984 0.83566 1 3 0.94996 2 end
more data szf=1.2 eps=1.0-7 ptc=1.0-8 end
'-----
' ASSEMBLY AND CYCLE PARAMETERS
```

Figure A.II.1: SAS2H Model, PWR, 4.5 w/o and 40 GWD/MTU

```

'-----
npin/assm=264 fuelngth=365.76 ncycles=1 nlib/cyc=1
printlevel=6
lightel=16 inplevel=1
numins= 1 ortube= 0.61214 srtube=0.5715 facmesh=1.4 end
power=17.3025 burn=1066.67 down=0 end
'power=18.456 burn=1000.0 down=0 end
'-----
' Light elements (kg) per assembly
'-----
c 0.05999 n 0.03377 o 62.14 al 0.04569
si 0.06586 p 0.1422 ti 0.04983 cr 2.340
mn 0.1096 fe 4.599 co 0.03344 ni 4.402
zr 100.8 nb 0.3275 mo 0.1816 sn 1.652
'-----
end

```

Figure A.II.1: SAS2H Model, PWR, 4.5 w/o and 40 GWD/MTU, cont.

```

=origens
0$$ a5 28 e
1$$ 1
1t
pwr nuclear data - sample case 1
'-----
'Uses SAS Updated Lib
'-----
3$$ 33 0 1 -88 a33 -88
'-----
2t
35$$ 0
4t
56$$ 10 a13 50 4 3 0 1 1 e
57** a3 1-14 e
95$$ 1
5t
pwr - 4.5% enriched u
mt of heavy metal charged to reactor
'-----
'Power specifications, 40 MW for 1000 Days
'-----
58** 10r40
60** 8i110 1000
'-----
'Nuclide identifies - charged nuclides
'-----
66$$ 1 a5 1 a9 1 e
73$$ 60120 130270 140280 140290 220460 220470 220480 220490
220500 240500 240520 240530 240540 250550 260540 260560 260570 260580
270590 280580 280600 280610 280620 280640 400900 400910 400920 400940
400960 410930 420920 420940 420950 420960 420970 420980 421000 501120
501140 501150 501160 501170 501180 501190 501200 501220 501240
922350 922380 922340
'-----
'Molar masses of charged nuclides
'-----
74** 1.5 4.0 .607 .034 .304 .277 2.771 .204 .2 5.04

```

Figure A.II.2: ORIGEN Model, PWR, 4.5 w/o and 40 GWD/MTU

```

57.423 6.415 1.574 0.327 4.037 61.018 1.439 0.31 0.915 111.862
41.783 1.869 5.645 1.609 1421.122 306.725 462.239 460.074 72.5 10.258
.957 .532 .926 .958 .546 1.357 .54 .321 .219 .113
4.681 2.47 7.729 2.739 10.392 1.467 1.823 191.45 4011.75 1.13
' - - - - -
75$$$ 47r1 3r2 t
56$$$ 0 10 a10 10 a14 5 a17 2 e

57** a3 1-14 e
95$$$ 1 5t
' - - - - -
'Decay time steps in years
' - - - - -
60** 1 5 10 100 50 500 1000 2500 5000 10000
' - - - - -
'Decay Output Specifications
' - - - - -
65$$$ 3z 1 2z 1 2z 1 5z 1 2z 1 5z 1 2z 1 2z 1 5z 1 2z 1 2z
1 5z 1 2z 1 e
'65$$$ 3z 1 20z 1 20z 1 e
' - - - - -
61** 5r1-14 1+6 1+4
81$$$ 2 0 26 1 e
82$$$ f2 6t
56$$$ f0 t
end

```

Figure A.II.2: ORIGEN Model, PWR, 4.5 w/o and 40 GWD/MTU, cont.

III. The BWR Model Using a UOX Fuel

The BWR model used in this study is adapted from a whole assembly SAS2H model in an Oak Ridge National Lab report concerning validation of SAS2H for BWR predictions (Figure A.III.1). The assembly is a General Electric type 7x7 fuel assembly with an active fuel length of 12.17 feet (370.84 cm) in a square pitch design. Fuel rods have a pitch of 1.875 cm and an outside diameter of 1.242 cm (no gap in this model). The model has been simplified from the mentioned report in that it has been homogenized (no burnable poisons or water holes) and has an initial enrichment of 4.5 w/o so as to match the PWR fuel in that regard. The fuel itself is UO₂ containing 190.71 kg of uranium in the proportions 4.50 w/o U-235, 95.472 w/o U-238 and 0.028 w/o U-234 and is volume fraction weighted (VF=0.5589) for the given fuel assembly based on the volume weighting method described in the SAS2H user's manual, i.e. VF depends on mass of fuel and volume of fuel assembly.

Cladding is zirc2 and the moderator is water. Average operating temperatures are 840, 620 and 558 degrees Fahrenheit for the fuel, clad and moderator respectively. Void fraction for the whole assembly model is handled by choosing an average moderator density based on the void fraction: $\rho_{\text{average}} = (\alpha)\rho_{\text{vapor}} + (1-\alpha)\rho_{\text{liquid}}$. The saturated liquid and vapor densities of water at 558 degrees Fahrenheit are 0.74178 and 0.03593 g/cm³ respectively and the void fractions used in this study were 0, 0.35, 0.50 and 0.65. The SAS2H model is burned at a specific power of 7.628 MW/assembly for 1000 days giving a total burnup of 40 GWD/MTU.

The corresponding ORIGEN model (Figure A.III.2), from which sampling is conducted, is one metric ton of the 4.5 w/o UOX fuel with approximately 271 kg of zirc2 cladding. The ORIGEN model is set to deplete the fuel using the binary cross section library generated from the fuel specific SAS2H model. Note: cross section perturbations are introduced directly into this binary working library during the sampling procedure. Fuel specific power density is 40 MW/MTU for a cycle length of 1000 days giving the same 40GWD/MTU burnup as the SAS2H Model. The ORIGEN model is set to “burn” the fuel for 10 equal time steps at 100% power and then print out decay isotopics at charge, discharge, 1, 5, 10, 50, 100, 500, 1000, 2500, 5000, and 10000 year times. ORIGEN also has the availability to print the decay heat, activity, and radiotoxicity for these times.

```
=sas2 parm='skipcellwt'
sas2 LWR UOX: 40 mwd/kgU, 7*7 pin, bwr, 1 cyc 50% Void
44groupndf5 latticecell
'-----
' FUEL COMPOSITION
'-----
uo2  1 0.5589 840 92234 0.028 92235 4.5 92238 95.472 end
'-----
' CLADDING
'-----
```

Figure A.III.1: SAS2H Model, BWR, 4.5 w/o and 40 GWD/MTU

```

zirc2 2 1 620 end
' -----
' MODERATOR / COOLANT
' -----
h2o 3 den=0.3889 1 558 end
end comp
' -----
' FUEL-PIN GEOMETRY
' -----

squarepitch 1.875 1.242 1 3 1.430 2 end
more data szf=1.2 eps=1.0-7 ptc=1.0-8 end
' -----
' ASSEMBLY AND CYCLE PARAMETERS
' -----

npin/assm=49 fuelngth=370.84 ncycles=1 nlib/cyc=1
printlevel=6
lightel=16 inplevel=1
numins= 1 ortube= 0.61214 srtube=0.5715 facmesh=1.4 end
power=7.6284 burn=1000 down=0 end
' -----
' Light elements (kg) per assembly
' -----
c 0.05999 n 0.03377 o 62.14 al 0.04569
si 0.06586 p 0.1422 ti 0.04983 cr 2.340
mn 0.1096 fe 4.599 co 0.03344 ni 4.402
zr 100.8 nb 0.3275 mo 0.1816 sn 1.652
' -----
end

```

Figure A.III.1: SAS2H Model, BWR, 4.5 w/o and 40 GWD/MTU, cont.

```

=origens
0$$$ a5 28 e
1$$$ 1 1t
bwr nuclear data - sample case 1
' -----
'Uses SAS Updated Lib
' -----
3$$$ 33 0 1 -88 a33 -88
' -----
2t
35$$$ 0 4t
56$$$ 10 a13 50 4 3 0 1 1 e
57** a3 1-14 e
95$$$ 1 5t
bwr - 4.5% enriched u
mt of heavy metal charged to reactor
' -----
'Power specifications, 40 MW for 1000 Days
' -----
58** 10r40
60** 8i110 1000
' -----
'Nuclide identifies - charged nuclides
' -----
66$$$ 1 a5 1 a9 1 e
73$$$ 60120 130270 140280 140290 220460 220470 220480 220490
220500 240500 240520 240530 240540 250550 260540 260560 260570 260580

```

Figure A.III.2: ORIGEN Model, BWR, 4.5 w/o and 40 GWD/MTU

```

270590 280580 280600 280610 280620 280640 400900 400910 400920 400940
400960 410930 420920 420940 420950 420960 420970 420980 421000 501120
501140 501150 501160 501170 501180 501190 501200 501220 501240
922350 922380 922340
'-----
'Molar masses of charged nuclides
'-----
74** 1.5 4.0 .607 .034 .304 .277 2.771 .204 .2 5.04
57.423 6.415 1.574 0.327 4.037 61.018 1.439 0.31 0.915 111.862
41.783 1.869 5.645 1.609 1421.122 306.725 462.239 460.074 72.5 10.258
.957 .532 .926 .958 .546 1.357 .54 .321 .219 .113

4.681 2.47 7.729 2.739 10.392 1.467 1.823 191.45 4011.75 1.13
'-----
75$$ 47r1 3r2 t
56$$ 0 10 a10 10 a14 5 a17 2 e
57** a3 1-14 e
95$$ 1 5t
'-----
'Decay time steps in years
'-----
60** 1 5 10 50 100 500 1000 2500 5000 10000
'-----
'Decay Output Specifications
'-----
65$$ 3z 1 2z 1 2z 1 5z 1 2z 1 5z 1 2z 1 2z 1 5z 1 2z 1 5z 1 2z 1 2z
1 5z 1 2z 1 e
'65$$ 3z 1 20z 1 20z 1 e
'-----
61** 5r1-14 1+6 1+4
81$$ 2 0 26 1 e
82$$ f2 6t
56$$ f0 t
end

```

Figure A.III.2: ORIGEN Model, BWR, 4.5 w/o and 40 GWD/MTU, cont.

IV. The PWR Separation Model Using a UOX Fuel

Since reprocessing hinges on chemical separation, we are also interested in uncertainty in the separation of SNF. Since chemistry only applied to elements we look at elemental uranium, neptunium, plutonium, americium, and curium – the key actinides produced by irradiating UOX fuel and those of interest to reprocessing and repository performance. This study examined heat loads produced by the separated elements in “lumps”. That is, at a given time after irradiation the key isotopes for a certain element at that time are placed into ORIGEN and decayed for the typical time steps already mentioned

in previous appendices and the total heat produced from that “lump”, regardless of daughters, is examined. This is equivalent to chemically separating that element, with 100% efficiency assumed, at the given time and then sitting that element away to decay. The procedure is repeated with +1 standard deviation of the isotopics as defined by the uncertainty in the PWR UOX fuel model which yields a heat +/- a heat uncertainty for each of the elements over their given decay times. A table of isotopics at 5, 10, and 25 years after irradiations is given in Table A.IV.1. Since the ORIGEN model used in this experiment is so general and uses a well known decay model, it is not presented.

Table A.IV.1: Isotopics of discharged UOX fuel at 5, 10, and 25 years after irradiation.

Nuclide	Mass at 5 Years		Mass at 10 Years		Mass at 25 Years	
	Grams	+/- Grams	Grams	+/- Grams	Grams	+/- Grams
u234	1.60E+02	2.53E+00	1.67E+02	2.64E+00	1.87E+02	2.96E+00
u235	1.23E+04	1.62E+02	1.23E+04	1.62E+02	1.23E+04	1.62E+02
u236	5.53E+03	3.94E+01	5.53E+03	3.94E+01	5.53E+03	3.94E+01
u237	3.75E-05	9.45E-07	2.95E-05	7.42E-07	1.43E-05	3.60E-07
u238	9.30E+05	7.21E+02	9.30E+05	7.21E+02	9.30E+05	7.21E+02
np237	5.69E+02	3.44E+00	5.73E+02	3.47E+00	5.95E+02	3.60E+00
np239	1.00E-04	1.37E-05	1.00E-04	1.37E-05	9.99E-05	1.36E-05
pu238	1.87E+02	1.96E+00	1.80E+02	1.88E+00	1.60E+02	1.67E+00
pu239	5.56E+03	4.48E+01	5.55E+03	4.48E+01	5.55E+03	4.48E+01
pu240	1.89E+03	4.85E+01	1.90E+03	4.86E+01	1.90E+03	4.88E+01
pu241	1.24E+03	3.12E+01	9.72E+02	2.45E+01	4.71E+02	1.19E+01
pu242	5.58E+02	1.45E+01	5.58E+02	1.45E+01	5.58E+02	1.45E+01
am241	3.79E+02	9.49E+00	6.41E+02	1.60E+01	1.12E+03	2.80E+01
am242m	8.97E-01	1.95E-02	8.76E-01	1.90E-02	8.13E-01	1.77E-02
am243	1.16E+02	1.59E+01	1.16E+02	1.59E+01	1.16E+02	1.58E+01
cm242	8.07E-03	1.75E-04	2.28E-03	4.96E-05	2.12E-03	4.60E-05
cm244	2.66E+01	3.02E+00	2.20E+01	2.49E+00	1.24E+01	1.40E+00
cm245	1.21E+00	1.24E-01	1.21E+00	1.24E-01	1.21E+00	1.24E-01

V. The PWR Model Using a MOX Fuel

For this study it was assumed that the MOX fuel would be burned in a conventional PWR and thus the SAS2H model (Figure A.V.1) for this fuel has the same geometry and operating parameters as that of the PWR UOX model described above with the exception that

fuel is now burned to 50 GWD/MTHM with a specific power of 23.070 MW/assembly for 1000 days. There is still 461.4 kg of heavy metal in the fuel but it is now divided between UO₂ and PuO₂. The composition of the MOX fuel is taken from an AFCI report from Los Alamos National Lab for Fiscal Year 2003, in which the fuel composition used in this study is designated “ALWR-2.” The 424.04 kg of uranium is in the proportions 1.40 w/o U-235, 98.572 w/o U-238 and 0.028 w/o U-234 and is volume fraction weighted at VF=0.82876. The 37.36 kg of plutonium is in the proportions 1.655 w/o Pu-238, 61.751 w/o Pu-239, 24.701 w/o Pu-240, 3.248 w/o Pu-241, 8.645 w/o Pu-242 and is volume fraction weighted at VF=0.06978. Since the sited report only specified a mass of Pu in the fuel, the isotopics vector was selected to approximate the discharged plutonium isotopic proportions of UOX fuel.

The corresponding ORIGEN model (Figure A.V.2), from which sampling is conducted, is one metric ton of the MOX fuel with approximately 271 kg of zirc2 cladding. The ORIGEN model is set to deplete the fuel using the binary cross section library generated from the fuel specific SAS2H model. Note: cross section perturbations are introduced directly into this binary working library during the sampling procedure. Fuel specific power density is 50 MW/ MTHM for a cycle length of 1000 days giving the same 50GWD/ MTHM burnup as the SAS2H Model. The ORIGEN model is set to “burn” the fuel for 10 equal time steps at 100% power and then print out decay isotopics at charge, discharge, 1, 5, 10, 50, 100, 500, 1000, 2500, 5000, and 10000 year times. ORIGEN also has the availability to print the decay heat, activity, and radiotoxicity for these times.

```
=sas2 parm='skipcellwt'  
sas2 ALWR-2 MOX: 50 mwd/kgHM, 17*17 pin, pwr, 1 cyc  
44groupndf5 latticecell
```

Figure A.V.1: SAS2H Model, MOX fuel in PWR, 50 GWD/MTHM

```

' -----
' FUEL COMPOSITION
' -----
uo2  1 0.82876 811 92234 0.028 92235 1.40 92238 98.572 end
puo2 1 0.06978 811 94238 1.655 94239 61.751 94240 24.701
' -----
' CLADDING
' -----
zirc2 2 1 620 end
' -----
' MODERATOR / COOLANT
' -----
h2o 3 den=0.733 1 570 end
co-59 3 0 1-20 570 end
end comp
' -----
' FUEL-PIN GEOMETRY
' -----
squarepitch 1.25984 0.83566 1 3 0.94996 2 end
more data szf=1.2 eps=1.0-7 ptc=1.0-8 end
' -----
' ASSEMBLY AND CYCLE PARAMETERS
' -----
npin/assm=264 fuelngth=365.76 ncycles=1 nlib/cyc=1
printlevel=6
lightel=16 inplevel=1
numins= 1 ortube= 0.61214 srtube=0.5715 facmesh=1.4 end
power=17.3025 burn=1333.3 down=0 end
'power=23.070 burn=1000.0 down=0 end
' -----
' Light elements (kg) per assembly
' -----
c 0.05999 n 0.03377 o 62.14 al 0.04569
si 0.06586 p 0.1422 ti 0.04983 cr 2.340
mn 0.1096 fe 4.599 co 0.03344 ni 4.402
zr 100.8 nb 0.3275 mo 0.1816 sn 1.652
' -----
end

```

Figure A.V.1: SAS2H Model, MOX fuel in PWR, 50 GWD/MTHM, cont.

```

=origens
0$$$ a5 28 e
1$$$ 1 1t
pwr nuclear data - sample case 1
3$$$ a4 -82 a11 0 0 a33 18 e
' -----
'Uses SAS Updated Lib
' -----
3$$$ 33 0 1 -88 a33 -88
' -----
54$$$ 5 e 2t
35$$$ 0 4t
56$$$ 10 a13 58 4 3 0 1 1 e
57** a3 1-14 e
95$$$ 1 5t
ALWR2 Fuel
  mt of heavy metal charged to reactor
' -----
'Power specifications, 50 MW for 1000 Days

```

Figure A.V.2: ORIGEN Model, MOX fuel in PWR, 50 GWD/MTHM

```

' - - - - -
58** 10r50
60** 8i100 1000
' - - - - -
'Nuclide identifies - charged nuclides
' - - - - -
66$$ 1 a5 1 a9 1 e
73$$ 60120 130270 140280 140290 220460 220470 220480 220490
220500 240500 240520 240530 240540 250550 260540 260560
260570 260580 270590 280580 280600 280610 280620 280640
400900 400910 400920 400940 400960 410930 420920 420940
420950 420960 420970 420980 421000 501120 501140 501150
501160 501170 501180 501190 501200 501220 501240 922340
922380 922350 942380 942390 942400 942410 942420 932370
952410 952430
' - - - - -
'Molar masses of charged nuclides
' - - - - -
74** 1.5 4 0.607 0.034 0.304 0.277 2.771 0.204
0.2 5.04 57.423 6.415 1.574 0.327 4.037 61.018
1.439 0.31 0.915 111.86 41.783 1.869 5.645 1.609
1421.1 306.73 462.24 460.07 72.5 10.258 0.957 0.532
0.926 0.958 0.546 1.357 0.54 0.321 0.219 0.113
4.681 2.47 7.729 2.739 10.392 1.467 1.823 1.13
3801.84 59.56 27.38 184.93 66.11 34.93 24.58 0.00
0.00 0.00
' - - - - -
75$$ 47r1 11r2 t
56$$ 0 10 a10 10 a14 5 a17 2 e
57** a3 1-14 e
95$$ 1 5t
' - - - - -
'Decay time steps in years
' - - - - -
60** 1 5 10 50 100 500 1000 2500 5000 10000
' - - - - -
'Decay Output Specifications
' - - - - -
65$$ 3z 1 2z 1 2z 1 5z 1 2z 1 5z 1 2z 1 2z 1 5z 1 2z 1 5z 1 2z 1 2z
1 5z 1 2z 1 e
'65$$ 3z 1 20z 1 20z 1 e
' - - - - -
61** 5r1-14 1+6 1+4
81$$ 2 0 26 1 e
82$$ f2 6t
56$$ f0 t
end

```

Figure A.V.2: ORIGEN Model, MOX fuel in PWR, 50 GWD/MTHM, cont.

VI. The PWR Model Using a MOX Fuel with Impurities

This model has the same geometry and operating conditions as the model described in the preceding section (Figure A.VI.1). The difference is now a portion of the U-238 mass has been removed and replaced with americium, Am, and neptunium, Np, heavy metal

impurities in the fuel in an effort to reflect a more realistic MOX fuel. The heavy metals have been added in the proportions 1 w/o Np-237 and 1.5 w/o Am-241 where the w/o is measured against the whole w/o of heavy metal in the fuel such that there is now 414.81 kg U, 37.36 kg Pu, 4.61 kg Np-237, and 6.92 kg Am-241. Due to the similarities in the model the only major change is the volume fraction of the UO₂ and PuO₂ and those of Am-241 and Np-137 which are now 0.809, 0.070, 0.0096, and 0.004 respectively.

The corresponding ORIGEN model (Figure A.VI.2), from which sampling is conducted, is one metric ton of the MOX fuel with approximately 271 kg of zirc2 cladding. The ORIGEN model is set to deplete the fuel using the binary cross section library generated from the fuel specific SAS2H model. Note: cross section perturbations are introduced directly into this binary working library during the sampling procedure. Fuel specific power density is 50 MW/MTHM for a cycle length of 1000 days giving the same 50GWD/ MTHM burnup as the SAS2H Model. The ORIGEN model is set to “burn” the fuel for 10 equal time steps at 100% power and then print out decay isotopics at charge, discharge, 1, 5, 10, 50, 100, 500, 1000, 2500, 5000, and 10000 year times. ORIGEN also has the availability to print the decay heat, activity, and radiotoxicity for these times.

```
=sas2 parm='skipcellwt'
sas2 ALWR-2 MOX: 50 mwd/kgHM,17*17 pin, pwr, 1 cyc
44groupndf5 latticecell
'-----
' FUEL COMPOSITION
'-----
uo2  1 0.82876 811 92234 0.028 92235 1.40 92238 98.572 end
puo2 1 0.06978 811 94238 1.655 94239 61.751 94240 24.701
      94241 3.248 94242 8.645 end
neptunium  1 0.0043 811 93237 100.0 end
americium  1 0.0096 811 95241 100.0 end
'-----
' CLADDING
'-----
zirc2 2 1 620 end
'-----
```

Figure A.VI.1: SAS2H Model, MOX with impurities fuel in PWR, 50 GWD/MTHM


```

' MODERATOR / COOLANT
' -----
h2o 3 den=0.733 1 570 end
co-59 3 0 1-20 570 end
end comp
' -----
' FUEL-PIN GEOMETRY
' -----
squarepitch 1.25984 0.83566 1 3 0.94996 2 end
more data szf=1.2 eps=1.0-7 ptc=1.0-8 end
' -----
' ASSEMBLY AND CYCLE PARAMETERS
' -----
npin/assm=264 fuelngth=365.76 ncycles=1 nlib/cyc=1
printlevel=6
lightel=16 inplevel=1
numins= 1 ortube= 0.61214 srtube=0.5715 facmesh=1.4 end
power=17.3025 burn=1333.3 down=0 end
'power=23.070 burn=1000.0 down=0 end
' -----
' Light elements (kg) per assembly
' -----
c 0.05999 n 0.03377 o 62.14 al 0.04569
si 0.06586 p 0.1422 ti 0.04983 cr 2.340
mn 0.1096 fe 4.599 co 0.03344 ni 4.402
zr 100.8 nb 0.3275 mo 0.1816 sn 1.652
' -----
end

```

Figure A.VI.1: SAS2H Model, MOX w/ impurities fuel in PWR, 50 GWD/MTHM, cont.

```

=origens
0$$ a5 28 e
1$$ 1 1t
pwr nuclear data - sample case 1
3$$ a4 -82 a11 0 0 a33 18 e
' -----
'Uses SAS Updated Lib
' -----
3$$ 33 0 1 -88 a33 -88
' -----
54$$ 5 e 2t
35$$ 0 4t
56$$ 10 a13 58 4 3 0 1 1 e
57** a3 1-14 e
95$$ 1 5t
ALWR2 Fuel
  mt of heavy metal charged to reactor
' -----
'Power specifications, 50 MW for 1000 Days
' -----
58** 10r50
60** 8i100 1000
' -----
'Nuclide identifies - charged nuclides
' -----
66$$ 1 a5 1 a9 1 e
73$$ 60120 130270 140280 140290 220460 220470 220480 220490
220500 240500 240520 240530 240540 250550 260540 260560
260570 260580 270590 280580 280600 280610 280620 280640
400900 400910 400920 400940 400960 410930 420920 420940

```

Figure A.VI.2: ORIGEN Model, MOX with impurities fuel in PWR, 50 GWD/MTHM

```

420950 420960 420970 420980 421000 501120 501140 501150
501160 501170 501180 501190 501200 501220 501240 922340
922380 922350 942380 942390 942400 942410 942420 932370
952410 952430
' - - - - -
'Molar masses of charged nuclides
' - - - - -
74** 1.5 4 0.607 0.034 0.304 0.277 2.771 0.204
0.2 5.04 57.423 6.415 1.574 0.327 4.037 61.018
1.439 0.31 0.915 111.86 41.783 1.869 5.645 1.609

1421.1 306.73 462.24 460.07 72.5 10.258 0.957 0.532
0.926 0.958 0.546 1.357 0.54 0.321 0.219 0.113
4.681 2.47 7.729 2.739 10.392 1.467 1.823 1.13
3696.816 59.56 27.38 184.93 66.11 34.93 24.58 42.186
62.226 0.00
' - - - - -
75$$ 47r1 11r2 t
56$$ 0 10 a10 10 a14 5 a17 2 e
57** a3 1-14 e
95$$ 1 5t
' - - - - -
'Decay time steps in years
' - - - - -
60** 1 5 10 50 100 500 1000 2500 5000 10000
' - - - - -
'Decay Output Specifications
' - - - - -
65$$ 3z 1 2z 1 2z 1 5z 1 2z 1 5z 1 2z 1 2z 1 5z 1 2z 1 5z 1 2z 1 2z
1 5z 1 2z 1 e
'65$$ 3z 1 20z 1 20z 1 e
' - - - - -
61** 5r1-14 1+6 1+4
81$$ 2 0 26 1 e
82$$ f2 6t
56$$ f0 t
end

```

Figure A.VI.2: ORIGEN Model, MOX with impurities in PWR, 50 GWD/MTHM, cont.

VII. The PWR Model Using TRITON

For purposes of conducting a comparison between using the SAS + ORIGEN scheme and using the driver program TRITON stand-alone, a TRITON model of the PWR fuel was created. The TRITON model represents a step up in the detail of modeling to a level closer to that of normal fuel analysis, in which a 2-D transport model is solved for each time step and new fluxes used to collapse a 44-group cross section library. A Wigner cell of the PWR fuel including the buffer region of extra water added by the water holes in the assembly is modeled. Two PWR models were constructed differing in the burnup steps while keeping all


```

power=36.53   burn=54.75   down=0       nlib=1   end
power=36.53   burn=54.75   down=0       nlib=1   end
power=36.53   burn=54.75   down=0       nlib=1   end
power=36.53   burn=54.75   down=0       nlib=1   end
power=36.53   burn=54.75   down=0       nlib=1   end
power=36.53   burn=54.75   down=0       nlib=1   end
power=36.53   burn=54.75   down=0       nlib=1   end
power=36.53   burn=54.75   down=0       nlib=1   end
end burndata
'-----
read opus
units=gram symnuc= pb-210 ra-226 ac-227 th-227 th-230 pa-231
u-234 u-235 u-236 u-237 u-238 np-237 np-239 pu-238 pu-239 pu-240 pu-241 pu-242
am-241 am-242m am-243 cm-242 cm-244 cm-245
c-14 se-79 sr-90 tc-99 i-129 cs-137 ba-137m y-90 cs-134 end
matl=0 1 end
end opus
'-----
read model
17x17 PWR Assembly, 4.5% 40 GWD
'-----
read parm
prtflux=no drawit=yes echo=yes
xnlib=1 run=yes collapse=yes fillmix=5 prtmxsec=no prtbroad=yes
sn=4 inners=10 outers=200 epsinner=1e-4 epsouter=1e-4
epseigen=1e-5 prtmxtab=yes
end parm
'-----
read materials
1 1 ! 4.5% enriched fuel, pin location 1 ! end
4 1 ! clad ! end
5 1 ! water ! end
end materials
'-----WIGNER CELL DOMAIN SPECIFICATION-----
read geom
cylinder 1 0.66 0.66 0.4178 !fuel - buffer! end
cylinder 4 0.66 0.66 0.4750 !clad - buffer! end
domain 1.32 1.32 4 4
boundary 1 1 1 1
end geom
'-----
end model
'***
'* end of newt transport model
'***
end
=origens
'-----ORIGEN DECAY ANALYSIS-----
0$$ a8 26 a11 -71 e 1t
sample case 3b
3$$ 21 0 1 -88 a33 -88
4** a4 1-35 2t
35$$ 0 4t
56$$ a13 -105 5 1 74 4 e
57** a3 1-14 e
95$$ 1 5t
sample case 3b
'Decay time steps in years
60** 1 5 10 50 100 500 1000 2500 5000 10000

```

```
'65$$$ 1 20z 2q21
65$$$ 3z 1 20z 1 20z 1 e
61** f1-14
81$$$ 2 0 26 1 e
82$$$ a10 2 6t
56$$$ 2z a10 10 e 6t
56$$$ f0 t
end
```

Figure A. VII.1: TRITON Model, PWR, 4.5 w/o and 40 GWD/MTU, cont.

VIII. TRITON FR Models Using Actinide Fuels

The fast reactor, FR models used in this study was created in reference to various fuel assemblies for Argonne National Lab's Advanced Burner Test Reactor (ABTR) which would use a fuel whose isotopics are based on 10 year decayed UOX that was 3.3 w/o fresh fuel and burned for 33 GWD/MTU. The metal fuel consists of depleted uranium, the transuranics: neptunium, plutonium, americium, and curium metals, and 10-20 w/o zirconium mixed into the metal. Three fuel types are analyzed that are intended to have conversion ratios of 0.25, 0.70 and 1.05 which are controlled by the TRU enrichment. Common among these assemblies are that the pins are in a triangular (hexagonal) pitch with an active fuel length of 80 cm. The composition data including volume fractions are included in Table A.VIII.1. The cladding is a material developed by Argonne and has the composition shown in Table A. VIII.2; it is namely an iron alloy. Finally, as with several other fast reactor design concepts, the coolant for this model is elemental sodium. Operating temperatures are 909, 783 and 783 degrees Fahrenheit for the fuel, clad and moderator, respectively, with the moderator density at 7.97 g/cm³. Specific powers, burnups, geometry and other important data are given in Table A. VIII.3. Note, TRITON automatically returns results in terms of 1 MTHM and the ORIGEN decay sequence is set for the standard charge, discharge, 1, 5, 10, 50, 100, 500, 1000, 2500, 5000, and 10000 year time steps. The TRITON models for CR= 1.05, 0.70, and

0.25 are presented in Figures A. VIII.1-3 respectively. For recycle sampling, consider these same models with input isotopics perturbed.

Table A.VIII.1: Fast Reactor Fuel Composition Data, by conversion ratio

Nuclide / Conversion Ratio:	Weight Percent in TRU		
	0.25	0.7	1.05
Np-237	18.635	7.334	9.907
Pu-238	0.855	1.253	0.000
Pu-239	32.764	48.058	72.150
Pu-240	14.983	21.973	4.469
Pu-241	4.936	7.241	0.250
Pu-242	2.956	4.335	0.000
Am-241	20.579	8.100	10.941
Am-242m	0.041	0.016	0.022
Am-243	3.565	1.403	1.895
Cm-244	0.689	0.271	0.366
Cm-245	0.041	0.016	0.022
Fissile Fraction, %	37.7	55.30	72.40
TRU Enrichment, %	59.2	20.6	16.2
Zr w/o	20	10	10
U-238, w/o	20.8	69.4	73.8

Table A. VIII.2: Cladding Composition Data

Cladding Composition	
Material	mass/cm ³
Iron	7.10E-02
Nickel	4.38E-04
Chromium	1.06E-02
Manganese-55	4.68E-04
Molybdenum	4.99E-04

Table A. VIII.3: Operating Conditions and Geometry Data

Conversion Ration	0.25	0.70	1.05
Specific Power of active core, MW/MT	114.8	47.7	41.2
Discharge Burnup, GWD.MT	94.3	78.4	67.7
Height, cm	80	80	80
Number of pins per assembly	217	169	127
Assembly lattice pitch, cm	14.834	14.834	14.834
Inter-assembly gap, mm	4.45	4.0	4.0
Duct thickness, mm	4.45	3.0	3.0
Pin pitch-to-diameter ratio	1.29	1.11	1.10
Cladding thickness, mm	0.75	0.41	0.41

```

=t-depl
Infinite lattice depletion model for a single pincell, 4 cycles @1 libs/cycle.
44groupndf
'-----FUEL COMPOSITION-----
read comp
'Fuel
uranium 1 0.4300 909.0
92235 0.192
92238 99.808 end
neptunium 1 0.000377 909.0
93237 100.0 end
plutoniumalp 1 0.0549 909.0
94238 1.038
94239 72.031
94240 23.356
94241 2.249
94242 1.326 end
americium 1 0.0015 909.0
95241 75.758
95243 18.182
95601 6.061 end
curium 1 0.00014 909.0
96244 66.667
96245 33.333
96246 0.000 end
zirconium 1 0.1108 909.0 40090 51.45 40091 11.22 40094 17.38 40096 2.8
          40092 17.15 end
sodium 2 den=4.8 1 909.0 end
'Moderator
sodium 5 den=6.15 1 783.0 end
'Clad
iron 4 0.8379 783.0 end
nickel 4 0.0048 783.0 end
chromium 4 0.1266 783.0 end
molybdenum 4 0.0078 783.0 end
'manganese 4 0.0427 783.0 end
MN-55 4 0.041 783 end
end comp
'-----GEOMETRY-----
read celldata
latticecell triangpitch pitch=1.21 5 fuelr=0.4407 1 cladr=0.5845 4 end
end celldata
'-----
read depletion
-1 4 2 5
end depletion
'-----POWER HISTORY-----
read burndata
power=41.2 burn=8.495 down=0 nlib=1 end
power=41.2 burn=8.495 down=0 nlib=1 end
power=41.2 burn=33.98 down=0 nlib=1 end
power=41.2 burn=33.98 down=0 nlib=1 end
power=41.2 burn=33.98 down=0 nlib=1 end
power=41.2 burn=33.98 down=0 nlib=1 end
power=41.2 burn=33.98 down=0 nlib=1 end
power=41.2 burn=84.9515 down=0 nlib=1 end

```

Figure A. VIII.1: TRITON Model, CR=1.05

```

power=41.2 burn=84.9515 down=0 nlib=1 end
power=41.2 burn=84.9515 down=0 nlib=1 end
power=41.2 burn=84.9515 down=0 nlib=1 end
power=41.2 burn=84.9515 down=0 nlib=1 end
power=41.2 burn=84.9515 down=0 nlib=1 end
power=41.2 burn=84.9515 down=0 nlib=1 end
power=41.2 burn=84.9515 down=0 nlib=1 end
power=41.2 burn=84.9515 down=0 nlib=1 end
power=41.2 burn=84.9515 down=0 nlib=1 end
power=41.2 burn=84.9515 down=0 nlib=1 end
power=41.2 burn=84.9515 down=0 nlib=1 end
power=41.2 burn=84.9515 down=0 nlib=1 end
power=41.2 burn=84.9515 down=0 nlib=1 end
power=41.2 burn=84.9515 down=0 nlib=1 end
power=41.2 burn=84.9515 down=0 nlib=1 end
power=41.2 burn=84.9515 down=0 nlib=1 end
power=41.2 burn=84.9515 down=0 nlib=1 end
power=41.2 burn=84.9515 down=0 nlib=1 end
power=41.2 burn=84.9515 down=0 nlib=1 end
end burndata
'-----
read opus
units=gram symnuc= pb-210 ra-226 ac-227 th-227 th-230 pa-231
u-234 u-235 u-236 u-237 u-238 np-237 np-239 pu-238 pu-239 pu-240 pu-241 pu-242
am-241 am-242m am-243 cm-242 cm-244 cm-245

c-14 se-79 sr-90 tc-99 i-129 cs-137 ba-137m y-90 cs-134
zr-90 zr-91 zr-92 zr-94 zr-96 end
matl=0 1 2 end
end opus
'-----
read model
ABTR Assembly, CR=0.25
'-----
read parm
prtflux=no drawit=yes echo=yes
xnlb=1 run=yes collapse=yes fillmix=5 prtmxsec=no prtbroad=yes
sn=4 inners=10 outers=200 epsinner=1e-4 epsouter=1e-4
epseigen=1e-5 prtmxtab=yes
end parm
'-----
read materials
  1 1 ! fuel ! end
  2 1 ! bond - sodium ! end
  4 1 ! clad ! end
  5 1 ! sodium ! end
end materials
'-----WIGNER CELL DOMAIN SPECIFICATION-----
read geom
cylinder 1 0.605 0.605 0.4407 !fuel! end
cylinder 2 0.605 0.605 0.5090 !gap! end
cylinder 4 0.605 0.605 0.5845 !clad! end
domain 1.21 1.21 3 3
boundary 1 1 1 1
end geom
'-----
end model

```

Figure A. VIII.1: TRITON Model, CR=1.05, cont.


```

****
'* end of newt transport model
****
end
=origens
'-----ORIGEN DECAY ANALYSIS-----
0$$ a8 26 a11 -71 e 1t
sample case 3b
3$$ 21 0 1 -88 a33 -88
4** a4 1-35 2t
35$$ 0 4t
56$$ a13 -109 5 1 74 4 e
57** a3 1-14 e
95$$ 1 5t
sample case 3b

'Decay time steps in years
60** 1 5 10 50 100 500 1000 2500 5000 10000

'65$$ 1 20z 2q21
65$$ 3z 1 20z 1 20z 1 e
61** f1-14
81$$ 2 0 26 1 e
82$$ a10 2 6t
56$$ 2z a10 10 e 6t
56$$ f0 t
end

```

Figure A. VIII.1: TRITON Model, CR=1.05, cont.

```

=t-depl
Infinite lattice depletion model for a single pincell, 4 cycles @1 libs/cycle.
44groupndf
'-----FUEL COMPOSITION-----
'Fuel
read comp
uranium 1 0.5682 909
92235 0.192
92238 99.808 end
neptunium 1 0.00225 909
93237 100.0 end
plutoniumalp 1 0.12825 909
94238 2.895
94239 55.307
94240 31.488
94241 4.469
94242 5.841 end
americium 1 0.01085 909
95241 64.348
95243 31.304
95601 4.348 end
curium 1 0.00218 909
96244 73.913
96245 17.391
96246 8.696 end
zirconium 1 0.232 909 40090 51.45 40091 11.22 40094 17.38 40096 2.8
          40092 17.15 end
sodium 2 den=11.175 1 909 end

```

Figure A. VIII.2: TRITON Model, CR=0.70

```

sodium 5 den=7.652 1 783 end
iron 4 0.8378 783 end
nickel 4 0.0048 783 end
chromium 4 0.1266 783 end
molybdenum 4 0.0078 783 end
'manganese 4 0.0427 783 end
MN-55 4 0.041 783 end
end comp
'-----GEOMETRY-----
read celldata
latticecell triangpitch    pitch=1.044 5 fuelr=0.4295 1 cladr=0.4705 4 end
end celldata
'-----
read depletion
-1 4 2 5
end depletion
'-----POWER HISTORY-----
read burndata
power=47.4 burn=8.439 down=0 nlib=1 end
power=47.4 burn=42.194 down=0 nlib=1 end
power=47.4 burn=42.194 down=0 nlib=1 end
power=47.4 burn=42.194 down=0 nlib=1 end
power=47.4 burn=42.194 down=0 nlib=1 end
power=47.4 burn=73.84 down=0 nlib=1 end
power=47.4 burn=73.84 down=0 nlib=1 end
power=47.4 burn=73.84 down=0 nlib=1 end
power=47.4 burn=73.84 down=0 nlib=1 end
power=47.4 burn=73.84 down=0 nlib=1 end
power=47.4 burn=73.84 down=0 nlib=1 end
power=47.4 burn=73.84 down=0 nlib=1 end
power=47.4 burn=73.84 down=0 nlib=1 end
power=47.4 burn=73.84 down=0 nlib=1 end
power=47.4 burn=73.84 down=0 nlib=1 end
power=47.4 burn=73.84 down=0 nlib=1 end
power=47.4 burn=73.84 down=0 nlib=1 end
power=47.4 burn=73.84 down=0 nlib=1 end
power=47.4 burn=73.84 down=0 nlib=1 end
power=47.4 burn=73.84 down=0 nlib=1 end
power=47.4 burn=73.84 down=0 nlib=1 end
power=47.4 burn=73.84 down=0 nlib=1 end
power=47.4 burn=73.84 down=0 nlib=1 end
power=47.4 burn=73.84 down=0 nlib=1 end
power=47.4 burn=73.84 down=0 nlib=1 end
end burndata
'-----
read opus
units=gram symnuc= pb-210 ra-226 ac-227 th-227 th-230 pa-231
u-234 u-235 u-236 u-237 u-238 np-237 np-239 pu-238 pu-239 pu-240 pu-241 pu-242
am-241 am-242m am-243 cm-242 cm-244 cm-245
c-14 se-79 sr-90 tc-99 i-129 cs-137 ba-137m y-90 cs-134
zr-90 zr-91 zr-92 zr-94 zr-96 end
matl=0 1 end
end opus
'-----
read model
ABTR Assembly, CR=0.7
'-----
read parm
prtflux=no drawit=yes echo=yes

```

Figure A. VIII.2: TRITON Model, CR=0.70, cont.

```

xnlib=1 run=yes collapse=yes fillmix=5 prtmxsec=no prtbroad=yes
sn=4 inners=10 outers=200 epsinner=1e-4 epsouter=1e-4
epseigen=1e-5 prtmxtab=yes
end parm
'-----
read materials
  1 1 ! fuel ! end
  2 1 ! bond - sodium ! end
  4 1 ! clad ! end
  5 1 ! sodium ! end
end materials
'-----WIGNER CELL DOMAIN SPECIFICATION-----
read geom
cylinder 1 0.531 0.531 0.3721 !fuel! end
cylinder 2 0.531 0.531 0.4295 !gap! end
cylinder 4 0.531 0.531 0.5017 !clad! end
domain 1.0623 1.0623 3 3
boundary 1 1 1 1
end geom
'-----
end model
'***
'* end of newt transport model
'***
end

=origens
'-----ORIGEN DECAY ANALYSIS-----
0$$$ a8 26 a11 -71 e 1t
sample case 3b
3$$$ 21 0 1 -88 a33 -88
4** a4 1-35 2t
35$$$ 0 4t
56$$$ a13 -101 5 1 74 4 e
57** a3 1-14 e
95$$$ 1 5t
sample case 3b

'Decay time steps in years
60** 1 5 10 50 100 500 1000 2500 5000 10000

'65$$$ 1 20z 2q21
65$$$ 3z 1 20z 1 20z 1 e
61** f1-14
81$$$ 2 0 26 1 e
82$$$ a10 2 6t
56$$$ 2z a10 10 e 6t
56$$$ f0 t
end

```

Figure A. VIII.2: TRITON Model, CR=0.70, cont.

```

=t-depl
Infinite lattice depletion model for a single pincell, 4 cycles @1 libs/cycle.
44groupndf
'-----FUEL COMPOSITION-----
read comp
'Fuel
uranium 1 0.2368 909.0

```

Figure A. VIII.3: TRITON Model, CR=0.25

```

92235 0.196
92238 99.804 end
neptunium 1 0.00785 909.0
93237 100.0 end
plutoniumalp 1 0.2837 909.0
94238 5.304
94239 35.902
94240 40.254
94241 6.936
94242 11.605 end
americium 1 0.0435 909.0
95241 60.470
95243 35.470
95601 4.060 end
curium 1 0.01175 909.0
96242 0.806
96244 70.968
96245 18.548
96246 9.678 end
zirconium 1 0.3626 909.0 40090 51.45 40091 11.22 40094 17.38 40096 2.8
          40092 17.15 end
sodium 2 den=7.00 1 909.0 end
'Moderator
sodium 5 den=17.73 1 783.0 end
'Clad
iron 4 0.8379 783.0 end
nickel 4 0.0048 783.0 end
chromium 4 0.1266 783.0 end
molybdenum 4 0.0078 783.0 end
'manganese 4 0.0427 783.0 end
MN-55 4 0.041 783 end
end comp
'-----GEOMETRY-----
read celldata
latticecell triangpitch  pitch=0.7793 5 fuelr=0.2057 1 cladr=0.3613 4
end
end celldata
'-----
read depletion
-1 4 2 5
end depletion
'-----POWER HISTORY-----
read burndata
power=114.8 burn=2.613 down=0 nlib=1 end
power=114.8 burn=17.42 down=0 nlib=1 end
power=114.8 burn=17.42 down=0 nlib=1 end
power=114.8 burn=19.60 down=0 nlib=1 end
power=114.8 burn=19.60 down=0 nlib=1 end
power=114.8 burn=39.20 down=0 nlib=1 end
power=114.8 burn=39.20 down=0 nlib=1 end
power=114.8 burn=39.20 down=0 nlib=1 end
power=114.8 burn=39.20 down=0 nlib=1 end
power=114.8 burn=39.20 down=0 nlib=1 end
power=114.8 burn=39.20 down=0 nlib=1 end
power=114.8 burn=39.20 down=0 nlib=1 end
power=114.8 burn=39.20 down=0 nlib=1 end
power=114.8 burn=39.20 down=0 nlib=1 end
power=114.8 burn=39.20 down=0 nlib=1 end
power=114.8 burn=39.20 down=0 nlib=1 end

```

Figure A. VIII.3: TRITON Model, CR=0.25, cont.

```

power=114.8 burn=39.20 down=0 nlib=1 end
power=114.8 burn=39.20 down=0 nlib=1 end
power=114.8 burn=39.20 down=0 nlib=1 end
power=114.8 burn=39.20 down=0 nlib=1 end
power=114.8 burn=39.20 down=0 nlib=1 end
power=114.8 burn=39.20 down=0 nlib=1 end
power=114.8 burn=39.20 down=0 nlib=1 end
power=114.8 burn=39.20 down=0 nlib=1 end
power=114.8 burn=39.20 down=0 nlib=1 end
power=114.8 burn=39.20 down=0 nlib=1 end
end burndata
'-----
read opus
units=gram symnuc= pb-210 ra-226 ac-227 th-227 th-230 pa-231
u-234 u-235 u-236 u-237 u-238 np-237 np-239 pu-238 pu-239 pu-240 pu-241 pu-242
am-241 am-242m am-243 cm-242 cm-244 cm-245
c-14 se-79 sr-90 tc-99 i-129 cs-137 ba-137m y-90 cs-134
zr-90 zr-91 zr-92 zr-94 zr-96 end
matl=0 1 2 end
end opus
'-----
read model
ABTR Assembly, CR=0.25
'-----
read parm
prtflux=no drawit=yes echo=yes
xnlib=1 run=yes collapse=yes fillmix=5 prtmxsec=no prtbroad=yes
sn=4 inners=10 outers=200 epsinner=1e-4 epsouter=1e-4
epseigen=1e-5 prtmxtab=yes
end parm
'-----
read materials
 1 1 ! fuel ! end
 2 1 ! bond - sodium ! end
 4 1 ! clad ! end
 5 1 ! sodium ! end
end materials
'-----WIGNER CELL DOMAIN SPECIFICATION-----
read geom
cylinder 1 0.363 0.363 0.2057 !fuel! end
cylinder 2 0.363 0.363 0.2375 !gap! end
cylinder 4 0.363 0.363 0.3613 !clad! end
domain 0.7253 0.7253 3 3
boundary 1 1 1 1
end geom
'-----
end model
'***
'* end of newt transport model
'***
end
=origens
'-----ORIGEN DECAY ANALYSIS-----
sample case 3b
3$$ 21 0 1 -88 a33 -88
4** a4 1-35 2t
35$$ 0 4t
56$$ a13 -97 5 1 74 4 e
57** a3 1-14 e

```

Figure A. VIII.3: TRITON Model, CR=0.25, cont.

```

95$$ 1 5t
sample case 3b
'Decay time steps in years
60** 1 5 10 50 100 500 1000 2500 5000 10000
'65$$ 1 20z 2q21
65$$ 3z 1 20z 1 20z 1 e
61** f1-14
81$$ 2 0 26 1 e
82$$ a10 2 6t
56$$ 2z a10 10 e 6t
56$$ f0 t
End

```

Figure A. VIII.3: TRITON Model, CR=0.25, cont.

Since the TRITON model used for the recycling experiment is the same as the CR = 0.70 fast reactor model, it is not repeated here. The burnup is adjusted to 41.4 GWD/MTHM, which is the end of cycle core average burnup, and the input isotopics for each element are different at each recycle step.

IX. REBUS Fast Reactor Model with Actinide Fuel and Recycle

The REBUS model was set up to reproduce the fuel loading and recycle as specified by Argonne's ABTR Preconceptual Design [26] report for the medium conversion ratio core. The model is set to recycle all of the fast reactor fuel transuranics after 1.5 years of cooling, and make up the mass and reactivity by using spent LWR fuel and depleted uranium. As described in the Results section, this model more closely matched the values in the report in terms of loading and operating parameters. The complete input is given in Figure A.IX.1.

```

BLOCK=OLD
DATASET=ISOTXS
BLOCK=STP027
DATASET=A. SUMMAR
01
02          Y          8          1
03          0
04          4LFP35
04          4LFP38
04          4LFP39
04          4LFP40
04          4LFP41
04          3P236I P236M P236O

```

Figure A.IX.1: REBUS Equilibrium Model, CR = 0.77.

```

04      3C242I C242M C242O
04      3C243I C243M C243O
04      3C244I C244M C244O
04      3C245I C245M C245O
04      3C246I C246M C246O
04      3A24MI A24MM A24MO
04      3A242I A242M A242O
05      PU2365SPEC 236.045761 P236I P236M P236O
05      CM2425SPEC 242.058426 C242I C242M C242O
05      CM2435SPEC 243.061035 C243I C243M C243O
05      CM2445SPEC 244.062637 C244I C244M C244O
05      CM2455SPEC 245.065247 C245I C245M C245O
05      CM2465SPEC 246.066849 C246I C246M C246O
05      AM242MSPEC 242.059433 A24MI A24MM A24MO
05      AM2425SPEC 242.059433 A242I A242M A242O
DATASET=A.STP027
01      0          0          0          0          0          0          0
02      0          0          0          1          0          1          0
03      1          1          1          1          1          1          1
06      1
DATASET=A.DIF3D
01      *****
01      A.DIF3D : 250MWt, 12-Month
01      *****
01
02      999000999000
03      0          0          0          50
04      0          0          0          00          000          10          100          0          0          0          0
05      .000001          .0001          .0001
05      1.0E-07          1.0E-05          1.0E-05          83.33E+6
06
DATASET=A.HMG4C
01      TURN OFF HMG4C EDITS
02      60000          1          0          0          0          1
DATASET=A.NIP3
01      *****
01      A.NIP3 : 250MWt, 12-Month
01      *****
01
02      0          1 90000          90000          1          1
03      126
04      7          4          0          4          4          4
07      TCORE ICO_D ICO_E ICO_F ICO_G ICO_H
07      TCORE MCO_D MCO_E MCO_F MCO_G MCO_H
07      TCORE OCO_D OCO_E OCO_F OCO_G OCO_H

07      ICORE ICO_D ICO_E ICO_F ICO_G ICO_H
07      MCORE MCO_D MCO_E MCO_F MCO_G MCO_H
07      OCORE OCO_D OCO_E OCO_F OCO_G OCO_H

09      Z          3 50.24          2 93.66          1 110.54
09      Z          1 127.42          1 144.30          1 161.18
09      Z          1 178.07          1 194.95          1 217.52
09      Z          4 280.36          1 300.46          1 315.54

```

Figure A. IX.1: REBUS Equilibrium Model, CR = 0.77, cont.

09 Z 2 345.68

* U-20TRU-10Zr, density = 15.73 g/cc, ANL-IFR-29

13	FUELI	U234I	1.0	U235I	1.0	U236I	1.0
13	FUELI	U238I	1.0	P236I	1.0	P238I	1.0
13	FUELI	P239I	1.0	P240I	1.0	P241I	1.0
13	FUELI	P242I	1.0	N237I	1.0	A241I	1.0
13	FUELI	A24MI	1.0	A243I	1.0	C242I	1.0
13	FUELI	C243I	1.0	C244I	1.0	C245I	1.0
13	FUELI	C246I	1.0	DUMP1	1.0	DUMP2	1.0
13	FUELI	LFP35	1.0	LFP38	1.0	LFP39	1.0
13	FUELI	LFP40	1.0	LFP41	1.0	ZIRCI	1.03839E-02

13	FUELO	U234O	1.0	U235O	1.0	U236O	1.0
13	FUELO	U238O	1.0	P236O	1.0	P238O	1.0
13	FUELO	P239O	1.0	P240O	1.0	P241O	1.0
13	FUELO	P242O	1.0	N237O	1.0	A241O	1.0
13	FUELO	A24MO	1.0	A243O	1.0	C242O	1.0
13	FUELO	C243O	1.0	C244O	1.0	C245O	1.0
13	FUELO	C246O	1.0	DUMP1	1.0	DUMP2	1.0
13	FUELO	LFP35	1.0	LFP38	1.0	LFP39	1.0
13	FUELO	LFP40	1.0	LFP41	1.0	ZIRCO	1.03839E-02

13	FUELM	U234M	1.0	U235M	1.0	U236M	1.0
13	FUELM	U238M	1.0	P236M	1.0	P238M	1.0
13	FUELM	P239M	1.0	P240M	1.0	P241M	1.0
13	FUELM	P242M	1.0	N237M	1.0	A241M	1.0
13	FUELM	A24MM	1.0	A243M	1.0	C242M	1.0
13	FUELM	C243M	1.0	C244M	1.0	C245M	1.0
13	FUELM	C246M	1.0	DUMP1	1.0	DUMP2	1.0
13	FUELM	LFP35	1.0	LFP38	1.0	LFP39	1.0
13	FUELM	LFP40	1.0	LFP41	1.0	ZIRCM	1.03839E-02

* Na coolant, density from Fink and Leibowitz (rho=0.850257 at 432.5 C)

13	CLNTI	NA23I	2.22724E-02
13	CLNTO	NA23O	2.22724E-02
13	CLNTM	NA23M	2.22724E-02
13	CLNTR	NA23R	2.22724E-02
13	CLNTS	NA23S	2.22724E-02

* HT9, density = 7.76 g/cc, ASTM A826-88

13	HT9	I	FE	I	7.10244E-02	NI	I	4.37911E-04	CR	I	1.05604E-02
13	HT9	I	MN	55I	4.67845E-04	MO	I	4.99271E-04			
13	HT9	O	FE	O	7.10244E-02	NI	O	4.37911E-04	CR	O	1.05604E-02
13	HT9	O	MN	55O	4.67845E-04	MO	O	4.99271E-04			
13	HT9	M	FE	M	7.10244E-02	NI	M	4.37911E-04	CR	M	1.05604E-02
13	HT9	M	MN	55M	4.67845E-04	MO	M	4.99271E-04			
13	HT9	R	FE	R	7.10244E-02	NI	R	4.37911E-04	CR	R	1.05604E-02
13	HT9	R	MN	55R	4.67845E-04	MO	R	4.99271E-04			
13	HT9	S	FE	S	7.10244E-02	NI	S	4.37911E-04	CR	S	1.05604E-02
13	HT9	S	MN	55S	4.67845E-04	MO	S	4.99271E-04			

* SS-316, density = 7.97 g/cc, /data/RA/PADB/SAMATL

13	S316R	FE	R	5.29276E-02	NI	R	1.08679E-02	CR	R	1.07851E-02
----	-------	----	---	-------------	----	---	-------------	----	---	-------------

Figure A. IX.1: REBUS Equilibrium Model, CR = 0.77, cont.

13	S316R	MN55R	1.69487E-03	MO	R	1.45080E-03		
* B4C (natural B), density = 2.268 g/cc, 90% TD, www.azom.com								
13	B4CPI	B-10I	0.0196760	B-11I	0.0791983	C-12I	0.0193455	
* B4C shield (Radial, 90% TD)								
13	B4CR	B-10S	0.0196760	B-11S	0.0791983	C-12S	0.0193455	
* 5% axial swelling, 0.596% radial expansion, 0.489% axial expansion								
14	ICSC	FUELI	0.385000	HT9 I	0.187000	CLNTI	0.300000	
14	OCSC	FUELO	0.385000	HT9 O	0.187000	CLNTO	0.300000	
14	MCSC	FUELM	0.385000	HT9 M	0.187000	CLNTM	0.300000	
14	LPSC	S316R	0.3	CLNTR	0.7			
14	LRSC	HT9 R	0.667897	CLNTR	0.320813			
14	UPSC1	HT9 R	0.227980	CLNTR	0.768166			
14	UPSC	HT9 R	0.227980	CLNTR	0.320813			
14	USSC	HT9 R	0.667897	CLNTR	0.320813			
* pellet volume fraction for B4C with thermal expansion								
14	CRBSC	HT9 I	0.263966	CLNTI	0.366908	B4CPI	0.308300	
14	CRCSC	HT9 I	0.076960	CLNTI	0.921739			
14	CRFSC	HT9 I	0.247787	CLNTI	0.748024			
14	CRPSC	HT9 R	0.263966	CLNTR	0.366908			
14	CRDSC	HT9 R	0.247787	CLNTR	0.748024			
* reflector and shield								
14	REFSC	HT9 R	0.828951	CLNTR	0.157036			
14	RS2SC	HT9 S	0.299011	CLNTS	0.173203	B4CR	0.421138	
14	BRSC	S316R	0.062	CLNTS	0.938			
* primary compositions								
14	ICPC	ICSC	1.0					
14	OCPC	OCSC	1.0					
14	MCPC	MCSC	1.0					
14	LPPC	LPSC	1.0					
14	LRPC	LRSC	1.0					
14	UPPC1	UPSC1	1.0					
14	UPPC	UPSC	1.0					
14	USPC	USSC	1.0					
14	BRPC	BRSC	1.0					
14	CRBPC	CRBSC	1.0					
14	CRCPC	CRCSC	1.0					
14	CRFPC	CRFSC	1.0					
14	CRPPC	CRPSC	1.0					
14	CRDPC	CRDSC	1.0					
14	REFPC	REFSC	1.0					
14	RS2PC	RS2SC	1.0					
15	LPPC	CR__A						
15	LRPC	CR__B						
15	CRCPC	CR__C						
15	CRFPC	CR__G						
15	CRBPC	CR__H						

Figure A. IX.1: REBUS Equilibrium Model, CR = 0.77, cont.

```

15   CRPPC CR__I
15   CRDPC CR__J
15   USPC  CR__K

15   LPPC  ICO_A
15   LPPC  OCO_A
15   LPPC  MCO_A

15   LRPC  ICO_B
15   LRPC  OCO_B
15   LRPC  MCO_B

15   ICPC  ICO_D ICO_E ICO_F ICO_G ICO_H
15   OCPD  OCO_D OCO_E OCO_F OCO_G OCO_H
15   MCPD  MCO_D MCO_E MCO_F MCO_G MCO_H

15   UPPC1 ICO_I
15   UPPC1 OCO_I
15   UPPC1 MCO_I

15   UPPC  ICO_J
15   UPPC  OCO_J
15   UPPC  MCO_J

15   USPC  ICO_K
15   USPC  OCO_K
15   USPC  MCO_K

15   REFPC REFLT
15   RS2PC SHILD
15   BRPC  BARRL

```

```

29           14.6850

```

SECTION	DESCRIPTION
A	LOWER STRUCTURE/POOL
B	LOWER REFLECTOR
D,E,F,G,H	ACTIVE CORE
I,J	FISSION-GAS PLENUM
K	UPPER STRUCTURE
REFLT	RADIAL REFLECTOR
SHILD	RADIAL SHIELD
BARRL	CORE BARREL/POOL

* Ring 1 = Control Rod

30	CR__A	1	0	0	0.0	50.24
30	CR__B	1	0	0	50.24	93.66
30	CR__C	1	0	0	93.66	178.07
30	CR__G	1	0	0	178.07	194.95
30	CR__H	1	0	0	194.95	280.36
30	CR__I	1	0	0	280.36	300.46
30	CR__J	1	0	0	300.46	315.54
30	CR__K	1	0	0	315.54	345.68

Figure A.IX.1: REBUS Equilibrium Model, CR = 0.77, cont.

* Ring 2 = Inner core						
30	ICO_A	2	0	0	0.0	50.24
30	ICO_B	2	0	0	50.24	110.54
30	ICO_D	2	0	0	110.54	127.42
30	ICO_E	2	0	0	127.42	144.30
30	ICO_F	2	0	0	144.30	161.18
30	ICO_G	2	0	0	161.18	178.07
30	ICO_H	2	0	0	178.07	194.95
30	ICO_I	2	0	0	194.95	217.52
30	ICO_J	2	0	0	217.52	315.54
30	ICO_K	2	0	0	315.54	345.68
* Ring 3 = Inner / CR/ Test						
30	ICO_A	3	0	0	0.0	50.24
30	ICO_B	3	0	0	50.24	110.54
30	ICO_D	3	0	0	110.54	127.42
30	ICO_E	3	0	0	127.42	144.30
30	ICO_F	3	0	0	144.30	161.18
30	ICO_G	3	0	0	161.18	178.07
30	ICO_H	3	0	0	178.07	194.95
30	ICO_I	3	0	0	194.95	217.52
30	ICO_J	3	0	0	217.52	315.54
30	ICO_K	3	0	0	315.54	345.68
30	CR_A	3	2	2	0.0	50.24
30	CR_B	3	2	2	50.24	93.66
30	CR_C	3	2	2	93.66	178.07
30	CR_G	3	2	2	178.07	194.95
30	CR_H	3	2	2	194.95	280.36
30	CR_I	3	2	2	280.36	300.46
30	CR_J	3	2	2	300.46	315.54
30	CR_K	3	2	2	315.54	345.68
30	MCO_A	3	4	4	0.0	50.24
30	MCO_B	3	4	4	50.24	110.54
30	MCO_D	3	4	4	110.54	127.42
30	MCO_E	3	4	4	127.42	144.30
30	MCO_F	3	4	4	144.30	161.18
30	MCO_G	3	4	4	161.18	178.07
30	MCO_H	3	4	4	178.07	194.95
30	MCO_I	3	4	4	194.95	217.52
30	MCO_J	3	4	4	217.52	315.54
30	MCO_K	3	4	4	315.54	345.68
30	MCO_A	3	12	12	0.0	50.24
30	MCO_B	3	12	12	50.24	110.54
30	MCO_D	3	12	12	110.54	127.42
30	MCO_E	3	12	12	127.42	144.30
30	MCO_F	3	12	12	144.30	161.18
30	MCO_G	3	12	12	161.18	178.07
30	MCO_H	3	12	12	178.07	194.95

Figure A.IX.1: REBUS Equilibrium Model, CR = 0.77, cont.

30	MCO_I	3	12	12	194.95	217.52
30	MCO_J	3	12	12	217.52	315.54
30	MCO_K	3	12	12	315.54	345.68

* Ring 4 = Inner / Test (reflector,so far)

30	ICO_A	4	0	0	0.0	50.24
30	ICO_B	4	0	0	50.24	110.54
30	ICO_D	4	0	0	110.54	127.42
30	ICO_E	4	0	0	127.42	144.30
30	ICO_F	4	0	0	144.30	161.18
30	ICO_G	4	0	0	161.18	178.07
30	ICO_H	4	0	0	178.07	194.95
30	ICO_I	4	0	0	194.95	217.52
30	ICO_J	4	0	0	217.52	315.54
30	ICO_K	4	0	0	315.54	345.68

30	MCO_A	4	1	1	0.0	50.24
30	MCO_B	4	1	1	50.24	110.54
30	MCO_D	4	1	1	110.54	127.42
30	MCO_E	4	1	1	127.42	144.30
30	MCO_F	4	1	1	144.30	161.18
30	MCO_G	4	1	1	161.18	178.07
30	MCO_H	4	1	1	178.07	194.95
30	MCO_I	4	1	1	194.95	217.52
30	MCO_J	4	1	1	217.52	315.54
30	MCO_K	4	1	1	315.54	345.68

30	REFLT	4	4	4	0.0	345.68
----	-------	---	---	---	-----	--------

* Ring 5 = Outer / CR

30	OCO_A	5	0	0	0.0	50.24
30	OCO_B	5	0	0	50.24	110.54
30	OCO_D	5	0	0	110.54	127.42
30	OCO_E	5	0	0	127.42	144.30
30	OCO_F	5	0	0	144.30	161.18
30	OCO_G	5	0	0	161.18	178.07
30	OCO_H	5	0	0	178.07	194.95
30	OCO_I	5	0	0	194.95	217.52
30	OCO_J	5	0	0	217.52	315.54
30	OCO_K	5	0	0	315.54	345.68

30	CR__A	5	3	3	0.0	50.24
30	CR__B	5	3	3	50.24	93.66
30	CR__C	5	3	3	93.66	178.07
30	CR__G	5	3	3	178.07	194.95
30	CR__H	5	3	3	194.95	280.36
30	CR__I	5	3	3	280.36	300.46
30	CR__J	5	3	3	300.46	315.54
30	CR__K	5	3	3	315.54	345.68

30	CR__A	5	7	7	0.0	50.24
30	CR__B	5	7	7	50.24	93.66

Figure A.IX.1: REBUS Equilibrium Model, CR = 0. 77, cont.

30	CR__C	5	7	7	93.66	178.07
30	CR__G	5	7	7	178.07	194.95
30	CR__H	5	7	7	194.95	280.36
30	CR__I	5	7	7	280.36	300.46
30	CR__J	5	7	7	300.46	315.54
30	CR__K	5	7	7	315.54	345.68

30	CR__A	5	23	23	0.0	50.24
30	CR__B	5	23	23	50.24	93.66
30	CR__C	5	23	23	93.66	178.07
30	CR__G	5	23	23	178.07	194.95
30	CR__H	5	23	23	194.95	280.36
30	CR__I	5	23	23	280.36	300.46
30	CR__J	5	23	23	300.46	315.54
30	CR__K	5	23	23	315.54	345.68

* Ring 6 = Outer core and blanket

30	REFLT	6	0	0	0.0	345.68
----	-------	---	---	---	-----	--------

30	OCO_A	6	3	4	0.0	50.24
30	OCO_B	6	3	4	50.24	110.54
30	OCO_D	6	3	4	110.54	127.42
30	OCO_E	6	3	4	127.42	144.30
30	OCO_F	6	3	4	144.30	161.18
30	OCO_G	6	3	4	161.18	178.07
30	OCO_H	6	3	4	178.07	194.95
30	OCO_I	6	3	4	194.95	217.52
30	OCO_J	6	3	4	217.52	315.54
30	OCO_K	6	3	4	315.54	345.68

30	OCO_A	6	8	8	0.0	50.24
30	OCO_B	6	8	8	50.24	110.54
30	OCO_D	6	8	8	110.54	127.42
30	OCO_E	6	8	8	127.42	144.30
30	OCO_F	6	8	8	144.30	161.18
30	OCO_G	6	8	8	161.18	178.07
30	OCO_H	6	8	8	178.07	194.95
30	OCO_I	6	8	8	194.95	217.52
30	OCO_J	6	8	8	217.52	315.54
30	OCO_K	6	8	8	315.54	345.68

30	OCO_A	6	29	29	0.0	50.24
30	OCO_B	6	29	29	50.24	110.54
30	OCO_D	6	29	29	110.54	127.42
30	OCO_E	6	29	29	127.42	144.30
30	OCO_F	6	29	29	144.30	161.18
30	OCO_G	6	29	29	161.18	178.07
30	OCO_H	6	29	29	178.07	194.95
30	OCO_I	6	29	29	194.95	217.52
30	OCO_J	6	29	29	217.52	315.54
30	OCO_K	6	29	29	315.54	345.68

* Ring 7 = reflector

Figure A.IX.1: REBUS Equilibrium Model, CR = 0.77, cont.

```

30 REFLT      7      0      0      0.0      345.68
    * Ring 8 = Shield and reflector
30 SHILD      8      0      0      0.0      345.68
30 REFLT      8      3      6      0.0      345.68
30 REFLT      8     10     11     0.0      345.68
30 REFLT      8     40     41     0.0      345.68
    * Ring 9 = Shield and BARREL
30 SHILD      9      3      7      0.0      345.68
30 SHILD      9     11     13     0.0      345.68
30 SHILD      9     45     47     0.0      345.68
30 BARRL      9      2      2      0.0      345.68
30 BARRL      9      8      8      0.0      345.68
30 BARRL      9     10     10     0.0      345.68
30 BARRL      9     48     48     0.0      345.68

```

DATASET=A. BURN

```

01
01 *****
01                      FFTF, 250MWt, 12-Month
01 *****
01
02          999000          0.001          0.001          0.0001          2          1
03          0          0.0          0.0          121.7          1.00          1          0
04          1.0000          0.001          1.0          0.170          0.210
06          CPL1          0.5
09 U-234          1U-235
09 U-234          2LFP35
09 U-234          5DUMP1
09 U-234          8DUMP1
25 U-234          8DUMP1          8.978-14
09 U-235          1U-236
09 U-235          2LFP35
09 U-235          5U-234
09 U-235          8DUMP1
25 U-235          8DUMP1          3.120-17
09 U-236          1NP237
09 U-236          2LFP35
09 U-236          5U-235
09 U-236          8DUMP1
25 U-236          8DUMP1          9.379-16
09 U-238          1PU239
09 U-238          2LFP38
09 U-238          5NP237
09 U-238          8DUMP1
25 U-238          8DUMP1          4.915-18
09 NP237          1PU238
09 NP237          2LFP38
09 NP237          5PU236          0.346U-236          0.374DUMP1          0.28

```

Figure A.IX.1: REBUS Equilibrium Model, CR = 0.77, cont.

09	NP237	8DUMP1				
25	NP237	8DUMP1	1.026-14			
09	PU236	1NP237				
09	PU236	2LFP35				
09	PU236	5DUMP1				
09	PU236	8DUMP1				
25	PU236	8DUMP1	7.703-09			
09	PU238	1PU239				
09	PU238	2LFP38				
09	PU238	5NP237				
09	PU238	8U-234				
25	PU238	8U-234	2.503-10			
09	PU239	1PU240				
09	PU239	2LFP39				
09	PU239	5PU238				
09	PU239	8U-235				
25	PU239	8U-235	9.109-13			
09	PU240	1PU241				
09	PU240	2LFP40				
09	PU240	5PU239				
09	PU240	8U-236				
25	PU240	8U-236	3.353-12			
09	PU241	1PU242				
09	PU241	2LFP41				
09	PU241	5PU240				
09	PU241	6AM241				
25	PU241	6AM241	1.494-09			
09	PU242	1AM243				
09	PU242	2LFP41				
09	PU242	5PU241				
09	PU242	8U-238				
25	PU242	8U-238	5.833-14			
09	AM241	1CM242	0.66AM242	0.20PU242		0.14
09	AM241	2LFP41				
09	AM241	5PU240				
09	AM241	8NP237				
25	AM241	8NP237	5.081-11			
09	AM242	1AM243				
09	AM242	2LFP41				
09	AM242	5AM241				
09	AM242	6CM242				
25	AM242	6CM242	1.189-10			
09	AM242	7PU242				
25	AM242	7PU242	2.487-11			
09	AM242	8PU238				
25	AM242	8PU238	7.225-13			
09	AM243	1CM244				
09	AM243	2LFP41				
09	AM243	5AM242	0.500PU242	0.086CM242		0.414
09	AM243	8PU239				
25	AM243	8PU239	2.976-12			
09	CM242	1CM243				
09	CM242	2LFP41				
09	CM242	5AM241	0.99NP237	0.01		

Figure A.IX.1: REBUS Equilibrium Model, CR = 0.77, cont.

09	CM242	8PU238				
25	CM242	8PU238	4.924-08			
09	CM243	1CM244				
09	CM243	2LFP41				
09	CM243	5CM242				
09	CM243	7AM243				
25	CM243	7AM243	2.003-12			
09	CM243	8PU239				
25	CM243	8PU239	7.685-10			
09	CM244	1CM245				
09	CM244	2LFP41				
09	CM244	5CM243				
09	CM244	8PU240				
25	CM244	8PU240	1.213-09			
09	CM245	1CM246				
09	CM245	2LFP41				
09	CM245	5CM244				
09	CM245	8PU241				
25	CM245	8PU241	2.592-12			
09	CM246	1DUMP2				
09	CM246	2LFP41				
09	CM246	5CM245				
09	CM246	8PU242				
25	CM246	8PU242	4.642-12			
09	LFP35	0				
09	LFP38	0				
09	LFP39	0				
09	LFP40	0				
09	LFP41	0				
09	DUMP1	0				
09	DUMP2	0				
10	U-234	U234I	U234M	U234O		
10	U-235	U235I	U235M	U235O		
10	U-236	U236I	U236M	U236O		
10	U-238	U238I	U238M	U238O		
10	NP237	N237I	N237M	N237O		
10	PU236	P236I	P236M	P236O		
10	PU238	P238I	P238M	P238O		
10	PU239	P239I	P239M	P239O		
10	PU240	P240I	P240M	P240O		
10	PU241	P241I	P241M	P241O		
10	PU242	P242I	P242M	P242O		
10	AM241	A241I	A241M	A241O		
10	AM242	A242I	A242M	A242O		
10	AM243	A243I	A243M	A243O		
10	CM242	C242I	C242M	C242O		
10	CM243	C243I	C243M	C243O		
10	CM244	C244I	C244M	C244O		
10	CM245	C245I	C245M	C245O		
10	CM246	C246I	C246M	C246O		
11	CPL1	0	1ICSC	ICPC	2ICSC	ICPC
11	CPL1	0	3ICSC	ICPC	4ICSC	ICPC
11	CPL1	0	5ICSC	ICPC	6ICSC	ICPC

Figure A.IX.1: REBUS Equilibrium Model, CR = 0.77, cont.

11	CPL1	0	7ICSC	ICPC	8ICSC	ICPC	
11	CPL1	0	9ICSC	ICPC	10ICSC	ICPC	
11	CPL1	0	11ICSC	ICPC	12ICSC	ICPC	
11	CPL1	0	13DISI				
11	CPL2	0	10CSC	OCPC	20CSC	OCPC	
11	CPL2	0	30CSC	OCPC	40CSC	OCPC	
11	CPL2	0	50CSC	OCPC	60CSC	OCPC	
11	CPL2	0	70CSC	OCPC	80CSC	OCPC	
11	CPL2	0	90CSC	OCPC	100CSC	OCPC	
11	CPL2	0	110CSC	OCPC	120CSC	OCPC	
11	CPL2	0	130CSC	OCPC	140CSC	OCPC	
11	CPL2	0	150CSC	OCPC			
11	CPL2	0	16DISO				
11	CPL3	0	1MCSC	MCPC	2MCSC	MCPC	
11	CPL3	0	3MCSC	MCPC	4MCSC	MCPC	
11	CPL3	0	5MCSC	MCPC	6MCSC	MCPC	
11	CPL3	0	7MCSC	MCPC	8MCSC	MCPC	
11	CPL3	0	9MCSC	MCPC	10MCSC	MCPC	
11	CPL3	0	11MCSC	MCPC	12MCSC	MCPC	
11	CPL3	0	13DISM				
12	CPL1		ICLOAD	0.0	0	1.00	
12	CPL2		OCLOAD	0.0	0	1.25	
12	CPL3		MCLOAD	0.0	0	1.13	
13	ICLOAD	U-234	3.64276E-02	U-235	3.62721E-02	U-236	3.61182E-02
13	ICLOAD	U-238	3.58140E-02				
13	ICLOAD	NP237	3.59654E-02				
13	ICLOAD	PU236	3.61181E-02	PU238	3.58141E-02	PU239	3.56639E-02
13	ICLOAD	PU240	3.55151E-02	PU241	3.53674E-02	PU242	3.52210E-02
13	ICLOAD	AM241	3.53673E-02	AM242	3.52209E-02	AM243	3.50757E-02
13	ICLOAD	CM242	3.52209E-02	CM243	3.50757E-02	CM244	3.49318E-02
13	ICLOAD	CM245	3.47888E-02	CM246	3.46472E-02		
13	ICLOAD	LFP35	3.65475E-02	LFP38	3.61589E-02	LFP39	3.59882E-02
13	ICLOAD	LFP40	3.58653E-02	LFP41	3.56998E-02		
13	OCLOAD	U-234	3.64276E-02	U-235	3.62721E-02	U-236	3.61182E-02
13	OCLOAD	U-238	3.58140E-02				
13	OCLOAD	NP237	3.59654E-02				
13	OCLOAD	PU236	3.61181E-02	PU238	3.58141E-02	PU239	3.56639E-02
13	OCLOAD	PU240	3.55151E-02	PU241	3.53674E-02	PU242	3.52210E-02
13	OCLOAD	AM241	3.53673E-02	AM242	3.52209E-02	AM243	3.50757E-02
13	OCLOAD	CM242	3.52209E-02	CM243	3.50757E-02	CM244	3.49318E-02
13	OCLOAD	CM245	3.47888E-02	CM246	3.46472E-02		
13	OCLOAD	LFP35	3.65475E-02	LFP38	3.61589E-02	LFP39	3.59882E-02
13	OCLOAD	LFP40	3.58653E-02	LFP41	3.56998E-02		
13	MCLOAD	U-234	3.64276E-02	U-235	3.62721E-02	U-236	3.61182E-02
13	MCLOAD	U-238	3.58140E-02				
13	MCLOAD	NP237	3.59654E-02				
13	MCLOAD	PU236	3.61181E-02	PU238	3.58141E-02	PU239	3.56639E-02
13	MCLOAD	PU240	3.55151E-02	PU241	3.53674E-02	PU242	3.52210E-02

Figure A.IX.1: REBUS Equilibrium Model, CR = 0.77, cont.

13	MCLOAD	AM241	3.53673E-02	AM242	3.52209E-02	AM243	3.50757E-02
13	MCLOAD	CM242	3.52209E-02	CM243	3.50757E-02	CM244	3.49318E-02
13	MCLOAD	CM245	3.47888E-02	CM246	3.46472E-02		
13	MCLOAD	LFP35	3.65475E-02	LFP38	3.61589E-02	LFP39	3.59882E-02
13	MCLOAD	LFP40	3.58653E-02	LFP41	3.56998E-02		

*Reprocessing Parameters

14	DISO	547.5						
14	DISI	547.5						
14	DISM	547.5						
15	DISO		REPRO	1.0				
15	DISI		REPRI	1.0				
15	DISM		REPRM	1.0				
16	REPRO	SFRF	CLSS	180.0				
16	REPRI	SFRF	CLSS	180.0				
16	REPRM	SFRF	CLSS	180.0				
17	SFRF		NP237	1.0	PU238	1.0	PU239	1.0
17	SFRF		PU240	1.0	PU241	1.0	PU242	1.0
17	SFRF		AM241	1.0	AM242	1.0	AM243	1.0
17	SFRF		CM242	1.0	CM243	1.0	CM244	1.0
17	SFRF		CM245	1.0	CM246	1.0		
18	CLSS		NP237	1.0	PU241	1.0	PU239	1.0
18	CLSS		PU240	1.0	PU238	1.0	PU242	1.0
18	CLSS		AM241	1.0	AM242	1.0	AM243	1.0
18	CLSS		CM242	1.0	CM243	1.0	CM244	1.0
18	CLSS		CM245	1.0	CM246	1.0		
19	CPL1		REPRI	1				
19	CPL2		REPRO	1				
19	CPL3		REPRM	1				

* Class - 1 : LWR-SNF

22	ESNF		NP237	4.59900-002	AM241	5.07600-002	AM242	6.00000-005
22	ESNF		PU238	1.34500-002	PU239	5.17730-001	PU240	2.36650-001
22	ESNF		PU241	7.80200-002	PU242	4.67400-002	AM243	8.80000-003
22	ESNF		CM243	3.00000-005	CM244	1.67000-003	CM245	9.00000-005
22	ESNF		CM246	1.00000-005				
21	ESNF	SNFS		1.0E30				
18	SNFS		NP237	1.0	PU236	1.0	PU238	1.0
18	SNFS		PU239	1.0	PU240	1.0	PU241	1.0
18	SNFS		PU242	1.0	AM241	1.0	AM242	1.0
18	SNFS		AM243	1.0	CM242	1.0	CM243	1.0
18	SNFS		CM244	1.0	CM245	1.0	CM246	1.0
19	CPL3		ESNF	2				
19	CPL1		ESNF	2				
19	CPL2		ESNF	2				

* Class - 2 : Depleted Uranium

22	EDU		U-238	0.998	U-235	0.002		
21	EDU	SDU		1.0E30				
18	SDU		U-234	0.0	U-235	0.0	U-236	0.0
18	SDU		U-238	0.0				

Figure A.IX.1: REBUS Equilibrium Model, CR = 0.77, cont.

20	CPL1	EDU	1						
20	CPL2	EDU	1						
20	CPL3	EDU	1						
24	U-234	0	92	234.040945					
24	U-235	1	92	235.043922					
24	U-236	0	92	236.045561					
24	U-238	0	92	238.050785					
24	NP237	0	93	237.048166					
24	PU236	0	94	236.046048					
24	PU238	0	94	238.049553					
24	PU239	1	94	239.052156					
24	PU240	0	94	240.053808					
24	PU241	1	94	241.056273					
24	PU242	0	94	242.058737					
24	AM241	0	95	241.056822					
24	AM242	0	95	242.059098					
24	AM243	0	95	243.061374					
24	CM242	0	96	242.058831					
24	CM243	0	96	243.061382					
24	CM244	0	96	244.062747					
24	CM245	0	96	245.065484					
24	CM246	0	96	246.067218					
24	LFP35	0	92	233.27263					
24	LFP38	0	92	235.77988					
24	LFP39	0	94	236.89792					
24	LFP40	0	94	237.71005					
24	LFP41	0	94	238.81227					
24	DUMP1	0	92	232.0371					
24	DUMP2	0	96	246.0672					
29	ICORE	MCORE	OCORE						
32		100.0	250.0	100.0	121.7	3	3		
34	15	0	0	0	0	0			
46	NP237	3PU236	1PU238	1PU239	1PU240		1		
46	PU241	1PU242	1AM241	3AM242	3AM243		3		
46	CM242	3CM243	3CM244	3CM245	3CM246		3		

Figure A.IX.1: REBUS Equilibrium Model, CR = 0.77, cont.

Appendix B: Graphical Verification of Model Linearity

Presented below is a collection of 6 plots (Figures B.1a-1f) of selected nuclides showing that the general depletion model, namely ORIGEN, is essentially linear over the range of cross section perturbations applicable to this problem. The range used is cross sections perturbations from 0 to +/- 25% of the nominal value. Further, a corresponding set of 6 histograms, of the same nuclides, are shown representing the result of random sampling for that nuclides after implementing the foreword perturbation model (Figures B.2a-2f). The reader can see that these histograms resemble a Gaussian distribution, as the input cross sections were perturbed in a Gaussian distribution; a proof of linearity.

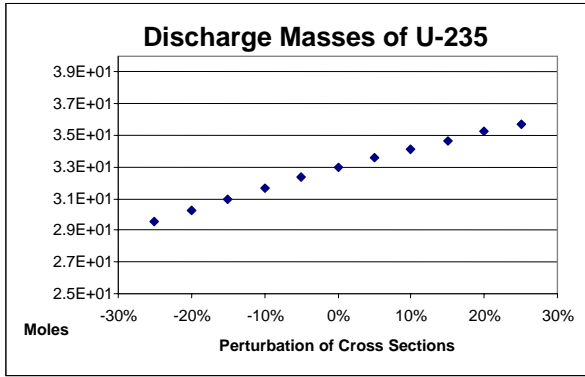


Figure B.1a: U-235 Linearity

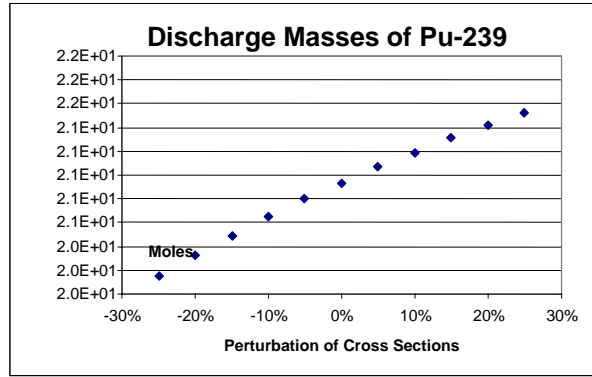


Figure B.1b: Pu-239 Linearity

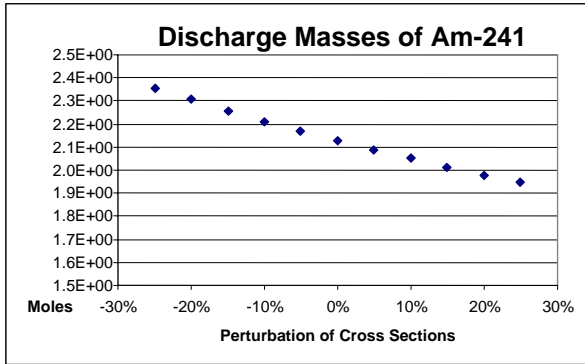


Figure B.1c: Am-241 Linearity

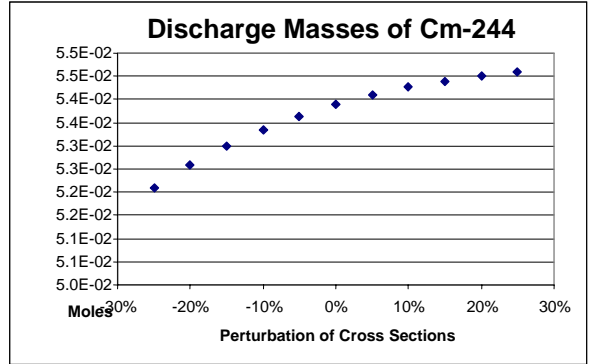


Figure B.1d: Cm-244 Linearity

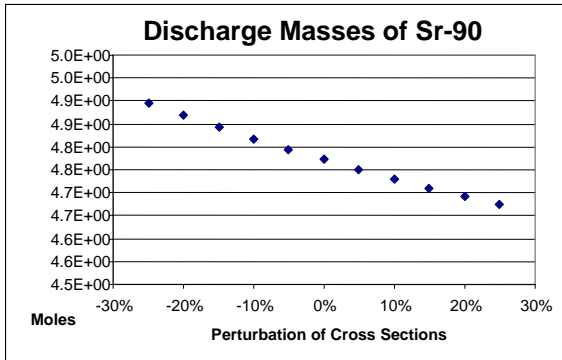


Figure B.1e: Sr-90 Linearity

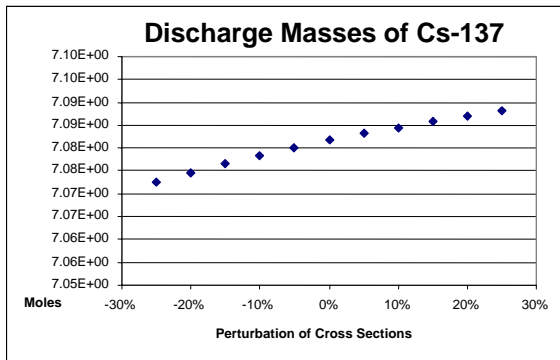


Figure B.1f: Cs-137 Linearity

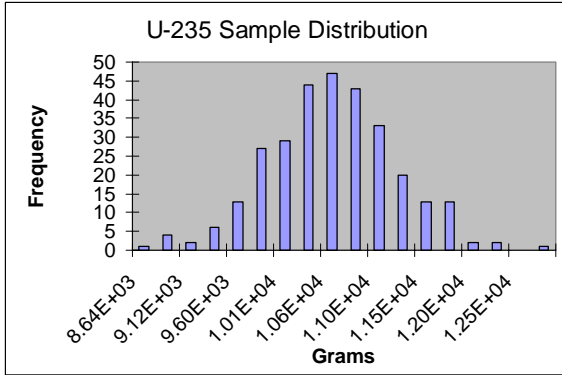


Figure B.2a: U-235 Distribution

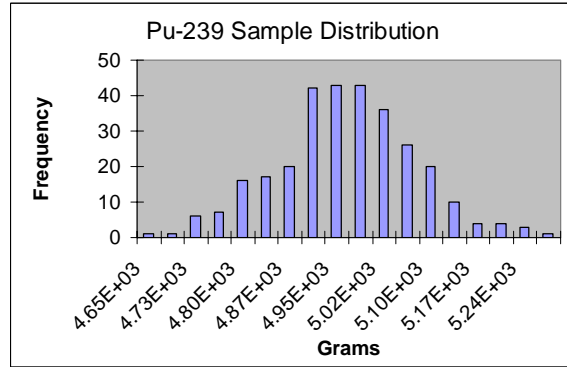


Figure B.2b: Pu-239 Distribution

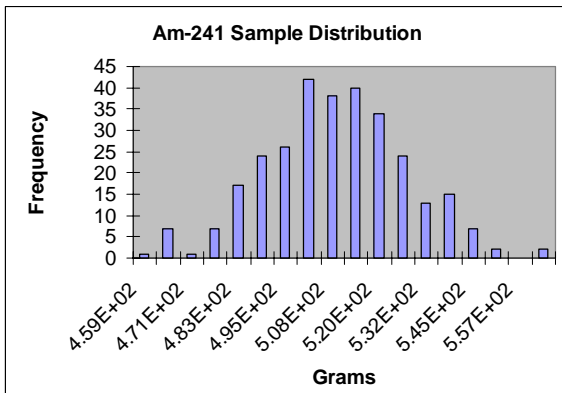


Figure B.2c: Am-241 Distribution

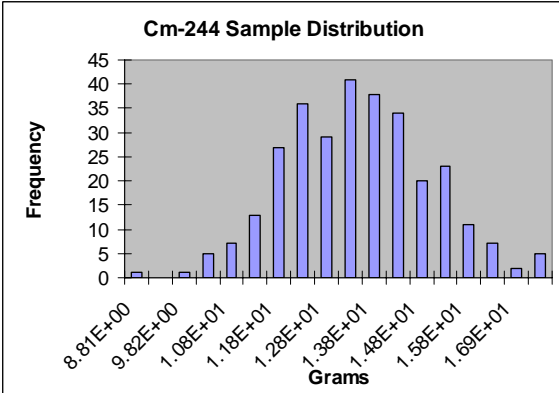


Figure B.2d: Cm-244 Distribution

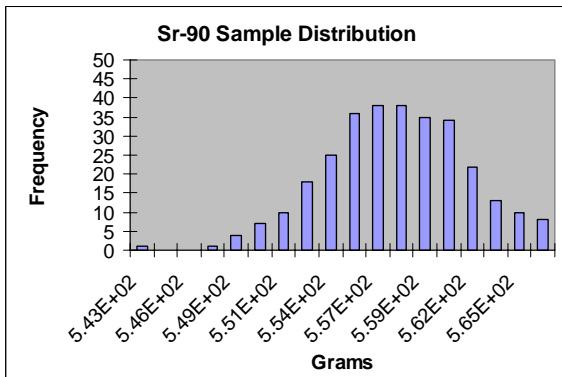


Figure B.2e: Sr-90 Distribution

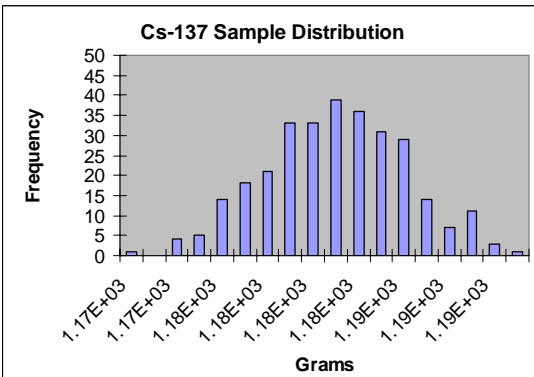


Figure B.2f: Cs-137 Distribution

Appendix C: Results Tables for Fuel Models

The following are the generalized results tables for each of the fuel models discussed in the Numerical Results section. The listing follows the order of models presented in the main body of the thesis. Since the nuclides between Pb-210 and Pa-231 were shown to contribute a negligible amount to any of the metrics, they were not included in the isotopics uncertainties lists. Tables are sub-labeled and include the absolute quantity and relative uncertainty to 95% confidence interval (1.96 standard deviations) for heat load, radioactivity, and radiotoxicity at various time steps, isotopic relative standard deviations for transuranics and fission products, main contributors to uncertainty heat load and radioactivity, and the 5 cross sections causing the most uncertainty in the model (simplified models only). The tables are somewhat different in format between the simplified ORIGEN models and the TRITON models but still follow the same principle. The table for the REBUS model follows the same format as the TRITON tables except “Charge” refers to BOC core loading and “discharge” refers to EOC core loading, both normalized to 1 MTHM.

Table C.1: Results table for the PWR model using ESM for uncertainty.

Results Table for PWR, 4.5 w/o UOX burned 40 GWD/MTU							
Uncertainty for Key Metrics					Isotopic Mass Uncertainties		
	Heat		Activity		Actinides (+/- %)		
	W	+/- %	Ci	+/- %			
Charge	5.817E-02	N/A	2.063E+00	N/A	u235	1.338	
Discharge	2.443E+06	N/A	2.325E+08	N/A	u236	0.702	
1 yr	1.178E+04	N/A	2.893E+06	N/A	u237	2.551	
5 yr	2.215E+03	1.152	7.205E+05	1.173	u238	0.076	
10 yr	1.423E+03	1.166	4.982E+05	1.119	np237	0.616	
50 yr	6.628E+02	3.037	1.603E+05	4.180	np239	13.870	
100 yr	3.567E+02	2.286	5.063E+04	0.601	pu238	1.058	
500 yr	1.126E+02	3.844	3.508E+03	3.752	pu239	0.885	
1000 yr	6.221E+01	3.280	1.966E+03	3.174	pu240	2.766	
2500 yr	2.481E+01	2.564	8.365E+02	2.540	pu241	2.551	
5000 yr	1.818E+01	2.642	6.274E+02	2.590	pu242	2.625	
10000 yr	1.346E+01	2.257	4.705E+02	2.199	am241	2.535	
	Inhalation Hazard		Ingestion Hazard		am242m	2.229	
	m³ air	+/- %	m³ water	+/- %	am243	13.870	
Charge	1.133E+13	N/A	5.380E+06	N/A	cm242	2.229	
Discharge	9.128E+17	N/A	6.723E+12	N/A	cm244	11.670	
1 yr	6.752E+17	N/A	7.972E+11	N/A	cm245	10.600	
5 yr	6.074E+17	3.295	3.862E+11	1.088	FP (+/- %)		
10 yr	5.968E+17	2.913	3.171E+11	1.092	c 14	0.490	
50 yr	5.184E+17	3.847	1.728E+11	2.339	se 79	0.382	
100 yr	4.405E+17	3.196	1.055E+11	2.512	sr 90	0.385	
500 yr	2.080E+17	3.621	3.913E+10	3.621	tc 99	1.880	
1000 yr	1.203E+17	3.049	2.262E+10	3.049	i129	0.449	
2500 yr	5.455E+16	2.610	1.026E+10	2.608	cs137	0.399	
5000 yr	4.133E+16	2.642	7.778E+09	2.639	ba137m	0.399	
10000 yr	3.053E+16	2.257	5.761E+09	2.255	y90	0.386	
	Main Contributors to Uncertainty in Decay Heat and Radioactivity					1-group Cross Sections Causing Uncertainty	
	Heat		Activity		Nuclide	Reaction	
5 yr	Cm-244		Pu241		Am-243	(n,γ)	
10 yr	Cm-244, Cs-134		Pu-241		Pu-240	(n,γ)	
50 yr	Cm-244, Cs-134		Pu-241		U-235	(fission)	
100 yr	Am-241		Am-241		Pu-239	(fission)	
500 yr	Am-241		Am-241		U-234	(n,γ)	
1000 yr	Am-241		Am-241				
2500 yr	Pu-240		Pu-240				
5000 yr	Pu-240 Pu-239		Pu-240, Pu-239				
10000 yr	Pu-240 Pu-239		Pu-240, Pu-239				

Table C.2: Results table for PWR fuel in the simplified model.

Results Table for PWR, 4.5 w/o UOX burned 40 GWD/MTU						
Uncertainty for Key Metrics					Isotopic Mass Uncertainties	
	Heat		Activity		Actinides (+/- %)	
	W	+/- %	Ci	+/- %		
Charge	5.817E-02	N/A	2.063E+00	N/A	u235	1.312
Discharge	2.443E+06	N/A	2.325E+08	N/A	u236	0.712
1 yr	1.178E+04	N/A	2.893E+06	N/A	u237	2.521
5 yr	2.215E+03	1.113	7.205E+05	1.156	u238	0.078
10 yr	1.423E+03	1.133	4.982E+05	1.103	np237	0.605
50 yr	6.628E+02	2.935	1.603E+05	4.122	np239	13.643
100 yr	3.567E+02	2.255	5.063E+04	0.588	pu238	1.050
500 yr	1.126E+02	3.788	3.508E+03	3.696	pu239	0.806
1000 yr	6.221E+01	3.215	1.966E+03	3.109	pu240	2.566
2500 yr	2.481E+01	2.396	8.365E+02	2.379	pu241	2.521
5000 yr	1.818E+01	2.457	6.274E+02	2.417	pu242	2.598
10000 yr	1.346E+01	2.094	4.705E+02	2.049	am241	2.502
	Inhalation Hazard		Ingestion Hazard		am242m	2.172
	m³ air	+/- %	m³ water	+/- %	am243	13.643
Charge	1.133E+13	N/A	5.380E+06	N/A	cm242	2.172
Discharge	9.128E+17	N/A	6.723E+12	N/A	cm244	11.340
1 yr	6.752E+17	N/A	7.972E+11	N/A	cm245	10.251
5 yr	6.074E+17	3.216	3.862E+11	1.059	FP (+/- %)	
10 yr	5.968E+17	2.846	3.171E+11	1.066	c 14	0.452
50 yr	5.184E+17	3.755	1.728E+11	2.278	se 79	0.366
100 yr	4.405E+17	3.152	1.055E+11	2.477	sr 90	0.375
500 yr	2.080E+17	3.564	3.913E+10	3.564	tc 99	1.970
1000 yr	1.203E+17	2.976	2.262E+10	2.976	i129	0.419
2500 yr	5.455E+16	2.430	1.026E+10	2.428	cs137	0.382
5000 yr	4.133E+16	2.452	7.778E+09	2.450	ba137m	0.382
10000 yr	3.053E+16	2.091	5.761E+09	2.089	y90	0.375
					cs134	1.138
Main Contributors to Uncertainty in Decay Heat and Radioactivity					1-group Cross Sections Causing Uncertainty	
	Heat		Activity		Nuclide	Reaction
5 yr	Cm-244		Pu241		Am-243	(n,γ)
10 yr	Cm-244, Cs-134		Pu-241		Pu-240	(n,γ)
50 yr	Cm-244, Cs-134		Pu-241		U-235	(fission)
100 yr	Am-241		Am-241		Pu-239	(fission)
500 yr	Am-241		Am-241		U-234	(n,γ)
1000 yr	Am-241		Am-241			
2500 yr	Pu-240		Pu-240			
5000 yr	Pu-240 Pu-239		Pu-240, Pu-239			
10000 yr	Pu-240 Pu-239		Pu-240, Pu-239			

Table C.3: Results table for typical LWR fuel simplified model.

Results Table for LWR, 4.5 w/o UOX burned 40 GWD/MTU					Isotopic Mass Uncertainties	
Uncertainty for Key Metrics					Actinides (+/- %)	
	Heat		Activity			
	W	+/- %	Ci	+/- %		
Charge	5.817E-02	N/A	2.063E+00	N/A	u235	6.184
Discharge	5.906E+04	N/A	2.255E+07	N/A	u236	1.364
1 yr	3.121E+03	N/A	7.167E+05	N/A	u237	3.708
5 yr	1.711E+03	1.148	5.456E+05	1.426	u238	0.089
10 yr	1.292E+03	0.966	4.494E+05	1.353	np237	1.032
50 yr	6.104E+02	1.649	1.562E+05	0.719	np239	12.698
100 yr	3.120E+02	3.037	4.902E+04	0.730	pu238	2.467
500 yr	9.464E+01	5.269	2.925E+03	5.124	pu239	2.202
1000 yr	5.463E+01	4.340	1.720E+03	4.181	pu240	2.837
2500 yr	2.434E+01	3.304	8.046E+02	3.222	pu241	3.708
5000 yr	1.815E+01	3.485	6.092E+02	3.362	pu242	3.995
10000 yr	1.309E+01	3.348	4.433E+02	3.200	am241	3.675
	Inhalation Hazard		Ingestion Hazard		am242m	3.169
	m³ air	+/- %	m³ water	+/- %	am243	12.698
Charge	1.133E+13	N/A	5.380E+06	N/A	cm242	3.169
Discharge	5.939E+17	N/A	1.504E+12	N/A	cm244	11.464
1 yr	4.983E+17	N/A	4.863E+11	N/A	cm245	11.231
5 yr	4.729E+17	3.570	3.530E+11	1.135	FP (+/- %)	
10 yr	4.671E+17	3.337	2.960E+11	1.158	c 14	0.683
50 yr	4.163E+17	4.057	1.551E+11	2.092	se 79	0.415
100 yr	3.581E+17	4.589	9.047E+10	3.424	sr 90	0.713
500 yr	1.776E+17	4.902	3.341E+10	4.902	tc 99	1.644
1000 yr	1.078E+17	3.994	2.026E+10	3.995	i129	0.569
2500 yr	5.414E+16	3.376	1.018E+10	3.373	cs137	0.335
5000 yr	4.149E+16	3.514	7.799E+09	3.511	ba137m	0.335
10000 yr	2.991E+16	3.381	5.623E+09	3.378	y90	0.713
					cs134	1.956
Main Contributors to Uncertainty in Decay Heat and Radioactivity					1-group Cross Sections Causing Uncertainty	
	Heat		Activity		Nuclide	Reaction
5 yr	Cm-244, Cs-134		Pu241		Am-243	(n,γ)
10 yr	Cm-244, Y-90		Pu-241		Pu-240	(n,γ)
50 yr	Am-241		Pu-241		U-235	(fission)
100 yr	Am-241		Am-241		Pu-239	(fission)
500 yr	Am-241		Am-241		U-234	(n,γ)
1000 yr	Am-241		Am-241			
2500 yr	Pu-240 Pu-239		Pu-240, Pu-239			
5000 yr	Pu-240 Pu-239		Pu-240, Pu-239			
10000 yr	Pu-240 Pu-239		Pu-240, Pu-239			

Table C.4: Results table for BWR fuel burned at 0% void.

Results Table for BWR, 0% Void, 4.5 w/o UOX burned 40 GWD/MTU						
Uncertainty for Key Metrics					Isotopic Mass Uncertainties	
	Heat		Activity		Actinides (+/- %)	
	W	+/- %	Ci	+/- %		
Charge	2.063E+00	N/A	5.817E-02	N/A	u235	1.360
Discharge	2.229E+08	N/A	2.368E+06	N/A	u236	0.481
1 yr	2.767E+06	N/A	1.095E+04	N/A	u237	2.105
5 yr	6.661E+05	0.491	2.014E+03	0.617	u238	0.055
10 yr	4.602E+05	0.426	1.304E+03	0.585	np237	0.541
50 yr	1.546E+05	0.719	5.510E+02	0.368	np239	8.910
100 yr	4.824E+04	1.430	2.536E+02	0.373	pu238	1.102
500 yr	2.098E+03	2.936	6.619E+01	2.851	pu239	0.817
1000 yr	1.256E+03	2.505	3.920E+01	2.422	pu240	2.157
2500 yr	6.293E+02	2.411	1.850E+01	2.336	pu241	2.105
5000 yr	4.829E+02	2.463	1.388E+01	2.354	pu242	2.011
10000 yr	3.510E+02	2.135	9.855E+00	2.017	am241	2.089
	Inhalation Hazard		Ingestion Hazard		am242m	1.807
	m ³ air	+/- %	m ³ water	+/- %	am243	8.910
Charge	1.133E+13	N/A	5.380E+06	N/A	cm242	1.806
Discharge	5.477E+17	N/A	6.431E+12	N/A	cm244	7.416
1 yr	3.662E+17	N/A	7.115E+11	N/A	cm245	6.816
5 yr	3.192E+17	1.854	3.352E+11	0.500	FP (+/- %)	
10 yr	3.155E+17	1.740	2.731E+11	0.510	c 14	0.392
50 yr	2.838E+17	2.243	1.326E+11	0.941	se 79	0.316
100 yr	2.455E+17	2.555	6.998E+10	1.693	sr 90	0.322
500 yr	1.252E+17	2.752	2.355E+10	2.752	tc 99	1.309
1000 yr	7.806E+16	2.387	1.468E+10	2.386	i129	0.362
2500 yr	4.122E+16	2.474	7.753E+09	2.472	cs137	0.326
5000 yr	3.164E+16	2.484	5.956E+09	2.482	ba137m	0.326
10000 yr	2.239E+16	2.157	4.226E+09	2.155	y90	0.322
					cs134	0.962
Main Contributors to Uncertainty in Decay Heat and Radioactivity					1-group Cross Sections Causing Uncertainty	
	Heat		Activity		Nuclide	Reaction
5 yr	Cm-244, Cs-134		Pu241		Am-243	(n,γ)
10 yr	Cm-244, Y-90, Ba-137m		Pu-241		Pu-240	(n,γ)
50 yr	Am-241		Pu-241		U-235	(fission)
100 yr	Am-241		Pu-241		Pu-239	(fission)
500 yr	Am-241		Am-241		U-234	(n,γ)
1000 yr	Am-241		Am-241			
2500 yr	Pu-240		Pu-240			
5000 yr	Pu-240 Pu-239		Pu-240, Pu-239			
10000 yr	Pu-240 Pu-239		Pu-240, Pu-239			

Table C.5: Results table for BWR fuel burned at 35% void.

Results Table for BWR, 35% Void, 4.5 w/o UOX burned 40 GWD/MTU						
Uncertainty for Key Metrics					Isotopic Mass Uncertainties	
	Heat		Activity		Actinides (+/- %)	
	W	+/- %	Ci	+/- %		
Charge	2.063E+00	N/A	5.817E-02	N/A	u235	1.472
Discharge	2.274E+08	N/A	2.405E+06	N/A	u236	0.608
1 yr	2.817E+06	N/A	1.128E+04	N/A	u237	2.390
5 yr	6.855E+05	0.674	2.087E+03	0.854	u238	0.065
10 yr	4.735E+05	0.631	1.344E+03	0.811	np237	0.593
50 yr	1.565E+05	0.982	5.912E+02	0.468	np239	11.086
100 yr	4.907E+04	1.853	2.916E+02	0.475	pu238	1.101
500 yr	2.632E+03	3.436	8.375E+01	3.343	pu239	0.867
1000 yr	1.533E+03	2.897	4.816E+01	2.798	pu240	2.381
2500 yr	7.191E+02	2.478	2.125E+01	2.418	pu241	2.390
5000 yr	5.470E+02	2.539	1.581E+01	2.447	pu242	2.252
10000 yr	4.023E+02	2.190	1.142E+01	2.093	am241	2.372
	Inhalation Hazard		Ingestion Hazard		am242m	2.071
	m³ air	+/- %	m³ water	+/- %	am243	11.086
Charge	1.133E+13	N/A	5.380E+06	N/A	cm242	2.070
Discharge	6.788E+17	N/A	6.560E+12	N/A	cm244	9.233
1 yr	4.769E+17	N/A	7.444E+11	N/A	cm245	8.431
5 yr	4.228E+17	2.369	3.535E+11	0.683	FP (+/- %)	
10 yr	4.171E+17	2.166	2.886E+11	0.698	c 14	0.441
50 yr	3.703E+17	2.562	1.472E+11	1.242	se 79	0.363
100 yr	3.180E+17	2.935	8.316E+10	2.117	sr 90	0.381
500 yr	1.569E+17	3.217	2.951E+10	3.217	tc 99	1.609
1000 yr	9.474E+16	2.710	1.782E+10	2.710	i129	0.408
2500 yr	4.713E+16	2.538	8.863E+09	2.536	cs137	0.374
5000 yr	3.602E+16	2.555	6.779E+09	2.553	ba137m	0.374
10000 yr	2.594E+16	2.206	4.894E+09	2.204	y90	0.381
					cs134	1.063
Main Contributors to Uncertainty in Decay Heat and Radioactivity					1-group Cross Sections Causing Uncertainty	
	Heat		Activity		Nuclide	Reaction
5 yr	Cm-244, Cs-134		Pu241		Am-243	(n,γ)
10 yr	Cm-244, Y-90, Ba-137m		Pu-241		Pu-240	(n,γ)
50 yr	Am-241		Pu-241		U-235	(fission)
100 yr	Am-241		Am-241		Pu-239	(fission)
500 yr	Am-241		Am-241		U-234	(n,γ)
1000 yr	Am-241		Am-241			
2500 yr	Pu-240		Pu-240			
5000 yr	Pu-240 Pu-239		Pu-240, Pu-239			
10000 yr	Pu-240 Pu-239		Pu-240, Pu-239			

Table C.6: Results table BWR fuel burned at 50% void.

Results Table for BWR, 50% Void, 4.5 w/o UOX burned 40 GWD/MTU						
Uncertainty for Key Metrics					Isotopic Mass Uncertainties	
	Heat		Activity		Actinides (+/- %)	
	W	+/- %	Ci	+/- %		
Charge	2.063E+00	N/A	5.817E-02	N/A	u235	1.757
Discharge	2.303E+08	N/A	2.425E+06	N/A	u236	0.731
1 yr	2.853E+06	N/A	1.153E+04	N/A	u237	2.492
5 yr	7.015E+05	0.880	2.146E+03	1.025	u238	0.069
10 yr	4.848E+05	0.858	1.379E+03	0.977	np237	0.638
50 yr	1.582E+05	1.171	6.249E+02	0.548	np239	12.685
100 yr	4.979E+04	2.098	3.230E+02	0.556	pu238	1.147
500 yr	3.074E+03	3.667	9.827E+01	3.574	pu239	0.874
1000 yr	1.763E+03	3.111	5.561E+01	3.010	pu240	2.637
2500 yr	7.953E+02	2.609	2.360E+01	2.560	pu241	2.492
5000 yr	6.019E+02	2.678	1.747E+01	2.597	pu242	2.437
10000 yr	4.463E+02	2.290	1.276E+01	2.207	am241	2.474
	Inhalation Hazard		Ingestion Hazard		am242m	2.156
	m³ air	+/- %	m³ water	+/- %	am243	12.685
Charge	1.133E+13	N/A	5.380E+06	N/A	cm242	2.155
Discharge	7.862E+17	N/A	6.652E+12	N/A	cm244	10.618
1 yr	5.685E+17	N/A	7.698E+11	N/A	cm245	9.687
5 yr	5.087E+17	2.786	3.686E+11	0.868	FP (+/- %)	
10 yr	5.013E+17	2.506	3.017E+11	0.881	c 14	0.483
50 yr	4.415E+17	2.710	1.595E+11	1.439	se 79	0.408
100 yr	3.778E+17	3.100	9.405E+10	2.347	sr 90	0.436
500 yr	1.831E+17	3.443	3.444E+10	3.443	tc 99	1.864
1000 yr	1.087E+17	2.906	2.043E+10	2.906	i129	0.444
2500 yr	5.218E+16	2.669	9.813E+09	2.667	cs137	0.413
5000 yr	3.979E+16	2.690	7.488E+09	2.688	ba137m	0.413
10000 yr	2.898E+16	2.302	5.467E+09	2.300	y90	0.436
					cs134	1.166
Main Contributors to Uncertainty in Decay Heat and Radioactivity					1-group Cross Sections Causing Uncertainty	
	Heat		Activity		Nuclide	Reaction
5 yr	Cm-244, Cs-134		Pu241		Am-243	(n,γ)
10 yr	Cm-244, Y-90, Ba-137m		Pu-241		Pu-240	(n,γ)
50 yr	Am-241		Pu-241		U-235	(fission)
100 yr	Am-241		Am-241		Pu-239	(fission)
500 yr	Am-241		Am-241		U-234	(n,γ)
1000 yr	Am-241		Am-241			
2500 yr	Pu-240		Pu-240			
5000 yr	Pu-240 Pu-239		Pu-240, Pu-239			
10000 yr	Pu-240 Pu-239		Pu-240, Pu-239			

Table C.7: Results table for BWR fuel burned at 65% void.

Results Table for BWR, 65% Void, 4.5 w/o UOX burned 40 GWD/MTU						
Uncertainty for Key Metrics					Isotopic Mass Uncertainties	
	Heat		Activity		Actinides (+/- %)	
	W	+/- %	Ci	+/- %		
Charge	2.063E+00	N/A	5.817E-02	N/A	u235	1.677
Discharge	2.346E+08	N/A	2.449E+06	N/A	u236	0.839
1 yr	2.907E+06	N/A	1.189E+04	N/A	u237	2.479
5 yr	7.286E+05	1.223	2.243E+03	1.226	u238	0.079
10 yr	5.046E+05	1.232	1.440E+03	1.175	np237	0.697
50 yr	1.613E+05	1.385	6.824E+02	0.649	np239	14.483
100 yr	5.111E+04	2.288	3.761E+02	0.657	pu238	1.172
500 yr	3.823E+03	3.706	1.229E+02	3.619	pu239	0.920
1000 yr	2.155E+03	3.138	6.835E+01	3.040	pu240	2.536
2500 yr	9.305E+02	2.390	2.777E+01	2.374	pu241	2.479
5000 yr	7.006E+02	2.459	2.048E+01	2.421	pu242	2.531
10000 yr	5.253E+02	2.130	1.518E+01	2.086	am241	2.462
	Inhalation Hazard		Ingestion Hazard		am242m	2.154
	m³ air	+/- %	m³ water	+/- %	am243	14.483
Charge	1.133E+13	N/A	5.380E+06	N/A	cm242	2.153
Discharge	9.632E+17	N/A	6.791E+12	N/A	cm244	12.041
1 yr	7.212E+17	N/A	8.098E+11	N/A	cm245	10.851
5 yr	6.526E+17	3.237	3.941E+11	1.146	FP (+/- %)	
10 yr	6.423E+17	2.862	3.242E+11	1.150	c 14	0.544
50 yr	5.615E+17	2.730	1.803E+11	1.624	se 79	0.465
100 yr	4.784E+17	3.106	1.125E+11	2.489	sr 90	0.496
500 yr	2.276E+17	3.482	4.281E+10	3.482	tc 99	2.238
1000 yr	1.326E+17	2.906	2.494E+10	2.906	i129	0.502
2500 yr	6.124E+16	2.427	1.152E+10	2.425	cs137	0.473
5000 yr	4.663E+16	2.457	8.775E+09	2.455	ba137m	0.473
10000 yr	3.450E+16	2.131	6.507E+09	2.129	y90	0.496
					cs134	1.305
Main Contributors to Uncertainty in Decay Heat and Radioactivity					1-group Cross Sections Causing Uncertainty	
	Heat		Activity		Nuclide	Reaction
5 yr	Cm-244, Cs-134		Pu241		Am-243	(n,γ)
10 yr	Cm-244, Y-90, Ba-137m		Pu-241		Pu-240	(n,γ)
50 yr	Am-241		Pu-241		U-235	(fission)
100 yr	Am-241		Am-241		Pu-239	(fission)
500 yr	Am-241		Am-241		U-234	(n,γ)
1000 yr	Am-241		Am-241			
2500 yr	Pu-240 Pu-239		Pu-240, Pu-239			
5000 yr	Pu-240 Pu-239		Pu-240, Pu-239			
10000 yr	Pu-240 Pu-239		Pu-240, Pu-239			

Table C.8: Results table for clean MOX fuel.

Results Table for PWR, MOX fuel burned 50 GWD/MTU						
Uncertainty for Key Metrics					Isotopic Mass Uncertainties	
	Heat		Activity		Actinides (+/- %)	
	W	+/- %	Ci	+/- %		
Charge	9.887E+05	N/A	3.926E+03	N/A	u235	1.367
Discharge	2.888E+08	N/A	2.990E+06	N/A	u236	1.037
1 yr	4.927E+06	N/A	2.543E+04	N/A	u237	1.929
5 yr	1.602E+06	11.670	7.824E+03	2.723	u238	0.092
10 yr	1.157E+06	11.020	6.267E+03	2.691	np237	0.790
50 yr	3.288E+05	4.158	3.765E+03	1.744	np239	24.978
100 yr	1.255E+05	2.058	2.567E+03	1.325	pu238	1.312
500 yr	2.354E+04	2.743	7.581E+02	2.777	pu239	1.384
1000 yr	1.287E+04	2.803	4.055E+02	3.009	pu240	2.361
2500 yr	5.661E+03	3.832	1.679E+02	4.423	pu241	1.929
5000 yr	4.153E+03	4.149	1.212E+02	4.742	pu242	2.590
10000 yr	2.909E+03	3.725	8.490E+01	4.263	am241	1.838
	Inhalation Hazard		Ingestion Hazard		am242m	1.213
	m³ air	+/- %	m³ water	+/- %	am243	24.978
Charge	9.004E+18	N/A	1.701E+12	N/A	cm242	1.213
Discharge	1.156E+19	N/A	1.021E+13	N/A	cm244	17.637
1 yr	1.015E+19	N/A	2.783E+12	N/A	cm245	14.425
5 yr	9.341E+18	8.639	2.037E+12	7.608	FP (+/- %)	
10 yr	8.825E+18	7.588	1.852E+12	6.863	c 14	0.837
50 yr	6.207E+18	2.906	1.238E+12	2.758	se 79	0.734
100 yr	4.600E+18	1.989	8.878E+11	1.944	sr 90	0.690
500 yr	1.410E+18	2.612	2.652E+11	2.611	tc 99	2.561
1000 yr	7.853E+17	2.697	1.477E+11	2.696	i129	0.764
2500 yr	3.658E+17	3.576	6.884E+10	3.573	cs137	0.759
5000 yr	2.717E+17	3.763	5.121E+10	3.761	ba137m	0.759
10000 yr	1.895E+17	3.386	3.591E+10	3.383	y90	0.690
	Main Contributors to Uncertainty in Decay Heat and Radioactivity				1-group Cross Sections Causing Uncertainty	
	Heat		Activity		Nuclide	Reaction
5 yr	Cm-244		Pu-241, Cm-244		Am-243	(n,γ)
10 yr	Cm-244		Pu-241, Cm-244		Pu-239	(fission)
50 yr	Cm-244		Pu-241, Cm-244		Pu-240	(fission)
100 yr	Pu-238, Am-241, Cm-244		Pu-238, Am-241, Cm-244		Pu-242	(n,γ)
500 yr	Am-241		Am-241		Pu-240	(n,γ)
1000 yr	Am-241, Am-243		Am-241, Am-243			
2500 yr	Pu-240, Am-243		Pu-240, Am-243			
5000 yr	Pu-240, Am-243		Pu-240, Am-243			
10000 yr	Pu-240, Am-243		Pu-240, Am-243			

Table C.9: Results table for MOX fuel with impurities.

Results Table for PWR, MOX fuel with Impurities burned 50 GWD/MTU						
Uncertainty for Key Metrics					Isotopic Mass Uncertainties	
	Heat		Activity		Actinides (+/- %)	
	W	+/- %	Ci	+/- %		
Charge	1.040E+06	N/A	5.643E+03	N/A	u235	1.354
Discharge	2.977E+08	N/A	3.134E+06	N/A	u236	1.059
1 yr	5.927E+06	N/A	6.168E+04	N/A	u237	1.863
5 yr	1.796E+06	6.146	1.419E+04	2.353	u238	0.096
10 yr	1.343E+06	5.588	1.232E+04	2.281	np237	0.373
50 yr	4.637E+05	2.103	8.179E+03	1.316	np239	23.074
100 yr	2.200E+05	1.265	5.641E+03	1.009	pu238	0.791
500 yr	3.481E+04	1.741	1.120E+03	1.788	pu239	1.354
1000 yr	1.656E+04	2.095	5.249E+02	2.310	pu240	2.299
2500 yr	6.460E+03	3.484	1.917E+02	4.053	pu241	1.863
5000 yr	4.640E+03	3.893	1.349E+02	4.459	pu242	2.393
10000 yr	3.332E+03	3.457	9.670E+01	3.955	am241	1.183
	Inhalation Hazard		Ingestion Hazard		am242m	1.162
	m³ air	+/- %	m³ water	+/- %	am243	23.074
Charge	1.196E+19	N/A	2.257E+12	N/A	cm242	1.162
Discharge	3.657E+19	N/A	1.502E+13	N/A	cm244	16.130
1 yr	2.528E+19	N/A	5.618E+12	N/A	cm245	13.127
5 yr	2.145E+19	3.866	4.323E+12	3.659	FP (+/- %)	
10 yr	2.046E+19	3.401	4.049E+12	3.259	c 14	0.946
50 yr	1.477E+19	1.565	2.856E+12	1.531	se 79	0.816
100 yr	1.057E+19	1.256	2.016E+12	1.244	sr 90	0.764
500 yr	2.069E+18	1.681	3.895E+11	1.679	tc 99	2.942
1000 yr	9.956E+17	2.074	1.874E+11	2.072	i129	0.828
2500 yr	4.101E+17	3.294	7.734E+10	3.288	cs137	0.819
5000 yr	2.976E+17	3.564	5.637E+10	3.557	ba137m	0.819
10000 yr	2.104E+17	3.194	4.041E+10	3.189	y90	0.764
					cs134	1.682
Main Contributors to Uncertainty in Decay Heat and Radioactivity					1-group Cross Sections Causing Uncertainty	
	Heat		Activity		Nuclide	Reaction
5 yr	Cm-244		Pu-241, Cm-244		Am-243	(n,γ)
10 yr	Cm-244		Pu-241, Cm-244		Pu-239	(fission)
50 yr	Cm-244		Pu-241, Cm-244		Pu-242	(n,γ)
100 yr	Pu-238, Am-241		Pu-238, Am-241		Pu-241	(fission)
500 yr	Am-241		Am-241		Pu-240	(n,γ)
1000 yr	Am-241, Am-243		Am-241, Am-243			
2500 yr	Pu-240, Am-243		Pu-240, Am-243			
5000 yr	Pu-240, Am-243		Pu-240, Am-243			
10000 yr	Pu-240, Am-243		Pu-240, Am-243			

Table C.10: Results table for TRITON PWR model, 48 GWD/MTU

Results Table for PWR, 4.5 w/o UOX burned 48 GWD/MTU					Isotopic Mass Uncertainties	
Uncertainty for Key Metrics					Actinides (+/- %)	
	Heat		Activity			
	W	+/- %	Ci	+/- %		
Charge	6.096E-02	N/A	2.160E+00	N/A	u235	0.620
Discharge	6.036E+04	N/A	2.249E+07	N/A	u236	1.052
1 yr	4.050E+03	N/A	8.538E+05	N/A	u237	2.067
5 yr	2.156E+03	0.696	6.427E+05	0.807	u238	0.015
10 yr	1.638E+03	0.779	5.280E+05	0.771	np237	1.609
50 yr	7.799E+02	1.020	1.825E+05	0.352	np239	3.878
100 yr	4.090E+02	1.736	5.788E+04	0.384	pu238	1.749
500 yr	1.205E+02	2.990	3.737E+03	2.906	pu239	1.065
1000 yr	6.878E+01	2.616	2.177E+03	2.525	pu240	2.486
2500 yr	3.045E+01	2.577	1.018E+03	2.481	pu241	2.065
5000 yr	2.263E+01	2.672	7.679E+02	2.539	pu242	3.897
10000 yr	1.625E+01	2.343	5.551E+02	2.212	am241	2.063
	Inhalation Hazard		Ingestion Hazard		am242m	2.121
	m³ air	+/- %	m³ water	+/- %	am243	3.884
Charge	1.188E+13	N/A	5.636E+06	N/A	cm242	2.121
Discharge	1.051E+18	N/A	1.654E+12	N/A	cm244	4.337
1 yr	8.750E+17	N/A	6.188E+11	N/A	cm245	4.673
5 yr	8.076E+17	2.334	4.527E+11	0.794	FP (+/- %)	
10 yr	7.801E+17	2.178	3.819E+11	0.845	c 14	0.360
50 yr	6.216E+17	2.233	2.036E+11	1.285	se 79	0.087
100 yr	5.075E+17	2.476	1.216E+11	1.945	sr 90	0.120
500 yr	2.257E+17	2.824	4.246E+10	2.823	tc 99	0.076
1000 yr	1.352E+17	2.509	2.542E+10	2.508	i129	0.174
2500 yr	6.736E+16	2.668	1.266E+10	2.665	cs137	0.025
5000 yr	5.144E+16	2.711	9.671E+09	2.708	ba137m	0.025
10000 yr	3.693E+16	2.378	6.944E+09	2.376	y90	0.120
	Main Contributors to Uncertainty in Decay Heat and Radioactivity				cs134	0.318
	Heat		Activity		k-effective Values	
					BOL	1.4181
5 yr	Cm-244		Pu241		EOL	0.9696
10 yr	Pu-238, Cm-244		Pu-241			
50 yr	Pu-238, Am-241		Pu-241			
100 yr	Am-241		Am-241			
500 yr	Am-241		Am-241			
1000 yr	Pu-240, Am-241		Pu-240, Am-241			
2500 yr	Pu-240 Pu-239		Pu-240, Pu-239			
5000 yr	Pu-240 Pu-239		Pu-240, Pu-239			
10000 yr	Pu-240 Pu-239		Pu-240, Pu-239			

Table C.11: Results table for fast reactor fuel of CR = 0.25.

Results Table for FR, CR=0.25, burned 94.3 GWD/MTU							
Uncertainty for Key Metrics					Isotopic Mass Uncertainties		
	Heat		Activity		Actinides (+/- %)		
	W	+/- %	Ci	+/- %			
Charge	6.397E+04	N/A	5.520E+06	N/A	u235	1.490	
Discharge	3.748E+05	N/A	3.982E+07	N/A	u236	1.795	
1 yr	8.308E+04	N/A	6.625E+06	N/A	u237	2.764	
5 yr	5.399E+04	14.160	5.170E+06	5.200	u238	0.205	
10 yr	4.820E+04	13.142	4.290E+06	5.104	np237	1.114	
50 yr	2.555E+04	6.068	1.339E+06	3.610	np239	10.752	
100 yr	1.677E+04	3.388	6.221E+05	2.753	pu238	3.371	
500 yr	5.375E+03	1.732	1.702E+05	1.708	pu239	1.468	
1000 yr	3.142E+03	1.581	1.014E+05	1.652	pu240	0.906	
2500 yr	1.639E+03	1.768	5.534E+04	1.978	pu241	2.764	
5000 yr	1.218E+03	1.867	4.150E+04	2.076	pu242	0.548	
10000 yr	8.012E+02	1.817	2.728E+04	2.009	am241	1.341	
	Inhalation Hazard		Ingestion Hazard		am242m	1.434	
	m³ air	+/- %	m³ water	+/- %	am243	10.752	
Charge	7.719E+19	N/A	1.458E+13	N/A	cm242	1.434	
Discharge	1.044E+20	N/A	2.136E+13	N/A	cm244	13.025	
1 yr	8.267E+19	N/A	1.612E+13	N/A	cm245	4.344	
5 yr	7.580E+19	10.165	1.471E+13	9.930	FP (+/- %)		
10 yr	6.983E+19	9.232	1.350E+13	9.048	c 14	1.655	
50 yr	4.339E+19	4.610	8.305E+12	4.559	se 79	1.137	
100 yr	3.108E+19	3.422	5.895E+12	3.410	sr 90	0.348	
500 yr	1.033E+19	1.623	1.944E+12	1.623	tc 99	0.319	
1000 yr	6.330E+18	1.486	1.190E+12	1.485	i129	0.412	
2500 yr	3.619E+18	1.664	6.805E+11	1.663	cs137	0.094	
5000 yr	2.735E+18	1.733	5.143E+11	1.732	ba137m	0.094	
10000 yr	1.797E+18	1.698	3.379E+11	1.697	y90	0.348	
	Main Contributors to Uncertainty in Decay Heat and Radioactivity					cs134	2.553
	Heat		Activity		k-effective Values		
					BOL	1.2856	
5 yr	Cm-244		Cm-244, Pu-241		EOL	1.1792	
10 yr	Cm-244		Cm-244, Pu-241				
50 yr	Cm-244, Pu-238		Cm-244, Pu-238				
100 yr	Pu-238, Am-241		Pu-238, Am-241				
500 yr	Am-241		Am-241				
1000 yr	Am-241		Am-241				
2500 yr	Am-243, Pu-240		Am-243, Pu-240				
5000 yr	Am-243, Pu-240		Am-243, Pu-240				
10000 yr	Am-243, Pu-239, Pu-240		Am-243, Pu-239, Pu-240				

Table C.12: Results table for fast reactor fuel of CR = 0.70.

Results Table for FR, CR=0.7, burned 78.4 GWD/MTU						
Uncertainty for Key Metrics					Isotopic Mass Uncertainties	
	Heat		Activity		Actinides (+/- %)	
	W	+/- %	Ci	+/- %		
Charge	9.086E+03	N/A	1.138E+06	N/A	u235	2.587
Discharge	1.300E+05	N/A	3.333E+07	N/A	u236	4.793
1 yr	1.763E+04	N/A	2.142E+06	N/A	u237	3.832
5 yr	1.208E+04	14.673	1.729E+06	4.552	u238	0.230
10 yr	1.068E+04	13.774	1.434E+06	4.416	np237	1.680
50 yr	6.002E+03	6.423	4.625E+05	2.845	np239	15.475
100 yr	4.051E+03	4.192	1.920E+05	2.680	pu238	4.824
500 yr	1.502E+03	2.777	4.738E+04	2.710	pu239	2.406
1000 yr	9.631E+02	2.588	3.085E+04	2.584	pu240	1.992
2500 yr	5.749E+02	2.903	1.896E+04	2.933	pu241	3.833
5000 yr	4.473E+02	3.009	1.482E+04	3.024	pu242	1.150
10000 yr	3.094E+02	2.993	1.024E+04	2.993	am241	2.369
	Inhalation Hazard		Ingestion Hazard		am242m	1.836
	m³ air	+/- %	m³ water	+/- %	am243	15.475
Charge	1.487E+19	N/A	2.809E+12	N/A	cm242	1.837
Discharge	2.039E+19	N/A	5.674E+12	N/A	cm244	16.925
1 yr	1.689E+19	N/A	3.633E+12	N/A	cm245	9.295
5 yr	1.571E+19	11.560	3.293E+12	10.454	FP (+/- %)	
10 yr	1.465E+19	10.447	3.025E+12	9.585	c 14	0.962
50 yr	9.804E+18	5.515	1.946E+12	5.256	se 79	0.627
100 yr	7.387E+18	4.353	1.422E+12	4.273	sr 90	0.180
500 yr	2.967E+18	2.627	5.580E+11	2.627	tc 99	0.472
1000 yr	2.003E+18	2.559	3.765E+11	2.558	i129	0.460
2500 yr	1.293E+18	2.922	2.431E+11	2.920	cs137	0.098
5000 yr	1.019E+18	2.998	1.916E+11	2.996	ba137m	0.092
10000 yr	7.050E+17	2.992	1.325E+11	2.991	y90	0.181
Main Contributors to Uncertainty in Decay Heat and Radioactivity					cs134	2.250
					k-effective Values	
					BOL	1.1779
					EOL	1.1195
	Heat		Activity			
5 yr	Cm-244		Cm-244, Pu-241			
10 yr	Cm-244		Cm-244, Pu-241			
50 yr	Cm-244, Pu-238		Cm-244, Pu-238, Pu-241			
100 yr	Pu-238, Am-241		Pu-238, Am-241			
500 yr	Am-241		Am-241			
1000 yr	Pu-240, Am-241		Pu-240, Am-241			
2500 yr	Pu-239, Pu-240		Pu-239, Pu-240			
5000 yr	Pu-239, Pu-240		Pu-239, Pu-240			
10000 yr	Pu-239, Pu-240		Pu-239, Pu-240			

Table C.13: Results table for fast reactor fuel of CR = 1.05.

Results Table for FR, CR=1.05, burned 67.7 GWD/MTU							
Uncertainty for Key Metrics					Isotopic Mass Uncertainties		
	Heat		Activity		Actindes (+/- %)		
	W	+/- %	Ci	+/- %			
Charge	1.632E+03	N/A	3.224E+05	N/A	u235	3.267	
Discharge	1.024E+05	N/A	3.537E+07	N/A	u236	5.535	
1 yr	6.572E+03	N/A	1.415E+06	N/A	u237	4.247	
5 yr	4.281E+03	6.259	1.149E+06	3.371	u238	0.255	
10 yr	3.682E+03	6.126	9.487E+05	3.213	np237	2.828	
50 yr	2.403E+03	3.672	3.106E+05	1.628	np239	15.989	
100 yr	1.735E+03	3.634	1.156E+05	1.685	pu238	5.204	
500 yr	8.261E+02	3.638	2.591E+04	3.572	pu239	2.800	
1000 yr	5.835E+02	3.513	1.852E+04	3.496	pu240	3.066	
2500 yr	3.873E+02	3.989	1.253E+04	3.966	pu241	4.246	
5000 yr	3.117E+02	4.060	1.011E+04	4.025	pu242	3.141	
10000 yr	2.240E+02	4.014	7.275E+03	3.977	am241	3.271	
	Inhalation Hazard		Ingestion Hazard		am242m	1.972	
	m³ air	+/- %	m³ water	+/- %	am243	15.989	
Charge	3.353E+18	N/A	6.323E+11	N/A	cm242	1.972	
Discharge	5.606E+18	N/A	3.066E+12	N/A	cm244	19.875	
1 yr	4.657E+18	N/A	1.334E+12	N/A	cm245	11.948	
5 yr	4.466E+18	6.841	1.169E+12	4.951	FP (+/- %)		
10 yr	4.339E+18	6.173	1.076E+12	4.714	c 14	0.708	
50 yr	3.603E+18	4.224	7.747E+11	3.707	se 79	0.544	
100 yr	3.061E+18	3.878	6.055E+11	3.695	sr 90	0.159	
500 yr	1.681E+18	3.508	3.159E+11	3.507	tc 99	0.554	
1000 yr	1.247E+18	3.560	2.344E+11	3.559	i129	0.494	
2500 yr	8.838E+17	4.036	1.661E+11	4.035	cs137	0.099	
5000 yr	7.181E+17	4.073	1.349E+11	4.072	ba137m	0.099	
10000 yr	5.161E+17	4.029	9.696E+10	4.028	y90	0.158	
	Main Contributors to Uncertainty in Decay Heat and Radioactivity					cs134	2.214
	Heat		Activity		k-effective Values		
					BOL	1.0234	
5 yr	Cm-244		Cm-244, Pu-241		EOL	1.0452	
10 yr	Cm-244		Cm-244, Pu-241				
50 yr	Cm-244, Pu-238		Cm-244, Pu-238, Pu-241				
100 yr	Pu-238, Am-241		Pu-238, Am-241				
500 yr	Pu-240, Am-241		Pu-240, Am-241				
1000 yr	Pu-238, Pu-240, Am-241		Pu-239, Pu-240, Am-241				
2500 yr	Pu-239, Pu-240		Pu-239, Pu-240				
5000 yr	Pu-239, Pu-240		Pu-239, Pu-240				
10000 yr	Pu-239, Pu-240		Pu-239, Pu-240				

Table C.14: Results table for equilibrium recycled fast reactor fuel of CR = 0.70.

Results Table for Recycled FR, CR=0.7, burned 41.4 GWD/MTU						
Uncertainty for Key Metrics					Isotopic Mass Uncertainties	
	Heat		Activity		Actinides (+/- %)	
	W	+/- %	Ci	+/- %		
Charge	9.086E+03	N/A	1.138E+06	N/A	u235	2.819
Discharge	1.331E+05	N/A	3.272E+07	N/A	u236	5.757
1 yr	1.770E+04	N/A	2.020E+06	N/A	u237	6.671
5 yr	1.220E+04	19.983	1.640E+06	8.875	u238	0.260
10 yr	1.100E+04	18.698	1.356E+06	8.585	np237	11.435
50 yr	6.348E+03	11.953	4.069E+05	6.594	np239	46.662
100 yr	4.433E+03	10.818	1.790E+05	8.118	pu238	12.869
500 yr	1.765E+03	8.443	5.555E+04	8.215	pu239	4.924
1000 yr	1.126E+03	7.500	3.599E+04	7.452	pu240	5.482
2500 yr	6.560E+02	7.838	2.160E+04	7.966	pu241	6.671
5000 yr	5.044E+02	7.979	1.669E+04	8.082	pu242	6.429
10000 yr	3.430E+02	7.500	1.134E+04	7.591	am241	7.244
	Inhalation Hazard		Ingestion Hazard		am242m	9.284
	m³ air	+/- %	m³ water	+/- %	am243	27.480
Charge	1.487E+19	N/A	2.809E+12	N/A	cm242	9.284
Discharge	2.265E+19	N/A	5.779E+12	N/A	cm244	19.265
1 yr	1.866E+19	N/A	3.736E+12	N/A	cm245	15.308
					FP (+/- %)	
5 yr	1.733E+19	16.097	3.442E+12	15.353	c 14	3.042
10 yr	1.615E+19	15.176	3.188E+12	14.555	se 79	1.548
50 yr	1.081E+19	12.097	2.092E+12	11.819	sr 90	0.410
100 yr	8.227E+18	11.132	1.566E+12	11.042	tc 99	0.514
500 yr	3.474E+18	7.866	6.533E+11	7.866	i129	0.854
1000 yr	2.333E+18	7.262	4.385E+11	7.261	cs137	0.144
2500 yr	1.475E+18	7.865	2.772E+11	7.861	ba137m	0.140
5000 yr	1.150E+18	7.919	2.161E+11	7.915	y90	0.410
10000 yr	7.816E+17	7.453	1.469E+11	7.449	cs134	2.966
Main Contributors to Uncertainty in Decay Heat and Radioactivity					k-effective Values	
	Heat		Activity		BOL	1.1731
5 yr	Cm-244		Cm-244, Pu-241		EOL	1.1468
10 yr	Cm-244		Cm-244, Pu-241			
50 yr	Cm-244, Pu-238		Cm-244, Pu-238, Pu-241			
100 yr	Pu-238, Am-241		Pu-238, Am-241			
500 yr	Pu-240, Am-241		Pu-240, Am-241			
1000 yr	Pu-239, Pu-240, Am-241		Pu-239, Pu-240, Am-241			
2500 yr	Pu-239, Pu-240		Pu-239, Pu-240			
5000 yr	Pu-239, Pu-240		Pu-239, Pu-240			
10000 yr	Pu-239, Pu-240		Pu-239, Pu-240			

Table C.15: Results table for REBUS equilibrium recycled fast reactor fuel.

Results Table for Recycled FR, CR=0.77, burned 76.5 GWD/MTU						
Uncertainty for Key Metrics				Isotopic Mass Uncertainties		
	Heat		Activity		Actinides (+/- %)	
	W	+/- %	Ci	+/- %		
Charge	3.474E+04	N/A	1.806E+06	N/A	u235	0.809
Discharge	3.871E+04	N/A	1.941E+06	N/A	u236	2.034
1 yr	1.634E+04	N/A	1.288E+06	N/A	u237	--
5 yr	9.725E+03	22.005	9.632E+05	15.819	u238	0.950
10 yr	8.980E+03	20.959	7.979E+05	15.327	np237	7.344
50 yr	5.699E+03	17.649	2.522E+05	13.526	np239	--
100 yr	4.192E+03	16.693	1.374E+05	15.399	pu238	18.616
500 yr	1.616E+03	11.382	5.039E+04	11.044	pu239	1.336
1000 yr	1.017E+03	9.549	3.194E+04	9.371	pu240	7.463
2500 yr	5.961E+02	8.750	1.912E+04	8.745	pu241	10.570
5000 yr	4.650E+02	8.556	1.498E+04	8.526	pu242	18.769
10000 yr	3.258E+02	7.269	1.050E+04	7.241	am241	10.163
	Inhalation Hazard		Ingestion Hazard		am242m	14.836
	m³ air	+/- %	m³ water	+/- %	am243	
Charge	1.779E+19	N/A	3.348E+12	N/A	cm242	8.856
Discharge	1.930E+19	N/A	3.631E+12	N/A	cm244	20.387
1 yr	1.712E+19	N/A	3.230E+12	N/A	cm245	38.508
5 yr	1.575E+19	19.334	2.974E+12	19.369	FP (+/- %)	
10 yr	1.482E+19	19.027	2.797E+12	19.062	c 14	--
50 yr	1.040E+19	18.267	1.962E+12	18.306	se 79	--
100 yr	7.993E+18	16.936	1.506E+12	16.977	sr 90	--
500 yr	3.182E+18	10.477	5.984E+11	10.479	tc 99	--
1000 yr	2.109E+18	9.062	3.964E+11	9.061	i129	--
2500 yr	1.342E+18	8.907	2.522E+11	8.902	cs137	--
5000 yr	1.061E+18	8.624	1.995E+11	8.619	ba137m	--
10000 yr	7.437E+17	7.322	1.398E+11	7.316	y90	--
	Main Contributors to Uncertainty in Decay Heat and Radioactivity				k-Effective Values	
	Heat		Activity		BOC	1.00638
5 yr	Pu-238, Cm-244		Cm-244, Pu-241		EOC	0.99925
10 yr	Cm-244, Pu-238		Cm-244, Pu-238, Pu-241		Conversion Ratio at EOC	
50 yr	Cm-244, Pu-238, Am241		Am-241, Pu-238, Pu-241		0.7695	
100 yr	Pu-238, Am-241		Pu-238, Am-241			
500 yr	Pu-240, Am-241		Pu-240, Am-241			
1000 yr	Pu-240, Am-241		Pu-240, Am-241			
2500 yr	Pu-239, Pu-240		Pu-239, Pu-240			
5000 yr	Pu-239, Pu-240		Pu-239, Pu-240			
10000 yr	Pu-239, Pu-240		Pu-239, Pu-240			